EC 13

VERIFICATION OF WAVE MODELS OUTPUT VERSUS MEASURED WAVE DATA FOR THE GREAT LAKES, EAST AND WEST COASTS OF CANADA

Final Report to

Atmospheric Environment Service
Environment Canada

February, 1995

Our File No.005859RE.O01

VERIFICATION OF WAVE MODELS FOR CANADIAN WATERS

Prepared for:
ATMOSPHERIC ENVIRONMENT SERVICE
ENVIRONMENT CANADA
4905 Dufferin Street
Downsview, Ontario
M3H 5T4

Prepared by
MACLAREN PLANSEARCH (1991) LIMITED
Suite 200, Park Lane Terraces
5657 Spring Garden Road
Halifax, Nova Scotia
B3J 3R4

and

OCEANWEATHER INC.
5 River Road
Cos Cob, Connecticut
U.S.A

1995

005859RE.O01

This work was partially funded by the Transport Canada Search and Rescue New Initiatives Fund and the Federal Panel on Energy Research and Development.

February 10, 1995

Atmospheric Environment Service
Environment Canada
Climate and Atmospheric Research Directorate
4905 Dufferin Street
Downsview, Ontario
M3H 5T4

Attention: Mr. Val Swail

Dear Mr. Swail:

RE: FINAL REPORT– VERIFICATION OF WAVE MODEL OUTPUT VERSUS MEASURED WAVE DATA FOR THE GREAT LAKES, EAST AND WEST COASTS OF CANADA.

We are pleased to submit the final report for the above referenced study. This revised version of the report includes all your comments and suggestions that you made on the draft report.

The report originals and a wordperfect file of the report on a diskette are enclosed. We trust this is satisfactory, but should you have any further requirements please contact the undersigned.

We would like to take this opportunity to thank you and the funding agencies for supporting this study.

Yours very truly,

MacLAREN PLANSEARCH (1991) LIMITED

Bassem M. Eid, P.Eng.,Ph.D.
Vice–President

BE/jc

cc: Vince Cardone, Oceanweather

STUDY PRINCIPAL INVESTIGATORS

MacLaren Plansearch (1991) Limited – Prime Contractor & Project Manager

- Dr. Bassem Eid, Project Manager
- Mr. Brian McGrath, Meteorologist
- Mr. Colin Calnan, Computer Programmer / Data Analyst

Oceanweather Inc. – Subcontractor

- Dr. Vince Cardone, Principal Advisor
- Mr. Brian Callahan, Meteorologist

STUDY SCIENTIFIC AUTHORITY

- Mr. Val Swail, AES, Downsview, Ontario

ACKNOWLEDGEMENTS

This study was carried out jointly by MacLaren Plansearch (1991) Limited, Halifax, Nova Scotia, Canada and Oceanweather Inc., Cos Cob, Connecticut, U.S.A. The study was funded by Transport Canada’s Search and Rescue New Initiatives Fund, and the Federal Panel on Energy R&D (PERD) and was managed by Atmospheric Environment Service of Environment Canada under Supply and Services Canada contract No. KM170–2–8930101–XSE.

The Authors wish to express their appreciation to Mr. Val Swail, the Scientific Authority for this study, for his support and valuable input throughout the course of the study.

The Authors also wish to thank the Marine Environmental Data Service (MEDS), and Atmospheric Environment Service (AES), for providing their data and supporting this and other wave hindcasting and forecasting projects.

EXECUTIVE SUMMARY

For a safe and economic design and operation of vessels, offshore platforms and other marine structures, an accurate description of the marine environment is required. Waves are one of the most important design and operation parameters of marine structures, therefore a good knowledge of the wave climate, with sufficient spatial and temporal data coverage, in the operating area is essential. Several wind and wave hindcasting studies have been carried out over the past number of years to provide wind/wave climatologies for Canadian waters. These model studies were used to fill the present data gaps in the measured database.

The purpose of this study was to verify the output of wave hindcasts made in these studies using contemporary wave models against measured wave data in Canadian waters, including the Great Lakes; the East Coast and West Coast of Canada. The focus, for the present work, is to document the expected accuracy or skill of the models considered in the context of the Search and Rescue, the funding agency.

For <u>the Great Lakes</u>, two main hindcast databases were reviewed:

a) the Ontario Ministry of Natural Resources hindcast study (1988) which provided a wave climate database of varying durations (20–35 years) using different models;

b) the U. S. Army Corps of Engineer, Waterways Experimental Station (WES) Wave Information Study (WIS), 1992, which contains 32 years prediction (continuous time series) using a spectral wave model.

For <u>the East Coast of Canada</u> the following data sets were considered:

a) Three year ODGP spectral wave model hindcast (1983–1986);

b) Extreme wave hindcast study (PERD–funded), where a total of 68 East Coast severe storms were hindcast;

c) Recent severe storms which were hindcast after the conclusion of (b) above, which includes the major ”Halloween Storm” (Oct. 31, 1991) in which the highest wave height ever recorded in this region (or anywhere else in the world) occurred.

For <u>the West Coast of Canada</u> the following hindcasts sets were included:

a) Three–year hindcast database produced in this study (1 Jan. 1987 – 31 Dec. 1989, inclusive);

b) Extreme wave hindcast study (CCC, 1992), where a total of 51 severe storms were hindcast;

c) Additional four new most severe storms from the most recent years (1990–1993) where wave height exceeded 10–12 m with good measured data coverage.

With the exception of the Great Lakes, where a number of different spectral and non–spectral models were used, all the studies listed above were made with the same model: i.e. the ODGP Spectral Ocean Wave Model, thus simplifying somewhat the study.

This study provided a comprehensive validation / evaluation of the above model predictions and presented extensive measures of the expected skills of these model hindcasts, both normals and extremes. Various error statistics, time series comparisons, regression analysis, etc. were applied to model hindcasts versus measured buoy data. Errors due to input winds, shallow water effects, and other topographical effects as well as model physics were discussed.

Despite the differences of approach and verifications, the errors in the ODGP hindcast results are not too different between the two basins (with scatter index at 31% in wave height). This was not the case for the Great Lakes where model skills varied from one lake to another and from one model to another.

The verification of storm hindcasts exhibit greater relative skill than the continuous hindcasts (i.e. scatter index of wave height in the order of 10–20%). This is mainly due to greater accuracy made in storms wind fields than the winds derived for the continuous (3 year) hindcasts period, and due to the large energy level of storms generated sea states than those of continuous hindcasts.

The model showed positive bias in the peak wave height (i.e. hindcast is greater than measured) particularly in the East Coast storm hindcast, which is attributed to the shallow water effects. However, while the bias in significant wave height in storm verification is positive in general in both basins, the model under predicted the peak sea states in the largest storm peaks, when peak H_S exceeds about 12 m. The sources of errors are discussed and recommendations were made in the report.

Study Findings And Recommendations

This study has identified the various sources of error in model predictions and provided the following conclusions:

1) Wind Errors

The errors in surface wind fields are the largest single source of error in all wave prediction model studies.

Better understanding of the accuracy of measured buoy surface wind is needed, particularly in high seastate conditions. This may be achieved by recording high–frequency, continuous wind data form various types of buoys and fixed platform in the vicinity of buoys. Buoy motion effects must also be studied.

2) Model Physics

The study has identified errors associated with model predictions due to:

- shallow water physics (e.g. east coast)
- wave–current interactions mechanism (e.g. west coast)

Additional hindcast and verification studies are needed to properly isolate the separate contributions of wind errors, shallow water refraction and alternations, current refraction, and deepwater source terms (i.e., atmospheric input, wave breaking and wave–wave interaction).

3. Model Numerics

The wave model temporal and spatial resolution should be compatible with the time and space of the deriving forces (i.e. wind fields associated with meteorological features and systems being modelled, jet streak features, and mesoscale or local effects) and topographical effects such as sheltering effects, funnelling, etc.

Further studies are required using models of various grid/time steps to define the optimum grid for nearshore wave field resolution and for assessment of the sensitivity of the wave solution to grid resolution for storm systems in which wave generation along dynamic fetch excites extreme waves.

4. Reliability of Simulated Wave Climate

a) Normals

– grid limitation prevented accurate resolution of nearshore gradients.

– physics limitations may lead to unrepresentative climate in shallow water areas and in areas susceptible to strong currents.

– short hindcast period limits the presentation of true long–term climate.

The hindcast period should be extended to cover at least a 10–year period (using the interactive graphics methods described in this study perhaps, with some further refinement). The wave model used should include the addition of shallow water terms, wave–current interactions, and extended domain for better resolution of distinct small sources.

b) Extremes

The model hindcast appeared to be underpredicting the wave height in very severe storms where measurement sites lie along the path of the rapidly propagating and energetic ”jet streak”.

Further detailed hindcast studies of recent severe storms which have been well sampled in the dense buoy network off the east and west coasts should be carried out to further characterize the dynamic fetch generation associated with low level jet streak.

TABLE OF CONTENTS

LIST OF TABLES

LIST OF FIGURES

Figure

ACRONYMS AND ABBREVIATIONS

AES	Atmospheric Environment Service
CCC	Canadian Climate Centre
CCIW	Canada Centre for Inland Waters
CMC	Canadian Meteorological Centre, Montreal, PQ
ECMWF	European Centre for Medium Range Weather Forecasting
GLERL	Great Lakes Environmental Research Lab
INGRED	Interactive Graphical Editor
MEDS	Marine Environmental Data Service
MPBL	Marine Planetary Boundary Layer
MPL	MacLaren Plansearch (1991) Limited
NDBC	National Data Buoy Center, USA
NMC	National Meteorological Center, USA.
NOAA	National Oceanic and Atmospheric Administration
NWP	Numeric Weather Prediction
ODGP	Ocean Data Gathering Program
OMNR	Ontario Ministry of Natural Resources
OWI	Oceanweather Inc.
PBL	Planetary Boundary Layer
PERD	Panel on Energy Research and Development. Also used to reference previously funded East Coast Hindcast Study by MPL and OWI
PWC	Pacific Weather Centre, Vancouver, B.C.
SMB	Sverdrup–Munk–Bretschneider
SOWM	Spectral Ocean Wave Model
SSW	Sandwell Swan Wooster Inc., Don Mills, ON.
TDC	Transport Development Centre, Transport Canada
USACE	United States Army Corps of Engineers
WES	Waterways Experimental Station, U.S. Army Engineers
WIS	Wave Information Study

1.0 INTRODUCTION

1.1 OBJECTIVES

An accurate description of a marine operating environment is a prerequisite for engineering design, precise performance analysis, and safe and economic operation of vessels, offshore platforms and other marine structures.

The ideal data set for providing such a description would consist of simultaneous measurement of wind, waves and other oceanographic parameters. These data would ideally be of long duration, large spatial coverage and great accuracy for providing reliable climate description of marine environments (both normals and extreme).

Waves are one of the most important design and operation parameters of marine structures. Therefore, a good knowledge of the wave climate in the operating areas is essential. It is important to have sufficient data coverage, both temporally and spatially, for planning, engineering design and operation of offshore structures, search and rescue, and emergency responses to marine disasters, etc.

Within the past decade several comprehensive wind and wave hindcasting studies have been completed using spectral ocean wave models to provide wind/wave climatologies for Canadian waters. The previous model hindcast studies included both continuous prediction over a number of years, for providing normal climate data, and severe storm events for providing extreme wave climate data.

The purpose of this study was to verify the output of wave hindcasts made in these studies versus measured wave data for three regions (or basins): (1) the Great Lakes; (2) the East coast of Canada; and (3) the West coast of Canada.

1.2 REVIEW OF CANADIAN WAVE CLIMATE PROGRAM

The present Canadian wave climate study program currently coordinated by the Canadian Waves Committee, with volunteer members from various Federal Government departments who are interested in this field, consists of four main components: (1) a measurement program; (2) a hindcast program which consists of development of hindcast techniques, evaluation of existing hindcast products, storm analysis and development of statistical techniques for extreme value analysis, and design parameters; (3) an archival service which makes available product developed in (1) and (2) above; and (4) database management and retrieval systems.

The database of instrumental wave measurement series, acquired mainly by the Marine Environmental Data Service (MEDS), Department of Fisheries and Oceans (DFO), is substantial. It contains large volumes of wave measurements from the East and West coasts of Canada, the Great Lakes and the Beaufort Sea. However, this database in itself does not satisfy the broad scope of planning and engineering requirements. Existing series are specific to sites of past interest, and measurements are not usually available for very long periods in new areas of industry interest. Also, at any given site, the measurement series are not continuous, since measurements were keyed, in general, to periods of active hydrocarbon exploratory drilling or related to specific application of short duration. These data gaps are particularly troublesome for applications which require duration and persistence–type wave statistics. Finally, most of the present waverider buoy measurements provide no directional wave information; such directional wave information could be very useful for both design and operation of offshore platforms, ship routing and seakeeping, etc.

To overcome the problems and limitations of the wave measurement database, model predictions (hindcasts) have been used to fill data gaps, and provide long–term directional wave information (i.e. 2–D spectra). Several models had been tested in Canada, United States and Europe. The hindcast component of the Canadian Wave Climate Program basically involves development of wave hindcast models and evaluation of existing hindcast models, creation of wave hindcast databases and use of such data for providing wave climatology for these waters.

The third element in these efforts is archival services which have been, to a great extent, the responsibility of MEDS and AES in Canada. MEDS's database includes both measured buoy data (including the U.S. NOAA buoys) and model hindcasts. Examples of model data archived are: 20–year hindcast using the U.S. Navy Spectral Ocean Wave Model, SOWM, the U.S. Army Wave Information System (WIS hindcast); and recent Canadian applications modelling the East coast (North Atlantic) and West coast (North Pacific Ocean) and the Beaufort Sea, using the ODGP (Ocean Data Gathering Program) spectral ocean wave model.

The last element of these efforts is the database management and retrieval system that integrates all marine climate information that is needed for planning, engineering design and operation (e.g. wind, wave, current, etc.) with an easy–to–access, on–line, digital database.

This study deals only with the second element of this program, i.e. evaluation of model predictions and creation of wave hindcast database for Canadian waters.

1.3 STUDY METHODOLOGY

The result of previously completed hindcast studies are compiled herein and evaluated within the context of Search and Rescue (SAR) main objectives, namely to verify model predictions and to provide a complete database for providing accurate description of wave climate in Canadian waters.

The present study covers three major areas:

1. **<u>The Great Lakes</u>**, where two main hindcast databases are reviewed:

(a) The Ontario Ministry of National Resources (OMNR) hindcast study, 1988 (20–35 years).

(b) The U.S. Army Corps of Engineers, Waterways Experimental Station (WES) wave information study (WIS), 1992 (32 years).

2. **<u>The East Coast of Canada</u>** where the following datasets are considered:

(a) Three–year ODGP spectral wave model hindcast database (1983 – 1986) carried out by MPL and OWI (Eid et. al., 1989);

(b) Extreme wave hindcast study carried out by MPL and OWI (CCC, 1991), where a total of 68 East coast severe storms over 32 years were hindcast;

(c) Recent severe storms which were hindcast after the conclusion of (b) above. This includes the major Halloween storm (October 31, 1991) in which the highest wave height ever recorded in this region was measured at an offshore buoy moored south of Nova Scotia.

3. **<u>The West Coast of Canada</u>**

(a) Three year hindcast database, which was produced as a part of this study, covering the period from January 01, 1987 to December 31, 1989;

(b) Extreme wave hindcast study by MPL and OWI (CCC, 1992), where a total of 51 severe storms were hindcast over 32 years;

(c) Four new most severe storms selected from most recent years (1990–1993) where good coverage of measured buoy data is available.

The first generation ODGP spectral ocean wave model was used to provide the database for the East and West Coast regions in the studies noted and for all additional hindcasts carried out in this study.

For the Great Lakes, various models were reviewed with more emphasis on the WES model hindcast database.

These data have been used to generate a wind and wave climate Atlas for the East Coast, the Great Lakes, and West Coast, for Transport Canada (MPL 1991, 1992 and 1993.)

1.4 REPORT ORGANIZATION

The Great Lakes model verification is described in Chapter 2.0 of this report. The East coast model verification is presented in Chapter 3.0 . Chapter 4.0 presents the West coast 3–year hindcast results. West coast storm verification is described in Chapter 4.0 . Summary, conclusions and recommendations are provided in Chapter 5.0 . Due to the large number of tables and figures, all tables and figures are placed at the end of each chapter or large section.

The 3–year continuous hindcast database for the Northern Pacific Ocean (i.e. gridded pressure field, wind field and wave data) and the wind/wave data for all additional storms hindcast were delivered to AES for archival in their marine climate database.

2.0 GREAT LAKES WAVE MODELLING

2.1 WIND/WAVE MODEL HINDCASTS

The Ontario Ministry of Natural Resources (OMNR) identified a need to develop a long term wave climate database for the Great Lakes, particularly for coastal areas along the Canadian side of the Great Lakes. In 1988, the Ontario Ministry of Natural Resources employed three consulting companies to model the wave climate of the Great Lakes. The companies contracted were: MacLaren Plansearch (MPL), which provided a 20–year (1964–1983) wave hindcast for Lake Superior and Lake Ontario; Philpott Associates, which provided a 35–year wave hindcast for Lake Huron and Georgian Bay (1952–1987); and Sandwell Swan Wooster (SSW), which provided a 16–year wave hindcast for lakes Erie and St. Clair (1971–1988). Lake Michigan was excluded from the OMNR Study, being entirely within the U.S. The results of these studies have been published in consultant's reports which were submitted to the Ontario Ministry of Natural Resources in March, 1988. The results of these hindcasts are summarized in this report.

Another major study of the Great Lakes, called Wave Information Study (WIS), was carried out by the U.S. Army Corps of Engineers, at Waterways Experimental Station (WES). The result was to supply a long term, continuous time series of winds and wave spectra for this area for 32 years (1956–1987). A full description of these results was reported in a series of WIS reports [Driver et al., (1992); Driver et al., (1991); Hubertz (1991); and Reinhard et al., (1991a and 1991b)]. The verification results from that study are summarized herein.

Concurrent to this, MPL compiled an atlas of wind and wave climate of the Great Lakes using the WES hindcasts, for the Transportation Development Centre (TDC) of Transport Canada. Included in that study for TDC was a verification study of the WES model versus measured buoy data. The results of that verification study are also presented in this report.

2.1.1 Model Verification

Models are deemed successful if their results have a high correlation to measured data that exists. Here, the models are verified against buoy data that have been compiled by NOAA and MEDS. General statistical analyses are performed and results are provided herein.

Variables considered include significant wave height (H_s), peak period (T_p), wave direction, wind direction (W_d), wind speed (W_s), time series plots of those parameters, and wave spectra. Verification analyses include: storms peak–to–peak comparison (usually of H_s, T_p) and standard statistics, such as mean error, root mean square error (RMSE), correlation coefficient, and scatter index (SI).

Results of these studies are discussed in the following sections.

2.2 OMNR/MPL: LAKES SUPERIOR AND ONTARIO

MPL was contracted to complete the modelling study of lakes Superior and Ontario. Documents were prepared by MPL, which included a discussion of the model used and verification of the model predictions (MPL, 1988). The results of that study are discussed below.

2.2.1 The Wave Model

The model employed by MPL was a two dimensional wave prediction model originally developed by Donelan (1978), at the Canada Centre for Inland Waters (CCIW) and later modified by Schwab et al. (1984) at the Great Lakes Environmental Research Laboratory (GLERL), NOAA, Ann Arbour, Michigan. This model had been used previously and tested in studies of the Great Lakes [Schwab et al. (1984 and 1986); and Clodman (1983), and in studies of the Beaufort Sea (Clodman and Eid (1988)).

The GLERL model is based on a momentum balance equation used in a finite difference environment. The terms in the equation include: a time rate of change of momentum, divergence of wave momentum flux, and a source term based on wind stress. The equation is solved by representing momentum flux in terms of the spreading of energy as waves propagate. Wave spectra variance, angle of propagation, and a spreading factor are the independent variables. This work is further described in Schwab et al. (1984).

The source term is specified by calculating wind stress from the input wind field. This term is dependent on wind velocity at 10 m, wave speed, drag coefficient, and an empirical factor, γ (gamma). The factor γ is the fraction of wind energy that causes the build up, or decay, of waves [see Donelan (1978)]. Ice edge was taken into account by redefining the boundary of the lake using the two–week median ice edge ($\geq$ 5/10 concentration) data, between 1972 and 1985.

2.2.2 The Wind Model

The wave model was driven by the source term which was derived from the input wind field. This field was derived from wind data recorded by coastal meteorological stations around the lake, after being converted to overwater values. An imperial relationship based on Phillips and Irbe (1978) was used to convert the over–land winds into the equivalent over–water values at a standard height (10m) above water surface. This relationship takes into account surface roughness (as a function of wave age or wind fetch) and atmospheric stability (as function of air–sea temperature difference) using relationships developed by Businger et al. (1971). The converted hourly winds were provided at a number of pre–selected locations in each lake (9 for Lake Ontario and 8 for Lake Superior); these values were then used to provide the wind field at all model grid points. The NOAA buoys measurements were used to calibrate and validate the wind model. It was found that in order to reproduce the buoy measured, Gilhousen (1987) found that NOAA buoy wind speeds are usually 10% too low, therefore, these winds were increased by 10% before input into the wave model. Winds were then interpolated onto a grid, to yield a wind field for the particular lake.

2.2.3 Model Verification

Lake Superior

The GLERL model was tested temporally and spatially. The temporal test used data from NOAA Buoy 45001, from April 25 to November 25, 1980. Time series plots of model output (i.e. wind speed and direction, wave height and period) and corresponding observations were provided in the MPL (1988) report. When model winds were highly correlated to the measured winds, the model predicted wave heights were in good agreement with measurements (see Figures 5–21, 5–24 of the MPL (1988) report). Errors in model predictions can be attributed to errors in the input wind field, and also to atmospheric stability.

The second analysis tested the model spatially. The time period was from September 1 to November 1, 1982, that included data from three NOAA buoys, namely 45001, 45004 and 45006.

The buoy observations were as follows:

NOAA Buoy	Wind Observation	Wave Observation
45001	September 1 to November 17, 1982	September 1 to October 8, 1982
45004	September 1 to November 17, 1982	September 1 to November 17, 1982
45006	September 1 to November 17, 1982	September 1 to November 6, 1982

Time series plots of wind speed, direction, wave height, and period were included in the MPL (1988) report. Model results were highly correlated for significant wave height (H_s) and wind speed (W_s), but correlations were not as strong for peak period (T_p), though it must be taken into account that T_p is an inherently variable statistic. Overall the model was successful in this domain. See Figures 5–21, 5–29, 5–31 and Table 5–34 of the MPL (1988) report. The results of model verification for Lake Superior are summarized in Table 2.1.

Lake Ontario

For Lake Ontario, the GLERL model was compared to actual data from two MEDS waverider buoys, B64 and B74. The test period was from August 1 to December 1, 1973. It was noted in the report (MPL, 1988) that buoy B74 was in shallow water which provided interesting information as to how the model handles such conditions. Time series plots of H_s, T_p, W_d, and W_s show excellent results for Site B64, but the model tended to over–predict wave height and period at the other site; particularly when the winds are northerlies or northwesterlies. This may be caused by shallow water effects as the model assumed deep water, it tends to over–predict waves at a shallow site, or it may be due to the model's sensitivity to wind direction in terms of affecting the fetch. i.e. small variation in wind direction can affect the fetch, and hence, the waves. The results of model verification for Lake Ontario are summarized in Table 2.2.

2.3 OMNR/SANDWELL SWAN WOOSTER – LAKES ST. CLAIR AND ERIE

The second part of the OMNR study was for lakes St. Clair and Erie and was carried out by Sandwell Swan Wooster (SSW). Two different models were used: a one–dimensional shallow water wave model for Lake St. Clair, and a two–dimensional wave predictor model for Lake Erie (similar to that used by MacLaren Plansearch in its study of Lakes Superior and Ontario). Wind input was again taken from AES land stations near each lake. The wave output from the model was compared to NOAA and MEDS buoys in the lakes. A verification study was completed by SSW and is summarized in this report. A more complete treatment is given in SSW (1988).

2.3.1 Lake St. Clair

The Wave Model

Input for this model was a meteorological data file that included data from the land stations around the lake; some corrections were applied to this data. First, the data were converted from the instrument height to a wind velocity at 10 m by a power law relation. Next, a speed dependent scaling factor was applied which accounted for dampening effects land features have on low winds. In other words, it boosted low wind velocities (0–10 m) by a maximum factor of 1.95, while leaving winds in excess of 10 m/s unchanged. The factors were derived from an overwater/overland wind factor graph (Resio and Vincent, 1976). A third correction applied to the wind data accounted for atmospheric instability caused by differences in land and water temperatures. These factors were taken from Resio and Vincent (1977).

The wave model is based on SMB shallow water equations which includes a wind stress forcing term that was calculated from the wind speed (CERC 1984). These data, along with calculated fetch and water depth, are independent variables for the model equations. Since Lake St. Clair is a shallow lake (water depths on the order of 5–6 m), the model was calibrated to account for refraction effects as wave refraction can have an effect on wave height and direction.

Model Verification

This model was verified against NOAA and MEDS buoy data during two periods: October 4–7, 1985, and September 23–36, 1985. During the calibration process, a phase lag of between 2–7 hours was noticed and later, this was accounted for by shifting the calibration plot by 4.5 hours.

For the first verification period, there was a good correlation for wave heights and periods (Figures 4–25 and 4–26 of the SSW report). The wave direction, however, showed marginal results (Figure 4–27 of the SSW report), but the inclusion of refraction effects did improve this comparison.

The second verification again showed a good correlation between model and measured wave heights and period. The wave direction correlation was poor during October 23th and 24th, but did improve on the 26th and 27th of that month. The inclusion of refraction effects did improve this comparison.

2.3.2 Lake Erie

The Wave Model

The model used for the wave study of Lake Erie was essentially the same used by MacLaren Plansearch to study the wave climate of lakes Superior and Ontario. The model is a two–dimensional hindcasting model, derived from Donelan (1978) and later revised by Schwab et al., (1984). Wind stress was derived from the input wind field and included the effects of atmospheric instability due to air–water temperature differences. The stress term included the factor Y, which acts to increase the momentum of the wave field by specifying the fraction of wind stress that leads to growth of waves. Ice front position was also allowed for in this model.

Model Verification

For a better understanding of the accuracy of this model, two verification sites were chosen. The first was a MEDS station, ERWVNE; the second was the GLERL research tower. These sites provide both temporal and spatial checks on the model results. The verifications took place over two time periods: December 3rd–6th, 1986 and October 1st–3rd, 1981.

Calibration results indicated that all major storm events in the month of December, 1973 were predicted (i.e. 5–7, 10, 13–14, 22–23, 28, 29–30). Smaller waves (micro–scale events) seemed to be underestimated by the model while macro–scale events appeared to be accurately predicted. A comparison of predicted and actual wave periods indicated that, below an apparent threshold value of 5 seconds, the model over–predicted wave periods; while above the threshold, the model under–predicted the wave periods. A correction factor was introduced to remedy this situation.

The first verification period indicated that wave heights of all major storm events were well predicted. Only one storm was under–predicted by the model which may have been caused by lower than expected wind speeds recorded at the two wind stations used. Wave periods were under–predicted, both below and above the 5 second threshold value, for the whole verification set.

The second verification set contained directional wave data (collected at the GLERL tower). Wave heights were well predicted for the first day of this period (October 1, 1981), but were under–predicted for the final two days (October 2–3, 1981). These discrepancies were also seen in the comparison between model and observed wave periods. Actual wind data was checked to reveal a dropping off of wind at the Simcoe Station, without a corresponding decrease at the GLERL tower or at Windsor. It was concluded that the discrepancies were due to a micro–scale weather event that was not reproducible by the model.

The comparison for wave directions from the model and observed values indicated a very good correlation. Typically, only a 10–20 degree difference was observed. A wind directional shift from 100 degrees to 250 degrees within a 10–hour span was accurately predicted by the model (see Figures 5–6, 5–7, 5–5, 5–4 of SSW (1988)).

A third verification was performed during October 18–20, 1981, but was not graphically represented in the report. Both wave heights and periods were well represented and discrepancies between measured and predicted wave directions were again not typically more than 10–20 degrees.

2.4 OMNR/PHILPOTT ASSOCIATES: LAKE HURON AND GEORGIAN BAY

The third part of the Great Lakes Study that was initiated by the Ontario Ministry of Natural Resources was completed by Philpott Associates Coastal Engineers, Limited. Their study implemented a wave hindcast model to look at the wave climate of Lake Huron and Georgian Bay. The model used was a parametric SMB model, referenced in CERC (1984). This was a similar approach to that taken by Sandwell Swan Wooster in their analysis of the wave climate of Lake St. Clair. Wind input was derived from one of AES' stations (Gore Bay) on the north shore of the lake. Wave model output was compared to buoy data from the Marine Environmental Data Service (MEDS).

The Wave Model

The wave hindcast model used was a one dimensional parametric SMB model. Wind speed and fetch are the independent variables. Through statistical analysis, wind data from a single station at Gore Bay was determined to be sufficient input for the wave model. Errors associated with using this set was low, because of a long record length and reasonable data accuracy (see Table 3.1 in Philpott Associates, 1988). Standard corrections were applied to the measured wind speeds to account for anemometer height, atmospheric stability derived from air/water temperature difference, and overland versus overwater boundary layer friction effects.

The model was adjusted by varying the method that fetches were determined, and the wind divergence angle. This angle specifies what range of wind data can be applied in the forcing term for wave generation. For example, a wider angle allows more wind forcing, and prolongs the duration of storm events.

Model Verification

The wave model results were compared to MEDS buoy data at six locations in the lake. Several storm events were compared during September–November, 1973; June – December, 1986; and July–November, 1987. Wave power, energy, significant wave height, and peak period were tested using standard statistical analysis. This was done using two sets of input wind data: Gore Bay and Sarnia.

The results show significant errors at various locations and times. A cumulative mean percentage error and mean standard deviation showed that there was no trend to the data. The hindcast results did not consistently over– or under–predict the measured wave data for any one site, or for all sites collectively.

A time lag did exist in most time series plots, so statistics for maximum, minimum and RMS instantaneous error of a storm event should be viewed with this in mind.

2.5 WIS: WIND/WAVE HINDCAST DATABASE

The Wave Information Study (WIS) was completed in 1991 by the U.S. Army Corps of Engineers, Waterways Experiment Station (WES) and was aimed at providing a long term, continuous wave hindcast database. A wave model was employed to compile observed wind data from land stations, and produce wave variables; such as significant wave height (H_s), peak period (T_p) and wave direction (W_d). Previous to a wave model run, the wind speeds were adjusted to a 10 m height using a power law relationship with an exponent of 1/7. Wind speed was also corrected for atmospheric stability due to air–sea temperature differences; and for frictional effects, due to differences in surface roughness between the land and water.

To construct a more realistic wind field, the land station wind data were interpolated to a grid using a scheme that employed weighting factors dependent on the location of land and buoy stations. Here, grid point wind speed was derived from a weighted sum of the products of wind speed at each land and buoy station. These interpolated winds were then verified by first calculating the field using land stations only, then comparing the result to NOAA buoy data at its corresponding location on the grid. A 32–year hindcast was compiled for the five Great Lakes. The complete reports have been published by USACE [Driver et al., (1992); Driver et al., (1991); Hubertz (1991); and Reinhard et al., (1991a, 1991b).

2.5.1 <u>The Wave Model</u>

The WES wave model used in this study was developed by Resio (1989). This is a discrete spectral model that simulates wave growth, dissipation and propagation in deep water. Forcing was implied through wind stress term; dependent on wind speed, peak frequency, frequency and direction of the wind and waves. Wind fields were calculated from measured data as described above. The WES model had been used and verified in other applications such as: Pacific storms, Gulf and Atlantic hurricanes and low–wave conditions of the Great Lakes.

2.5.2 <u>Model Verification</u>

The wave output was verified using measured wave data from NOAA and MEDS buoys in each lake which, unfortunately, measure non–directional data, such as wave height and period and wind speed and direction. The wave direction determined from the model is a an important variable, and its verification with real data is of interest. Fortunately, a field experiment by NOAA's Great Lakes Environmental Research Laboratory (GLERL) in 1981 produced a small, but valuable data set of wave parameters. The data was recorded by a tower, situated 6 km from the shoreline of Lake Erie. Therefore, a verification of wave direction is possible for this lake.

Verification studies were completed by USACE in the WIS reports and privately by MacLaren Plansearch (unpublished). USACE verified its results using NOAA buoy data measured at varied times from 1980 to 1986; except in Lake Ontario, where data from MEDS buoys was used for the period April–November, 1972. MacLaren Plansearch verified the model output primarily with measured data from the spring, summer, and fall months of 1987; but for one grid point in Lake Ontario, the verification period was from April–November, 1972. A summary of the verification results is provided in Tables 2.1 to 2.7.

a) Model Verification by WIS

The model was verified in each lake separately, so results may vary from lake to lake. Overall, the model performed very well under the verification tests. H_s, T_p and W_d (for Lake Erie) were the verified variables. Time series comparisons, scattergrams and standard statistical analysis were used in this process.

For Lake Erie (WIS Report 22 Driver et al., 1991) percent distributions showed agreement between model and measured results for W_s, H_s and T_p (Figure 10 of WIS report). The largest difference in H_s occurred for the smallest waves (0.15 m), where the model over–predicted the results by approximately nine percent. Time series plots showed that agreement was good, though there was a tendency for the model to over–predict the peaks. The correlation coefficient for the entire wave height data set was approximately 0.7; with peak period (a highly variable parameter) having expectedly lower correlations, particularly during times of low wave energy.

Data from the GLERL tower showed reasonably good agreement for wave direction for directions greater than 180 degrees, but there was disagreement for directions less than 180 degrees (see Figure 15c of the WIS report). This is most likely a result of the way fetch–limited conditions are handled by the model. Overall, agreement was good for wave direction predicted by the model. Verification results (i.e. error statistics) are summarised in Table 2.5.)

Lake Superior (WIS Report 23 Driver et al., 1992) showed good verification results. The correlation coefficients ranged from 0.73 to 0.85 for wave heights, and 0.63 to 0.76 peak periods. (See Table 2.1 for summary of error statistics).

For Lake Michigan (WIS Report 24 Hubertz, 1991), both H_s and T_p were biased slightly high with respect to NOAA buoy measurements. This was compensated for by a simple reduction of all wind speeds by 3 knots. After this adjustment, the model was deemed to accurately represent the wave climate. Maximum wave heights from the model and buoys were compared to be within 0.5 m, while peak periods were generally within 1.0 seconds, though sometimes they differed by 2.0 seconds. Correlation coefficients for H_s ranged from 0.89 to 0.94, and for T_p ranged from 0.67 to 0.80. (A summary of verification results is presented in Table 2.4).

For Lake Ontario (WIS Report 25 Reinhard et al., 1991b), results of the verification tests were good. Excellent results were obtained at Buoy 65; whereas the model tended to over–predict the measured wave height at Buoy 60. The largest difference in H_s occurred in small waves less than 0.5 m (Figure 13a), where the model results exceeded measured values by approximately 15%. (Table 2.2 provides a summary of verification statistics).

Lake Huron (WIS Report 26 Reinhard et al., 1991a) again showed good agreement in corresponding peaks and troughs in the time series plots of H_s and T_p. The mean and maximum values were in close agreement, with correlation coefficients ranging from 0.71 to 0.77 for H_s and 0.59 to 0.66 for T_p. (See Table 2.3).
Through these verification analyses, it was assessed by the WIS group that the model accurately simulated the wave climate of the Great Lakes.

b) Model Verification by MacLaren Plansearch

In 1992, MacLaren Plansearch completed its report to verify the WIS wind and wave hindcast model for use in the wind/wave climate Atlas prepared for Transport Canada. Here, data were represented through time series plots, scattergrams and standard statistical analyses for each lake. It was determined that the results of the model were in good agreement with measured values of H_s, T_p, W_s, and W_d. Wave direction was not tested due to a lack of comparison data. Particular attention was given to the modelling of significant wave height (H_s). The verification results are summarized in Tables 2.1 to 2.7

The root mean square error between the modelled and measured H_s was generally less than 0.5 m for the entire comparison period for each lake, while the absolute mean error in W_s ranged from 3.3 to 5.8 knots. The buoy and model W_d were highly correlated; mean errors ranged from 1.9 degrees for Lake Michigan to 15.7 degrees for Lake Huron.

Different lakes showed different results in the accuracy of the model, and some small seasonal variations occur. The modelling of Lake Superior showed an over–estimation of the wave climate in the late spring and the early summer months. In Lake Huron, the model over–estimated H_s in the spring and summer, while under–estimating the wave climate from September to the end of the verification period. Wave climate was under–estimated in Lake Michigan throughout the verification period. The trend in Lake Ontario was to under–estimate H_s from August–October, 1987, while Lake Erie showed no noticeable seasonal trend.

Overall, when the modelled and measured values for H_s differed by more than one metre, the model tended to under–predict the measured values. T_p was calculated to within two seconds of the observed data; at times, this difference was greater.

It was determined by MacLaren Plansearch through its analyses that, the WIS wave hindcast model gave a reasonably accurate description of the wave climate of the Great Lakes.

Table 2.1: Lake Superior: Verification Results for Hs and Tp

Variable	Study	Verification Date	Buoy (NOAA)	Records	Average Observ.	Average Model	Mean Error	Absolute Error	RMSE	Scatter Index	Correlation Coefficient
Hs (m)	WIS Report 23	1981-1986	45006	7232	0.64	0.68	0.04	*	0.41	64	0.73
			45001	7827	0.87	0.94	0.07	*	0.40	46	0.85
			45004	5954	0.75	0.88	0.13	*	0.44	59	0.82
	MacLaren Plansearch	Jul. 1, 1986 -	45006	1493	0.65	0.66	0.01	0.30	0.44	66.02	0.75
	(Unpublished)	Jul. 31, 1987	45001	2615	0.87	0.98	0.11	0.34	0.49	49.03	0.80
	WIS Hindcast		45004	1529	0.72	0.80	0.09	0.28	0.39	48.39	0.87
	MacLaren Plansearch:	Sept- Nov 1982	45001	861	1.07	0.87	-0.20	0.35	0.48	45.29	0.68
	Report to Ontario Min.		45004	1831	1.01	1.15	0.14	0.35	0.45	44.53	0.88
	of Natural Resources		45006	1564	0.99	0.92	-0.07	0.33	0.49	49.24	0.76
Tp (s)	WIS Report 23	1981-1986	45006	7232	3.84	3.83	-0.01	*	1.01	26	0.63
			45001	7827	4.27	4.41	0.14	*	0.95	22	0.76
			45004	5954	4.13	4.37	0.24	*	1.00	24	0.70
	MacLaren Plansearch	Jul. 1, 1986 -	45006	1547	4.08	3.67	-0.42	0.88	1.15	31.46	0.60
	(Unpublished)	Jul. 31, 1987	45001	2666	4.67	4.44	-0.23	0.81	1.07	24.08	0.71
	WIS Hindcast		45004	1582	4.22	4.13	-0.09	0.68	0.87	20.95	0.74
	MacLaren Plansearch:	Sept- Nov 1982	45001	859	4.48	3.99	-0.49	0.96	1.23	27.48	0.50
	Report to Ontario Min.		45004	1831	4.55	4.48	-0.07	0.89	1.15	25.35	0.71
	of Natural Resources		45006	1569	4.35	4.06	-0.29	0.95	1.28	29.38	0.59

Table 2.2: Lake Ontario: Verification Results for Hs and Tp

Variable	Study	Verification Date	Buoy	Records	Average Observ.	Average Model	Mean Error	Absolute Error	RMSE	Scatter Index	Correlation Coefficient
Hs (m)	WIS Report 25	Apr-Dec 1973	Meds 64	1867	0.49	0.32	-0.17	*	*	*	*
		Aug-Nov 1973	Meds 74	750	0.48	0.50	0.02	*	*	*	*
		Apr-Nov 1972	Meds 60	1250	0.60	0.39	-0.21	*	*	*	*
		Jul-Oct 1972	Meds 65	964	0.34	0.28	-0.06	*	*	*	*
	MacLaren Plansearch (Unpublished) WIS 35 Year Hindcast	Apr-Oct 1987	ONWVSW	1391	0.46	0.27	-0.19	0.28	0.40	114.73	0.49
		Apr-Nov 1972	Meds 60	1050	0.58	0.36	-0.22	0.32	0.42	115.38	0.63
	MacLaren Plansearch Report to Ontario Min. of Natural Resources	Jul-Nov 1972	Meds 65	844	0.35	0.48	0.13	0.20	0.26	74.53	0.69
			Meds 60	689	0.59	0.59	0.00	0.24	0.32	53.24	0.75
Tp (s)	WIS Report 25	Apr-Dec 1973	Meds 64	1867	3.57	3.29	-0.28	*	*	*	*
		Aug-Nov 1973	Meds 74	750	3.36	3.32	-0.04	*	*	*	*
		Apr-Nov 1972	Meds 60	1250	3.75	3.25	-0.50	*	*	*	*
		Jul-Oct 1972	Meds 65	964	3.19	3.09	-0.10	*	*	*	*
	MacLaren Plansearch (Unpublished) WIS 35 Year Hindcast	Apr-Oct 1987	ONWVSW	1391	3.47	2.90	-0.57	0.84	1.11	38.16	0.38
		Apr-Nov 1972	Meds 60	1050	3.66	3.09	-0.58	0.86	1.10	35.49	0.50
	MacLaren Plansearch Report to Ontario Min. of Natural Resources	Jul-Nov 1972	Meds 65	848	3.21	2.83	-0.39	0.90	1.22	37.86	0.16
			Meds 60	689	3.70	3.20	-0.50	0.79	1.06	28.69	0.64

Table 2.3: Lake Huron: Verification Results for Hs and Tp

Variable	Study	Verification Date	Buoy (NOAA)	Records	Average Observ.	Average Model	Mean Error	Absolute Error	RMSE	Scatter Index	Correlation Coefficient
Hs (m)	WIS Report 26	1980-1986 1981-1986	45003 45008	9658 8285	0.82 0.84	0.83 0.75	0.01 -0.09	* *	0.44 0.50	54 60	0.77 0.71
	MacLaren Plansearch (Unpublished) WIS Hindcast	Mar-Nov 1987	45008 45003	1709 1627	0.79 0.71	0.77 1.08	-0.03 0.37	0.33 0.51	0.44 0.67	56.78 62.36	0.72 0.60
Tp (s)	WIS Report 26	1980-1986 1981-1986	45003 45008	9658 8285	4.17 4.04	4.14 4.18	-0.03 0.14	* *	1.02 1.14	25 28	0.66 0.59
	MacLaren Plansearch (Unpublished) WIS Hindcast	Mar-Nov 1987	45008 45003	1749 1677	4.10 4.21	4.12 4.43	0.02 0.22	0.89 0.88	1.10 1.09	26.69 24.62	0.59 0.53

Table 2.4: Lake Michigan: Verification Results for Hs and Tp

Variable	Study	Verification Date	Buoy (NOAA)	Records	Average Observ.	Average Model	Mean Error	Absolute Error	RMSE	Scatter Index	Correlation Coefficient
Hs (m)	WIS Report 24	Apr-Nov 1981	45002	1711	*	*	*	*	*	*	0.93
		Apr-Dec 1982	45002	1851	*	*	*	*	*	*	0.92
		Mar-Dec 1983	45002	1936	*	*	*	*	*	*	0.84
		Apr-Dec 1984	45002	1487	*	*	*	*	*	*	0.94
		Jul-Nov 1981	45007	942	*	*	*	*	*	*	0.93
		Mar-Dec 1982	45007	2090	*	*	*	*	*	*	0.91
		May-Nov 1983	45007	1493	*	*	*	*	*	*	0.94
		Apr-Oct 1984	45007	1794	*	*	*	*	*	*	0.91
	MacLaren Plansearch (Unpublished) WIS Hindcast	Mar-Nov 1987	45007	1260	0.86	0.57	-0.28	0.32	0.42	73.61	0.86
			45002	1271	0.92	0.51	-0.41	0.42	0.48	95.36	0.87
Tp (s)	WIS Report 24	Apr-Nov 1981	45002	1711	*	*	*	*	*	*	0.71
		Apr-Dec 1982	45002	1851	*	*	*	*	*	*	0.77
		Mar-Dec 1983	45002	1936	*	*	*	*	*	*	0.71
		Apr-Dec 1984	45002	1487	*	*	*	*	*	*	0.80
		Jul-Nov 1981	45007	942	*	*	*	*	*	*	0.76
		Mar-Dec 1982	45007	2090	*	*	*	*	*	*	0.67
		May-Nov 1983	45007	1493	*	*	*	*	*	*	0.78
		Apr-Oct 1984	45007	1794	*	*	*	*	*	*	0.72
	MacLaren Plansearch (Unpublished) WIS Hindcast	Mar-Nov 1987	45007	1260	5.28	3.60	-1.68	1.70	1.88	52.12	0.64
			45002	1271	5.17	3.34	-1.82	1.85	2.06	61.74	0.46

Table 2.5: Lake Erie: Verification Results for Hs and Tp

Variable	Study	Verification Date	Buoy (NOAA)	Records	Average Observ.	Average Model	Mean Error	Absolute Error	RMSE	Scatter Index	Correlation Coefficient
Hs (m)	WIS Report 22	1980-1986	45005	9797	0.61	0.63	0.02	*	0.32	53	0.70
		1980	45005	1230	0.62	0.62	0.00	*	0.27	43	0.74
		1981	Tower	289	0.76	0.93	0.17	*	0.41	54	0.77
	MacLaren Plansearch (Unpublished)	Apr-Oct 1987	45005	1435	0.47	0.61	0.14	0.29	0.38	61.71	0.46
Tp (s)	WIS Report 22	1980-1986	45005	9797	3.35	3.69	0.34	*	0.92	27	0.54
		1980	45005	1230	3.29	3.59	0.30	*	0.84	26	0.51
		1981	Tower	289	4.20	4.18	-0.02	*	1.11	26	0.63
	MacLaren Plansearch (Unpublished)	Apr-Oct 1987	45005	1491	3.49	3.67	0.17	0.70	0.88	23.88	0.50

Table 2.6: Verification Results for Wind Data: Wind Direction

Group	Lake	Verification Date	Buoy (NOAA)	Records	Average Observ.	Average Model	Mean Error	Absolute Error	RMSE	Scatter Index	Correlation Coefficient
MacLaren Plansearch (Unpublished) WIS Hindcast	Superior	July 1986 - July 1987	45006 45001 45004	1457 2316 1460	99.10 92.70 131.60	87.50 84.60 100.70	-6.47 -10.76 -15.74	41.02 35.88 36.16	56.30 49.45 50.75	64.32 58.42 50.38	0.86 0.90 0.90
	Erie	Mar-Nov 1987	45005	1385	176.20	128.70	-9.83	36.12	50.20	39.01	0.85
	Huron	Mar-Nov 1987	45008 45003	1640 1570	128.60 112.10	175.50 133.20	3.90 15.55	36.54 44.32	52.13 60.15	29.71 45.16	0.89 0.85
	Michigan	Mar-Nov 1987	45007 45002	1528 1397	140.60 96.00	148.90 92.60	-3.15 -1.96	7.00 4.68	14.68 7.27	9.86 7.94	0.99 1.00
	Ontario				NO DATA AVAILABLE						
MacLaren Plansearch: Report to Ontario Min. of Natural Resources	Superior	Sept-Nov 1982	45001 45004 45006	1848 1840 1570	* * *	* * *	-0.47 -3.76 4.45	29.61 31.25 32.51	44.49 44.44 48.11	* * *	* * *
WIS Reports					NO DATA AVAILABLE						

Table 2.7: Verification Results for Wind Data: Wind Speed (m/s)

Group	Lake	Verification Date	Buoy (NOAA)	Records	Average Observ.	Average Model	Mean Error	Absolute Error	RMSE	Scatter Index	Correlation Coefficient
MacLaren Plansearch (Unpublished) WIS Hindcast	Superior	July 1986 - July 1987	45006	1568	8.35	9.20	0.85	3.66	4.73	51.42	0.66
			45001	2332	10.92	12.09	1.16	3.93	5.21	43.10	0.65
			45004	1567	8.23	9.43	1.21	3.33	4.33	45.86	0.72
	Erie	Mar-Nov 1987	45005	1447	9.08	10.14	1.06	4.30	5.49	54.12	0.41
	Huron	Mar-Nov 1987	45008	1693	10.14	9.37	-0.77	3.78	4.76	50.82	0.63
			45003	1652	9.48	13.70	4.22	5.76	7.35	53.61	0.49
	Michigan	Mar-Nov 1987	45007	1818	9.48	6.48	-3.01	3.56	4.02	62.04	0.88
			45002	1643	10.14	6.92	-3.22	3.41	3.58	51.67	0.96
	Ontario				NO DATA AVAILABLE						
MacLaren Plansearch: Report to Ontario Min. of Natural Resources	Superior	Sept-Nov 1982	45001	1848	13.69	12.60	-1.09	3.94	5.09	37.15	0.69
			45004	1840	11.81	13.07	1.26	3.43	4.51	38.17	0.71
			45006	1578	12.13	12.13	0.00	3.86	4.92	40.60	0.63
WIS Reports					NO DATA AVAILABLE						

3.0 THE EAST COAST

This chapter contains results from studies that modelled the wave climate of the North west Atlantic Ocean. The Datasets considered in this study are:

a) A three year spectral wave model hindcast database (1983 – 1986) carried out by MPL and OWI;

b) An extreme wave hindcast study carried out by MPL and OWI, in which a total of 68 East coast severe storms over the period 1957–1989 were hindcast;

c) Recent severe storms hindcast including the major Halloween storm (October 31, 1991), which produced the highest ever recorded wave height in this, or any other, region.

In each of these studies, the wave model used was the Ocean Data Gathering Program (ODGP) model. This is a deep water, fully discretized directional spectral wave model that evolved from the Spectral Ocean Wave Model (SOWM) of the U.S. Navy (Pierson, Tick and Baer, 1966). Wave parameters such as significant wave height, peak period, wave direction, wind speed and direction are represented on a grid pattern as seen in Figure 3.1. The model, when driven by a wind field of accuracy $\pm$ 2 m/s in speed and $\pm$ 20 degrees in direction, can provide output (H_S and Tp) with a scatter index of about 10–20 percent. It has been used in many wave climate studies in the past and found to be highly reliable. Further information on this model can be found in CCC, (1991), Cardone et al. (1976), Reece and Cardone (1982), MPL (1985), and Eid et al. (1989).

3.1 THREE–YEAR HINDCAST DATABASE

The first major study to model the wave climate of the North Atlantic Ocean using the ODGP wave model was completed by MacLaren Plansearch and Oceanweather in 1988. References for this study can be found in Eid et al. (1989) and MPL (1985). As indicated in Eid et al. (1989), there exists a need to produce modelled wave information to supplement the on–site data acquired from buoys and ship reports. On–site data tends to be recorded in areas and at times of hydrocarbon exploration and drilling; therefore these data are usually insufficient to satisfy requirements where a continuous dataset is necessary. In addition, wave directional data were usually not provided by the buoys.

Other models (SOWM and WES) have been evaluated in previous studies (e.g. Baird and Readshaw, 1981; MPL, 1985) but were found to be deficient in estimating the wave climate in the study area, particularly coastal areas. There have been some recommendations for a continuous 20–year hindcast of the area, but it was decided that a shorter study duration (3–5 year), that also paid particular attention to severe storms, would be sufficient for providing a complete description of the wave climate (both normals and extremes) with sufficient accuracy. The three–year hindcast provided such a product.

Shallow water areas (< 100 m) exist on the East coast due to proximity to land masses and the presence of shallow banks. The ODGP model used in these studies is a first generation deep water wave model. An assessment of shallow water effects on model prediction is provided in this study.

The three–year hindcast study produced a data base that extended from October 01, 1983 to September 30, 1986, and is now maintained by Marine Environmental Data Service (MEDS), DFO Ottawa. Spectral wave data was produced at a pre–selected 54 grid points, and wave parameters such as significant wave height, peak periods, vector mean wave direction, wind speed and direction, and frictional velocity were generated. Time series plots were provided and standard statistics were compiled in order to verify the model against buoy data from the area (see Table 3.1 – 3.3).

As shown, model results compare well with measured data. The model tends to over predict wave heights in water of depths of less than 100 m, which can be explained by error induced by shallow effects. However, a mean error of 0.4 m and RMSE in the range of 0.64 m to 0.86 m with correlation coefficients in the range of 0.82 to 0.86 were found over the 3 year period in the 3 regions (Grand Banks (GB), Scotian Shelf (SS), and Georges Bank (EB)). The peak period was predicted with a bias in the range of –0.31 s to 0.66 s and RMSE in the range of 2.07 s to 2.43 s over the 3 year period.

3.1.1 Verification of the 3–Year Hindcasts

With respect to the validation of hindcast integrated properties of the wave spectrum such as H_s and T_p, the errors shown are among the lowest reported in other hindcast studies of continuous series. For example, Table 3.1 indicates a scatter index in deep water model hindcasts of H_s in Canadian waters of about 30%. For only the stormy periods (Table 3.2) the scatter index is only slightly lower, and the rms differences and the correlation coefficients are basically the same as those found for the 3–year continuous period as a whole. Errors in the wind fields are an important, if not dominant, contributor to the hindcast wave errors since the same wave hindcast model has provided storm hindcasts with errors about a factor of 2 lower than indicated above when wind fields of the maximum achievable accuracy are used to drive the model. Such wind fields must be analyzed essentially by hand (e.g. Cardone and Callahan, 1992). It should be recalled that the 3–year hindcast was driven by a file of 6–hourly ”analysis” wind fields generated as part of a real–time analysis–forecast cycle operated by MPL/OWI as a joint venture during the three–year period. These fields therefore could not benefit from synoptic data available after real–time and the hand analysis kinematic procedures usually applied in storm hindcasts.

An additional, though small, error in the 3–year wave hindcasts has been identified by Juszko and Graham (1992), exhibited as a deficiency in low background swell components in the hindcast directional spectra. The two most likely sources of this error are again wind field errors and grid domain limitations. We surmise this from the experience of the LEWEX ’87 (Labrador Extreme Wave Experiment) program (Beal, 1991) in which 7 different wave hindcast models were applied to hindcast directional spectra for evaluation against directional wave spectra measured by several different systems deployed east of Newfoundland. The wave regime sampled during LEWEX happened to be swell dominated, and common difficulties exhibited by all models in tracking the swell were ultimately attributed to the difficulty in specifying accurate winds fields in the multiple distant sources of swell inferred from the directional wave measurements. Swells were identified from source zones in the far northern Labrador Sea, the northeastern Atlantic Ocean, the subtropical eastern North Atlantic Ocean, and the Sargasso Sea. These areas lie well outside the main North Atlantic shipping lanes, hence no marine data is available, so wind errors are larger there in both operational and hindcast wind fields. In the three–year hindcast some swell components are not resolved simply because some of these source zones are not included in the grid system used. The LEWEX experience suggests that precise specification of swell off the east coast of Canada in a model derived wave climate will require not only a wave model grid which covers essentially the whole of the North Atlantic Ocean but also wind fields of greater accuracy that can be specified from conventional historical meteorological data.

3.2 VERIFICATION OF STORM HINDCASTS

3.2.1 Selection of Verification Cases

The main objective of this section is to verify the output of the North west Atlantic version of the wave model by comparing storm predictions against measured data. In a previously completed study, carried out by MacLaren Plansearch and Oceanweather, Canadian Climate Centre, 1991) 68 storm events were hindcast in order to describe the extreme wave climate on the east coast of Canada. This section is meant to summarize previous work and provide additional model verification.

In the previous study, a verification of the ODGP wave model was performed by comparing the model results to buoy data from selected storms in the area. Sixty–eight storms were selected as the most severe events of a 32 year period from 1957 to 1988 in three areas off the east coast of Canada: the Grand Banks, the Scotian Shelf, and Georges Bank. Table 3.4 lists the 68 east coast storms. Of these 68 events, 10 storms were selected to verify the accuracy of the ODGP model. Time series analysis, energy spectra analysis, and standard statistics were used to determine the validity of the model output. In this study, an attempt was made to further quantify the accuracy of this model by extending the list of verification cases from the original number of 10 storms to the maximum number of storms for which model and buoy data exists. As opposed to the previous study, only events that occurred on the Grand Banks or on the Scotian Shelf were considered here.

A number of criteria had to be met in the selection of storms to be used for this additional validation. Firstly, the most severe storms which generated the highest wave heights were the target of this selection; it was also necessary to select storms of long duration (of at least a few days). A second criteria for storm selection was that adequate buoy data existed so that a comparison with the model results could be made. It was found that during some storm periods, especially those that occurred in the 60's and 70's, there was sparse data due to a lack of buoys in the study area. In other events, some buoys exhibited gaps in their data. Time series plots aided in determining whether a certain storm event met the above criteria.

As a result, a total of 16 storms were selected to verify the model on the Grand Banks (Table 3.5), and 20 storms to represent the Scotian Shelf area (Table 3.6). Buoy data were obtained from MEDS and were compared to model predictions at the nearest model grid point to the buoy location (see Figures 3.2 and 3.3 and Tables 3.7 and 3.8 for list of waverider buoys, location, names, etc.). In some instances, one storm event provided several verification opportunities due to the presence of more than one buoy, sometimes for both areas. As a result of this overlap, the storm populations selected provide 34 verification cases for the Grand Banks and 44 for the Scotian Shelf. Error statistics are presented in Tables 3.9–3.15.

3.2.2 Measured Buoy Data

The primary data sources used in the preparation of the wind fields (i.e. kinematic analysis) and validation of model predictions are:

1. meteorological and oceanographic (MET/OCEAN) buoys which provided wind and wave measurements; and

2. MEDS waverider buoys in relatively shallow waters of the east coast of Canada. These buoys provided only wave measurements.

The wind measurements from the MET/OCEAN buoys were used in the wind field analysis and in the evaluation of model wind prediction. The wave model verification results presented in the next section (Tables 3.9 – 3.15) were based only on MEDS waverider buoys data.

The following paragraphs provide a brief description of this data source.

Meteorological and Oceanographic Buoys

Buoy observations were available from two different sources. In Canadian waters, Environment Canada operates six 6m NOMAD buoys, offshore in deep water; along the eastern seaboard of the United States NOAA operates a series of buoys, both along the coast in relatively shallow water and offshore in deep water.

a. Canadian NOMAD Buoys

The Canadian NOMAD buoys measure and transmit data each hour via GOES. Parameters measured include wind direction and speed (dual wind monitors), barometric pressure (dual), air and water temperature, and significant and peak wave height, peak period and non–directional frequency spectra.

The following paragraphs provide more detail on the wind and wave measurements and processing.

Wind

The wind sensors are R.M. Young helicoid propeller and vane which sense the wind over two second intervals. The two wind sensors are mounted on the two arms of the rear mast. The first anemometer is located on the starboard side, at an elevation of 5.36 m; the second (backup) anemometer is located on the port side, at an elevation of 4.59 m.

For the Canadian east coast NOMAD buoys the wind measurements are taken over a ten–minute period beginning 5 minutes prior to the hour until 5 minutes past the hour. Successive 2–second samples taken over the 10–minute sampling interval are vector–averaged to provide the 10–minute mean wind speed and direction. This differs from present NDBC practice where the mean winds are scalar–averaged. Gilhousen (1987) showed that the underestimate of the scalar wind by vector averaging is about 7% for wind speeds greater than 8m/s; this difference may increase with higher wind speeds and wave heights. The highest running 8–second scalar mean gust is also recorded and transmitted in the GOES message.

Waves

The heave sensor is turned on for two minutes to allow it to stabilize before measurements begin. A collection of 256 heave magnitude samples is made at 1–second intervals, and a Fourier analysis is used to break up the data into spectral bands. This is repeated 8 times and the results are averaged. The bands are indicated in Table 2. This whole process takes about 35 minutes. The observing period for the wave sample on east coast NOMAD buoys is from 18 minutes after the preceding hour to 55 minutes after the preceding hour. This is followed immediately by the meteorological sample.

The significant and maximum wave height in tenths of metres and peak period in tenths of seconds computed from the sample is transmitted, followed by the 1–D wave spectral data.

b. NOAA Buoy Network

The NOAA buoys also transmit once per hour via GOES, values of wind speed and direction (dual anemometers), atmospheric pressure, air and water temperature, significant wave height, average and dominant wave period, and non–directional wave frequency spectra.

During the study period NOAA operated several different buoy hulls, with different payloads. The following paragraphs provide more detail on the NOAA wind and wave measurements and data processing.

Wind

The wind is measured at NOAA buoys by dual R.M. Young aerovane wind sensors. The wind speed is either the mean value from an 8 minute scalar average of instantaneous measurements sampled at a rate of 1 Hz, or an 8.5 minute vector average depending on the type of buoy. Wind directions for both payloads are vector averages. The anemometer heights vary between the different hull types, from 5 m on the 3 m discus buoys and NOMAD buoys, to 13.8 m for the Large Navigational Buoys.

In the analysis and verification, buoy wind measurements were adjusted to ”effective neutral” 20 m values as described in Cardone et al. (1980).

Waves

The wave measurement system on the NOAA buoys uses an accelerometer to record buoy heave motion. An NDBC onboard wave data analyzer computes the wave spectral data from the time series of buoy motion. Directional wave data, where available, are estimated from records of the buoy’s heave, pitch and roll motions. For details see Steele and Mettlach (1993).

3.2.3 Comparison of Storm Hindcasts and Measurements

The storm hindcast verification was made first in terms of standard time series comparisons of measured and hindcast H_s and T_p for each of 34 verification cases on the Grand Banks and 44 cases on the Scotian Shelf. For each ”case”, the peak hindcast sea state (H_s and the associated T_p) and the peak measured sea state were identified from these time–history comparisons for further statistical analysis. The time of occurrence of these respective peaks was allowed to differ, so long as the peaks appeared to occur in the same storm event. Table 3.9 gives the peak–peak comparisons selected for the Grand Banks cases and Table 3.10 gives the peak–peak comparisons for the Scotian Shelf cases. These tables also include the positive or negative lag, in hours, between the hindcast and measured peak H_s and the H_s difference. In these comparisons, the model grid point closest to the buoy was used, as shown in Figures 3.2 and 3.3.

These peak–peak differences are summarized in various ways. First, a general impression of the directional distribution of the measured storm peaks is gained from the polar plots shown in Figure 3.4 which display the measured winds (where available) associated with the peak sea states, and Figure 3.5 which shows the hindcast vector mean wave direction associated with the peak sea state. On the Grand Banks, clearly the preponderance of cases are for wind and wave approach directions between Northwest and Southwest. On the Scotian Shelf, northeasterly approach directions are also represented. In both areas there are very few cases of approach from the southeast which for both basins would be the direction from the deepest water. The directional distribution of the differences between hindcast and measured peak storm H_s is shown for each region in Figure 3.6. There is no clear stratification of the errors in H_s by direction except for a slight tendency for the largest differences to occur for southwesterly approach directions.

Peak–peak comparisons in terms of scatter plots of H_s and T_p are shown in Figure 3.7 for Grand Banks and Figure 3.8 for Scotian Shelf. Peak–peak statistics are given in Table 3.14. At GB the skill, expressed in terms of scatter index in H_s, of 15% is comparable to the skill found in the more limited (in terms of cases) validation phases of the previous Hibernia hindcast study (Cardone et al., 1989) and the east coast hindcast study (Swail et al., 1989, 1992). However, there is now seen to be a systematic positive bias in hindcast H_s at the higher sea states (H_s greater than about 10 m). The mean difference in H_s is +0.84m with associated T_p bias of +1.05 seconds.

A positive bias in hindcast peak H_s is also seen in the comparisons made for SS, shown in Figure 3.8 and Table 3.14. The mean difference in H_s is 0.88 m with T_p bias of 0.70 seconds. At SS however, the scatter is somewhat greater than seen in previous studies. Note however, that no attempt has been made in these comparisons to factor in the effect of water depth. Figure 3.9 and 3.10 show the distribution of the peak–peak differences in H_s by water depth in each region. At GB, all but one hindcast peak exceeds the measured peak at depths below 100 meters, while in deeper water the differences are divided about evenly between positive and negative differences. At SS there is also a correlation shown between the sign of the differences and the water depth with positive bias at shallow water sites. This suggests that the absence of shallow water physics in the version of ODGP used for these storm hindcasts is contributing to the hindcast error. The period statistics are probably also affected by neglect of shallow water.

Comparisons were also made for continuous ”analysis” periods within each case. The analysis period was typically a twenty–four hour period before and after the occurrence of the largest wave height. Comparison statistics for these analysis periods are given for each case and region in Tables 3.11 through, 3.13, with summary statistics given in Table 3.15. Scatter plots between hindcast and measured H_s and T_p are given in Figure 3.11 for analysis periods. These comparisons indicate the usual increase found in hindcast RMSE and scatter index for continuous series over peak–peak series. However, these also indicate that the positive bias in H_s and associated T_p is not confined just to the storm peaks but are a characteristic of the entire stormy periods as well. This is to be expected if neglect of shallow water processes in the wave model used is the dominant source of this bias.

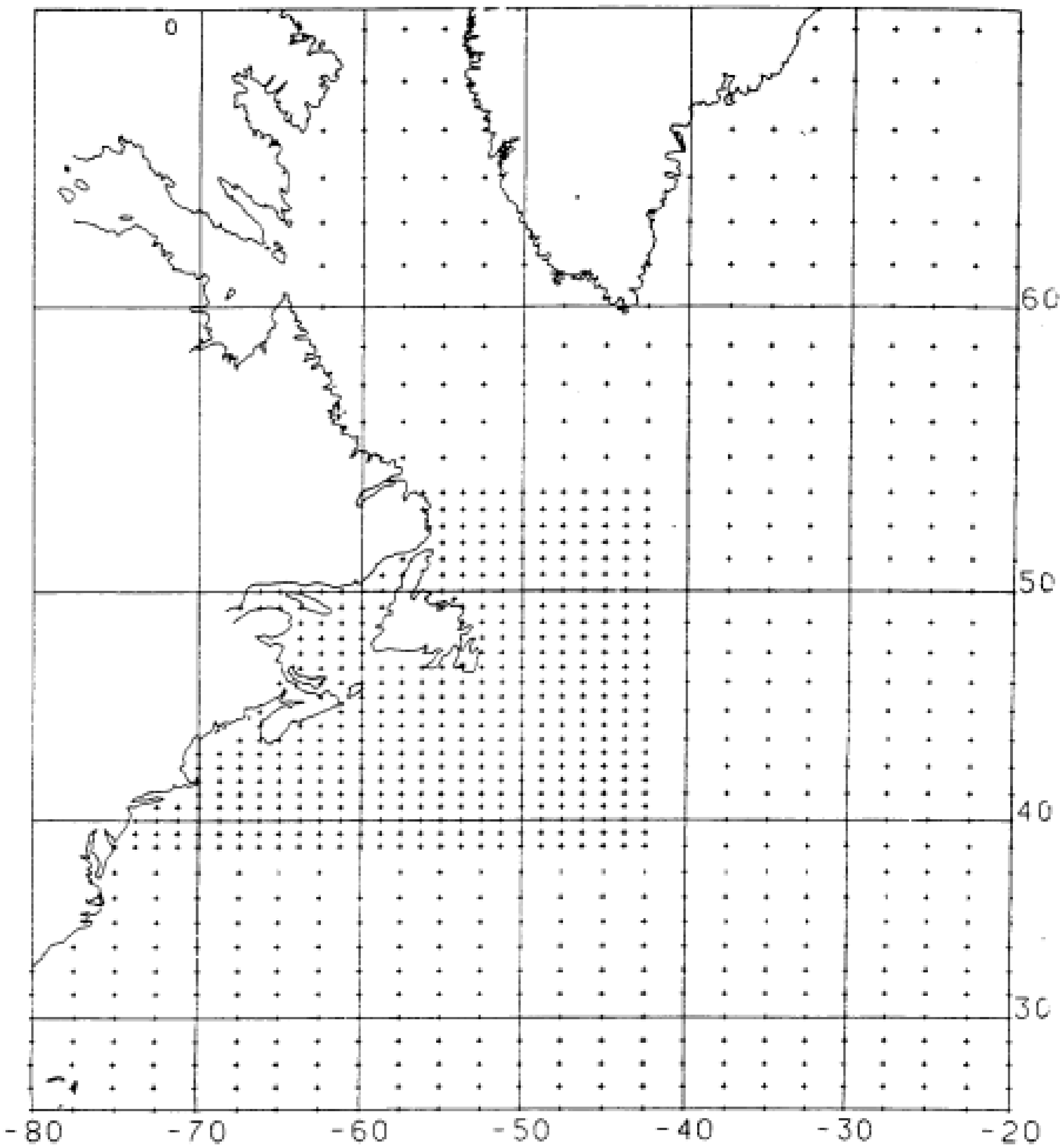

Figure 3.1 East Coast ODGP (NATWAV) Grid

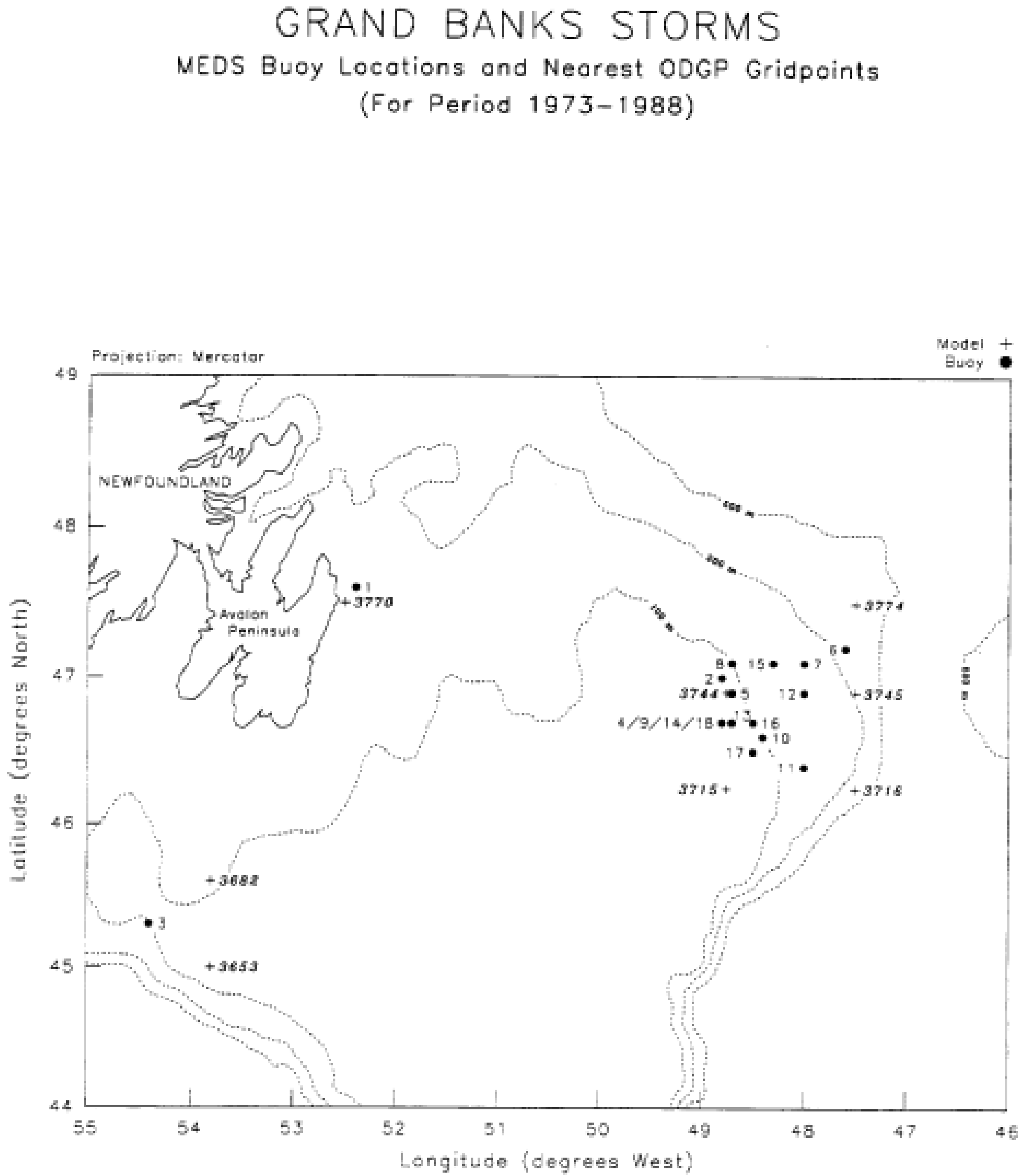

Figure 3.2 Grand Banks Map Showing Buoy Locations and the Nearest ODGP Grid Points

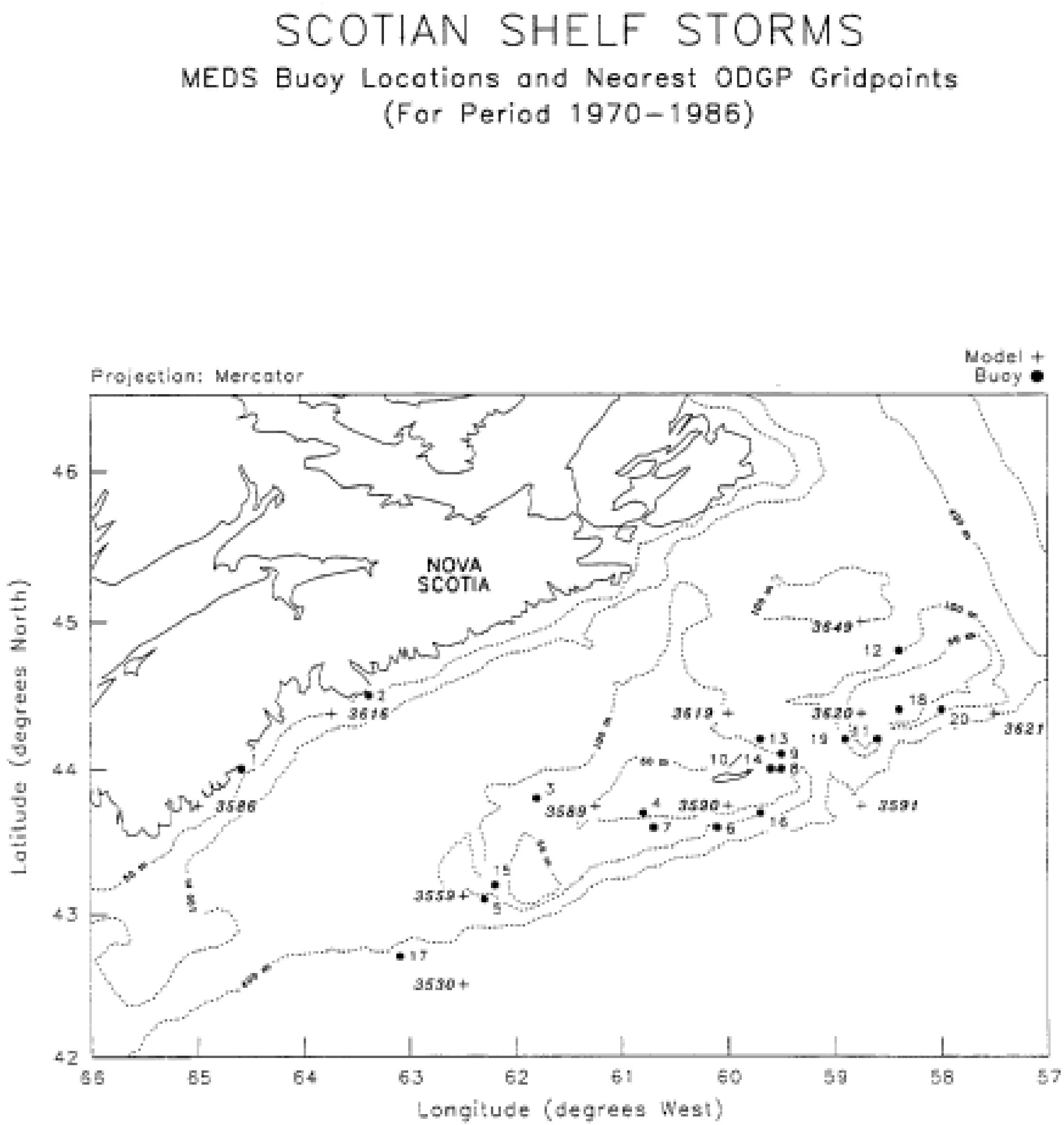

Figure 3.3 Scotian Shelf Map Showing Buoys Location and the Nearest ODGP Grid Points

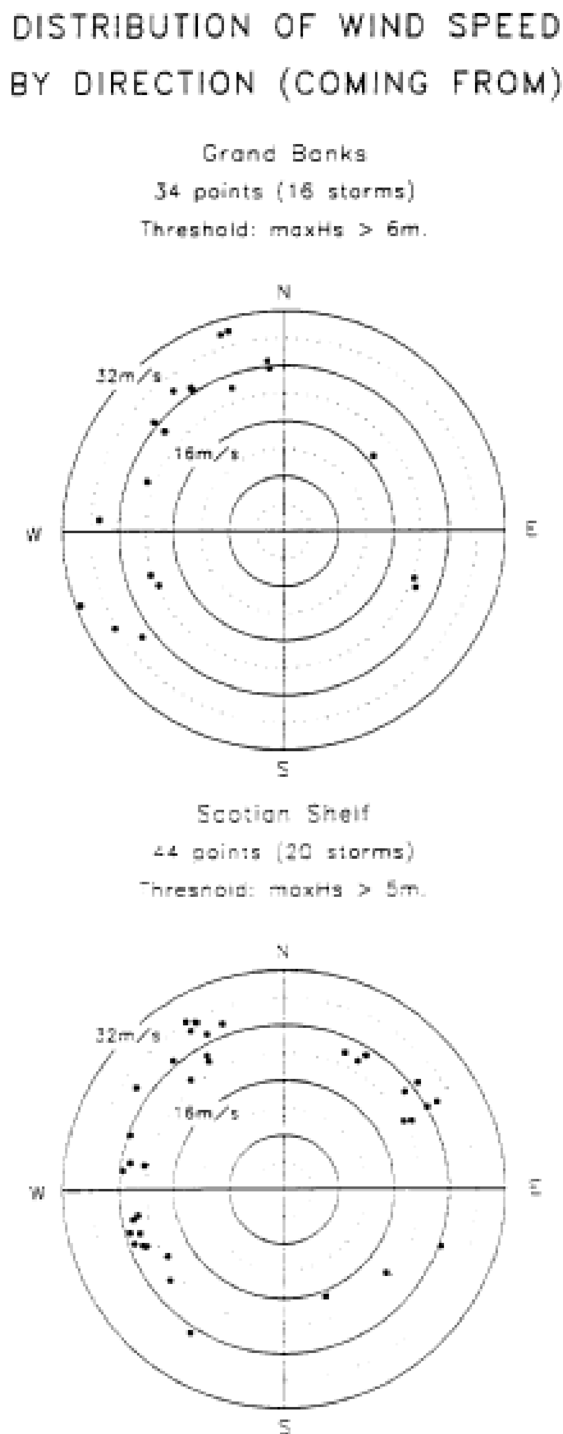

Figure 3.4 Distribution of Wind Speed by Direction for East Coast Storms

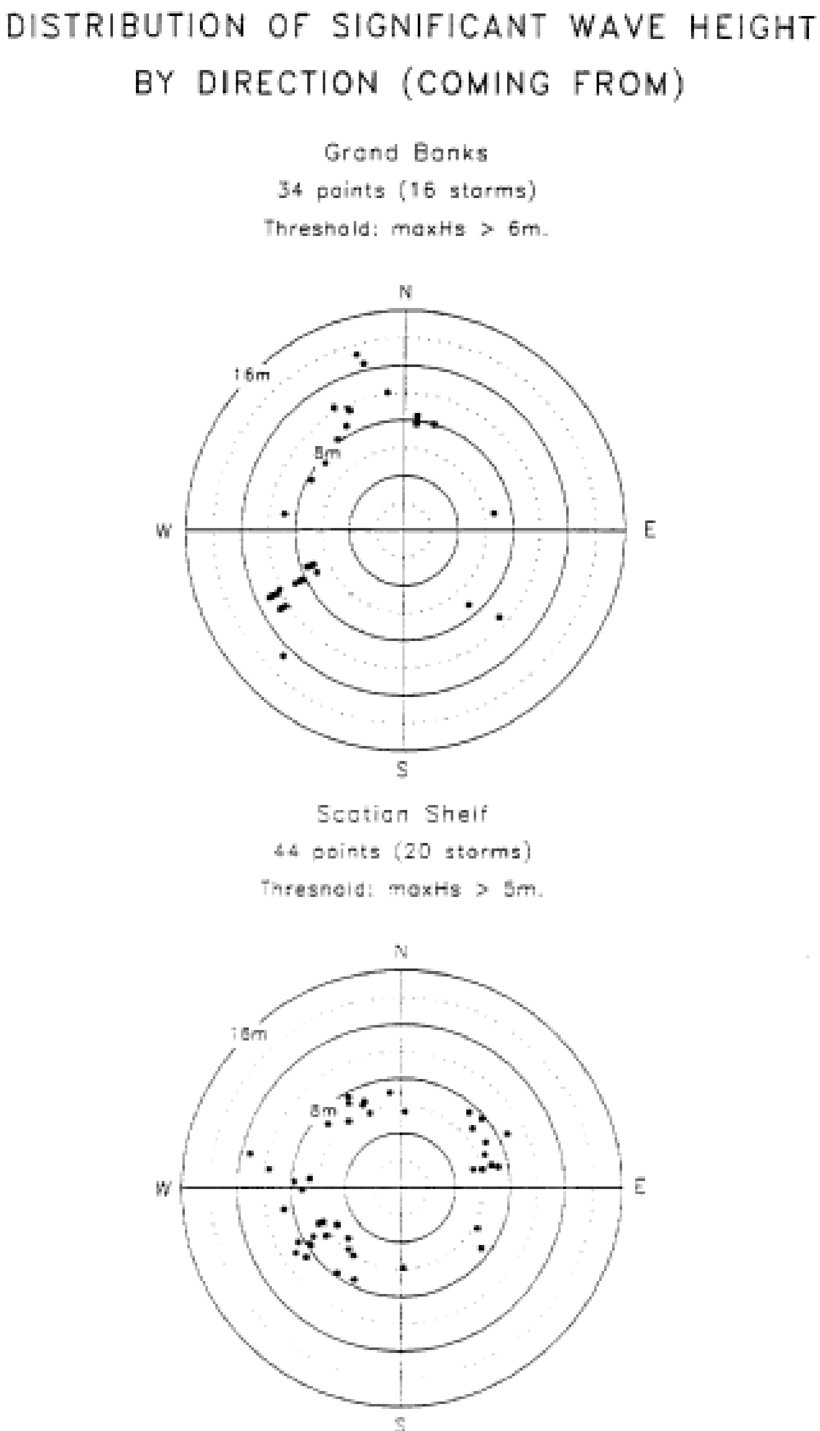

Figure 3.5 East Coast Significant Wave Height Directional Distribution

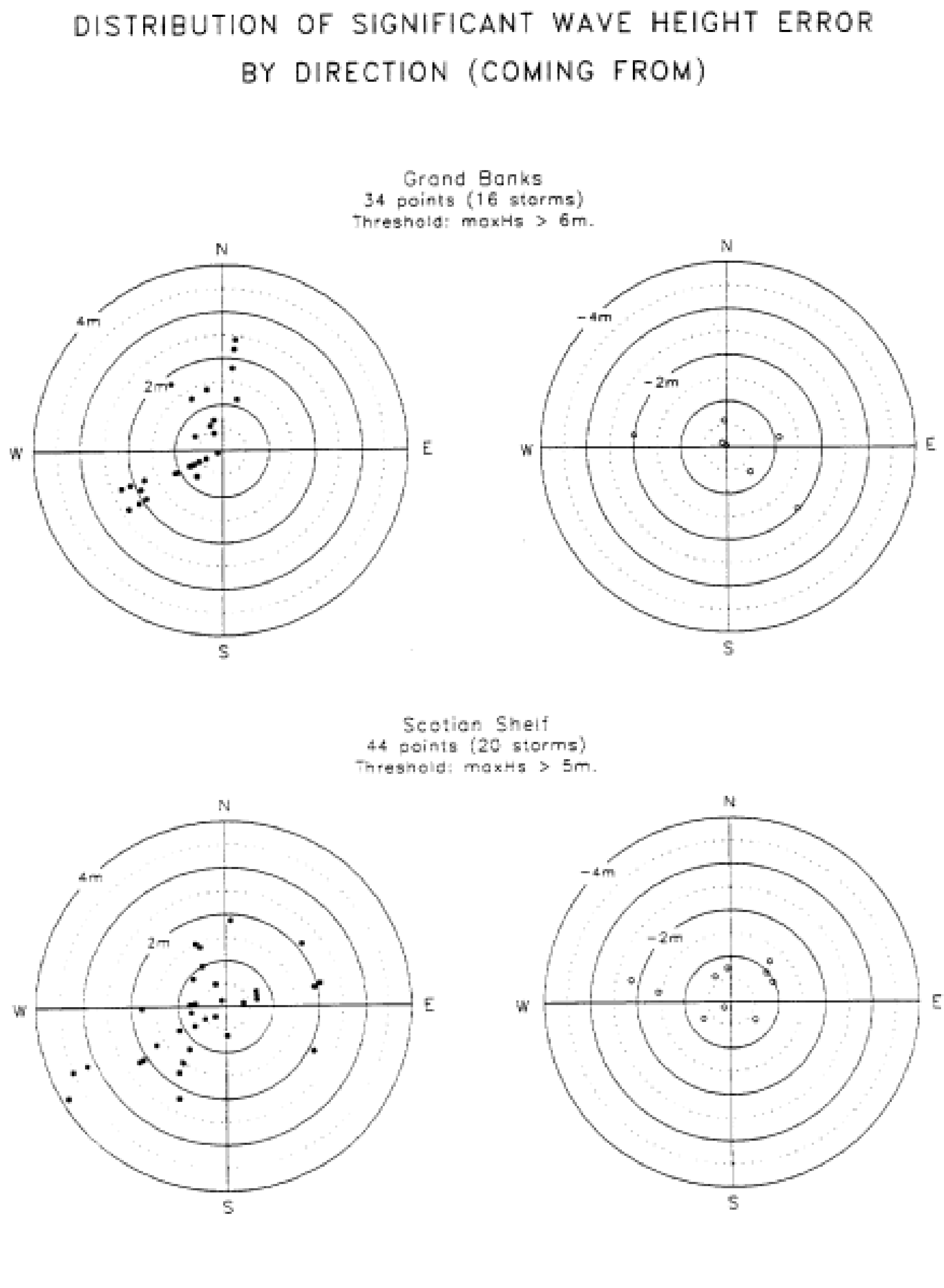

Figure 3.6 East Coast Significant Wave Height Error Directional Distribution

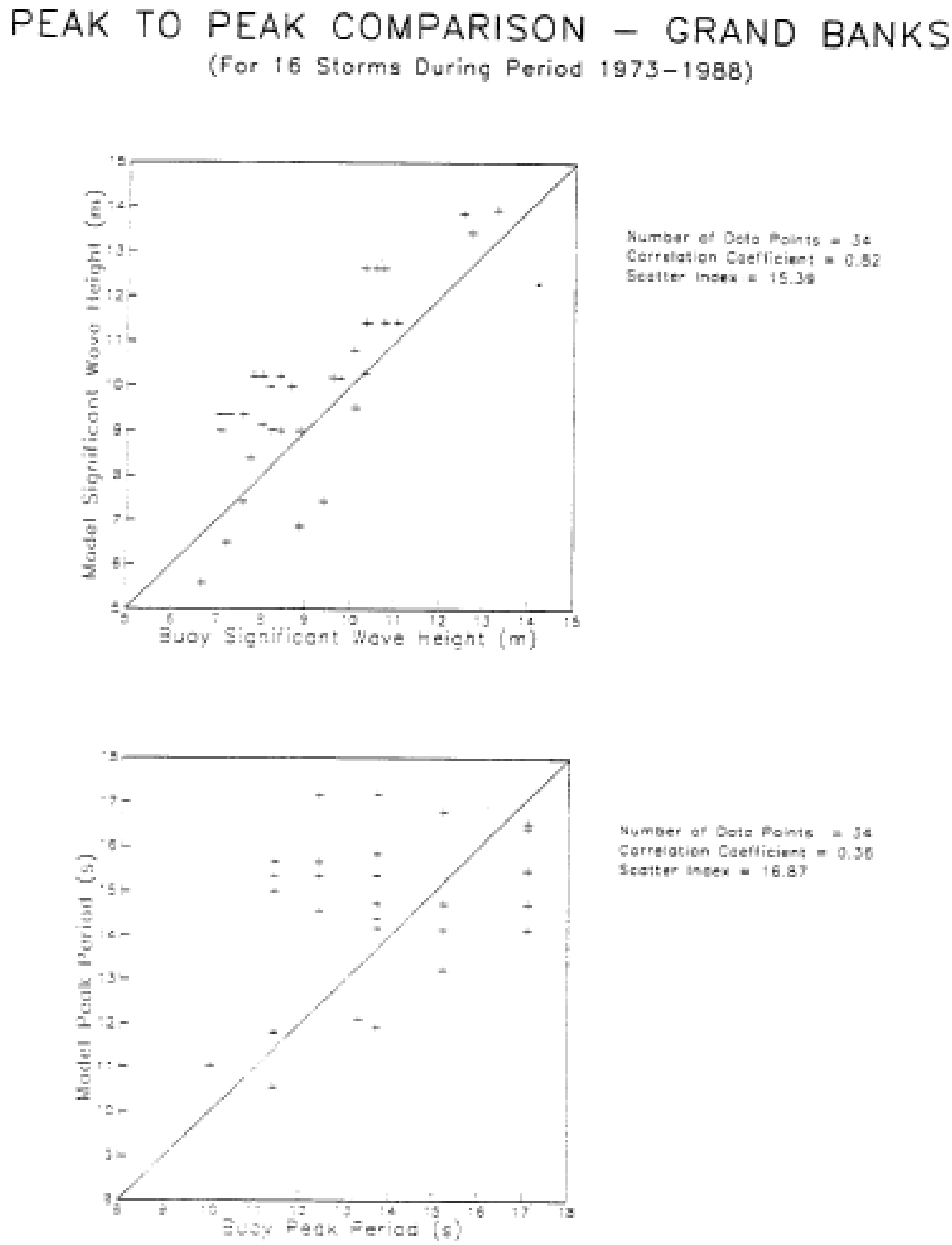

Figure 3.7 Grand Banks: Storm Peak to Peak Scattergram (H_s, T_p)

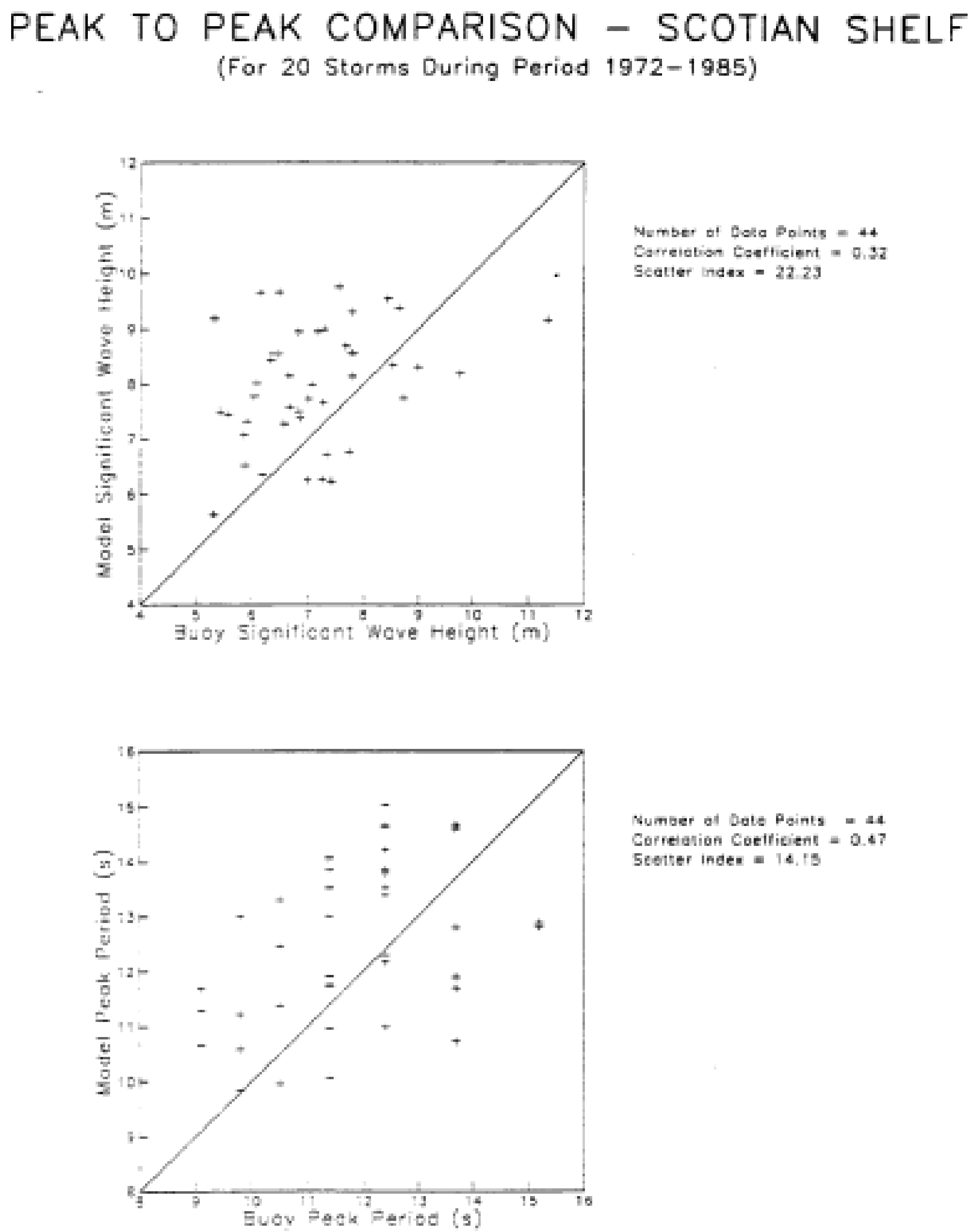

Figure 3.8 Scotian Shelf: Storm Peak to Peak Scattergram (H_s, T_p)

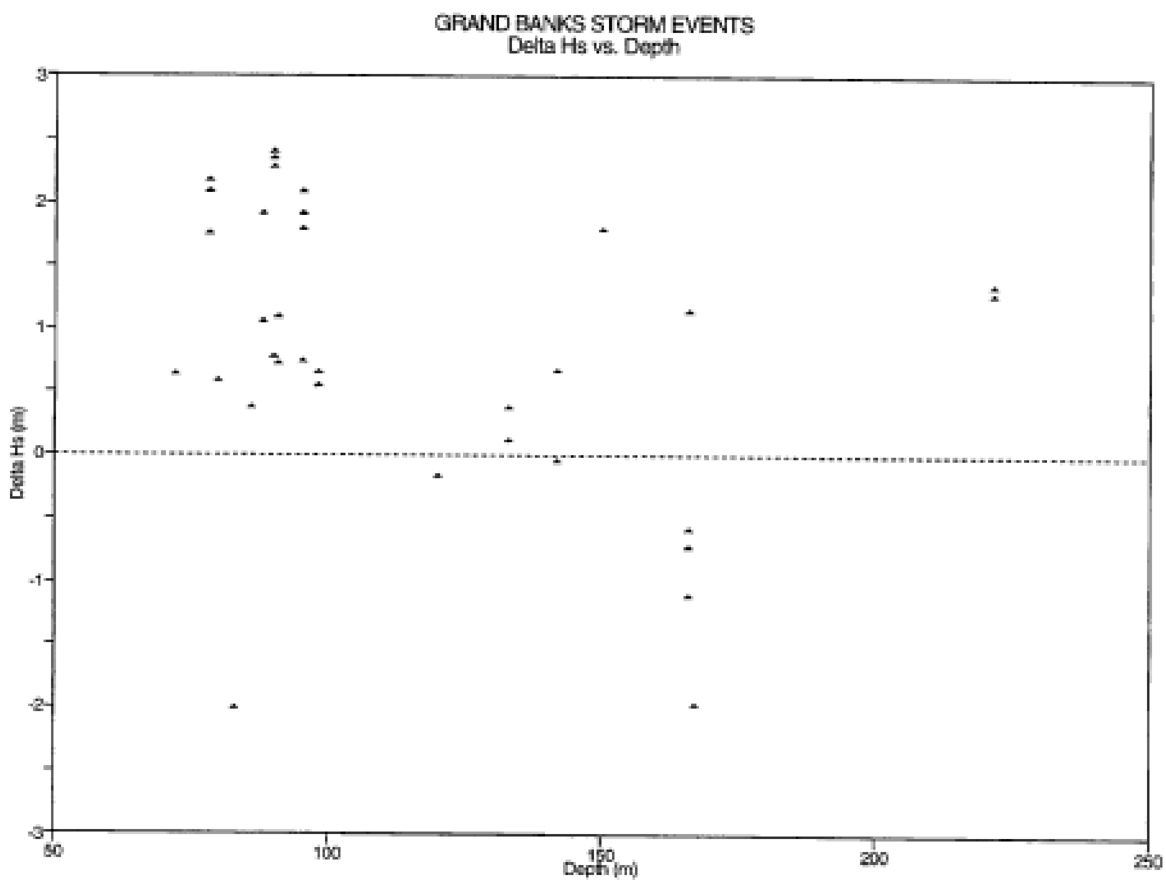

Note: ΔH_S (Delta H_S)= Hindcast – observed heights

Figure 3.9 Grand Bank Storms: Peak – Peak Differences (Bias) in H_S versus Water Depth

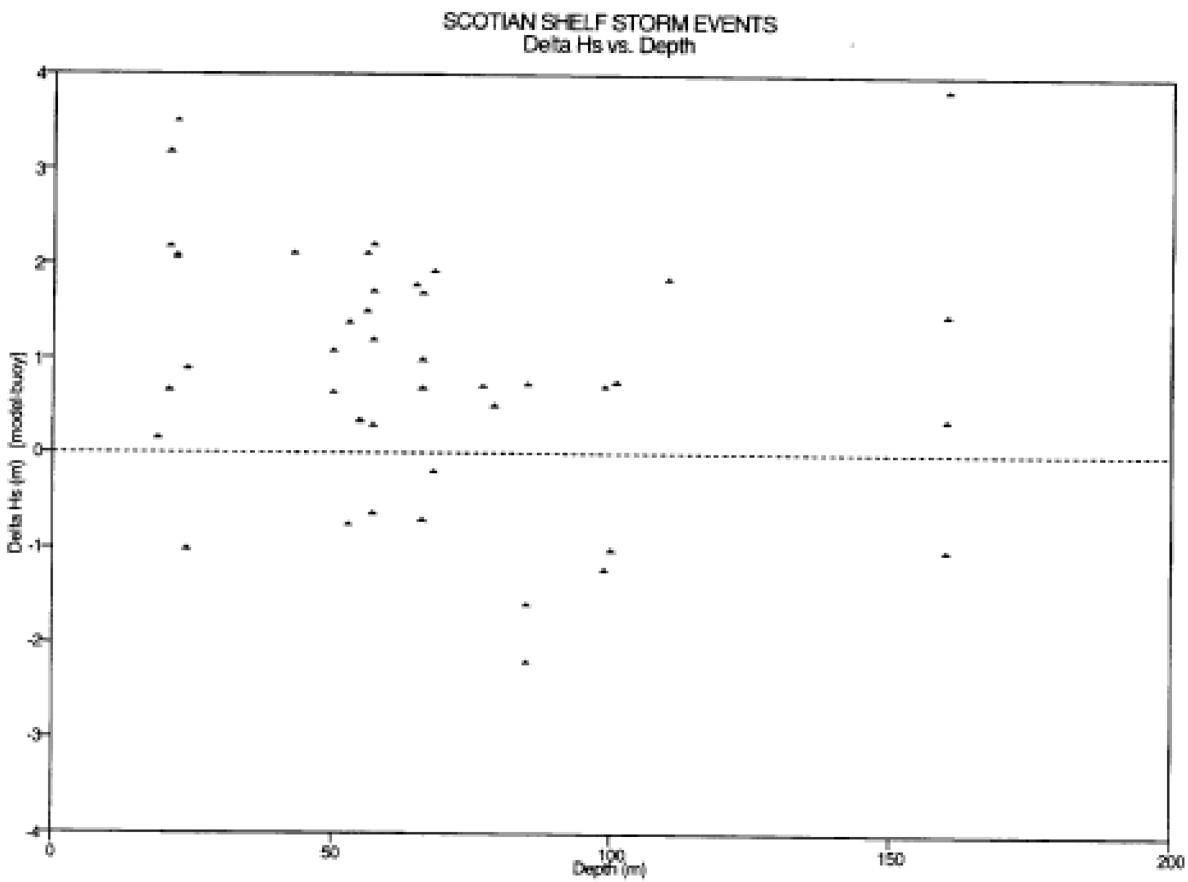

ΔH_S= Hindcast = Observed height

Figure 3.10 Scotian Shelf Storms: Peak to Peak Differences (Bias) in H_S versus Water Depth

STORM COMPARISON GRAND BANKS

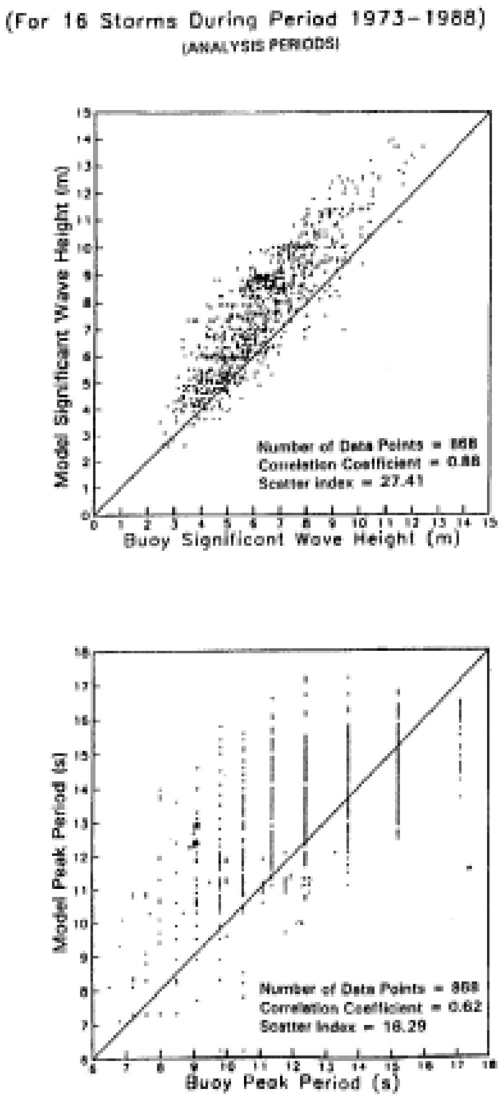

STORM COMPARISON SCOTIAN SHELF

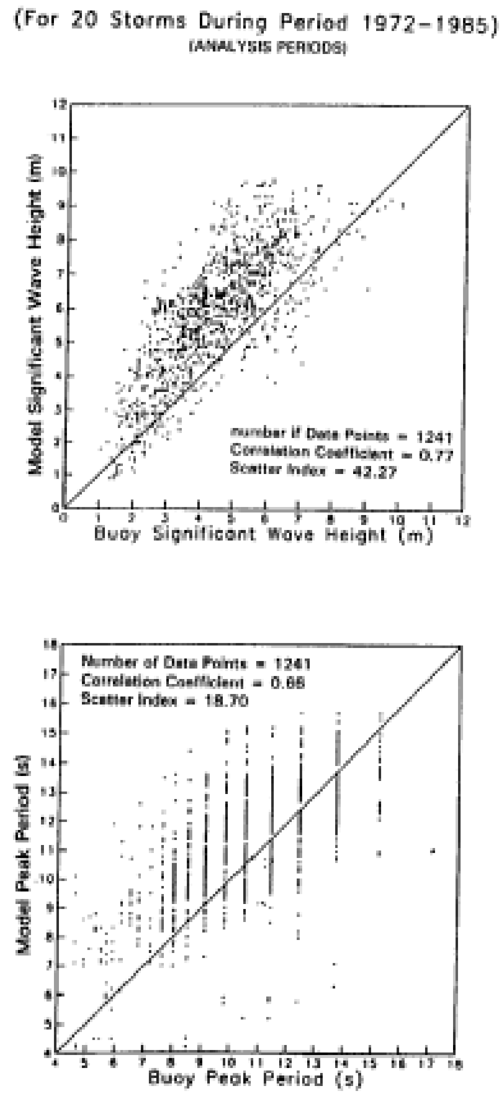

Figure 3.11 Storm Period Scattergram (Hs, Tp) for the Grand Banks and Scotian Shelf

Table 3.1 Three Year Overall Statistics for East Coast.

VAR	AREA	POINTS	AVE. OBS.	STD. DEV.	AVE. MODEL	STD. DEV.	BIAS	RMSE	SCATTER INDEX	CORR. COEF.
Hs (m)	EB	3563	1.72	1.03	1.81	1.07	0.08	0.64	37.24	0.82
	SS	2402	2.33	1.31	2.49	1.32	0.16	0.70	30.13	0.87
	GB	3025	2.75	1.39	3.08	1.52	0.33	0.86	31.21	0.86
Tp (s)	EB	3499	6.42	1.91	7.08	2.03	0.66	2.43	37.80	0.30
	SS	2402	8.47	2.10	8.16	1.97	–0.31	2.07	24.46	0.49
	GB	2913	9.83	2.33	9.24	1.86	–0.59	2.37	24.14	0.42

Table 3.2 Three Year Storm Statistics for East Coast.

VAR	AREA	POINTS	AVE. OBS.	STD. DEV.	AVE. MODEL	STD. DEV.	BIAS	RMSE	SCATTER INDEX	CORR. COEF.
Hs (m)	EB	230	2.80	1.58	2.78	1.54	–0.02	0.84	29.98	0.86
	SS	186	3.43	1.57	3.68	1.67	0.25	0.82	23.87	0.89
	GB	229	4.12	1.65	4.55	1.86	0.43	1.08	26.21	0.85
Tp (s)	EB	227	7.44	2.72	8.48	2.27	1.04	3.10	41.64	0.33
	SS	186	9.52	2.27	9.45	1.73	–0.07	1.96	20.55	0.55
	GB	196	11.16	1.94	10.84	1.82	–0.32	2.02	18.07	0.44

Table 3.3 Three Year Shallow Water Statistics for East Coast.

VAR	AREA	POINTS	AVE. OBS.	STD. DEV.	AVE. MODEL	STD. DEV.	BIAS	RMSE	SCATTER INDEX	CORR. COEF.
Hs (m)	EB	129	1.75	1.03	1.48	0.92	–0.28	0.65	37.31	0.82
	SS	186	1.78	1.13	1.55	0.98	–0.23	0.62	34.70	0.86
	GB	184	1.40	0.96	1.32	0.89	–0.08	0.48	34.57	0.87
	ALL	499	1.63	1.06	1.44	0.94	–0.19	0.58	35.67	0.85
Tp (s)	EB	129	9.02	2.41	8.22	2.45	–0.80	2.66	29.48	0.46
	SS	186	9.13	2.51	8.09	2.22	–1.04	2.40	26.27	0.59
	GB	184	9.43	2.38	8.11	2.43	–1.31	2.91	30.91	0.42
	ALL	499	9.21	2.44	8.13	2.36	–1.08	2.67	28.93	0.49

Table 3.4 East Coast 68 Storm List

Storm #	Storm Period Start – End	GB	SS	EB
1	59020612–59021012*			
2	60010900–60011300*			
3	61011912–61012312*			
4	61121412–61121912*			
5	62030600–62030912	*	*	
6	62111412–62111912		*	
7	62123000–63010218	*	*	
8	63111400–63111818*			
9	63121900–63122118	*	*	
10	64011212–64011718*			
11	64020800–64021018*			
12	64031512–64031912*			
13	64113000–64120312		*	
14	65012112–65012512*			
15	66010812–66011212*			
16	66012612–66013012	*	*	
17	66021318–66021812*			
18	67022100–67022500*	*	*	
19	67042700–67050200	*		
20	68010418–68010800*			
21	69020900–69021218	*	*	
22	69122600–69123012	*	*	
23	70012000–70012400	*		
24	70122600–70123000	*		
25	71011518–71011918*			
26	71030300–71030700		*	
27	72021812–72022200	*		
28	72032612–72033100	*		
29	72121512–72121912		*	
30	73032112–73032500		*	
31	73102600–73102912*			
32	73110100–73110512		*	
33	74010200–74010700*			
34	74020400–74020800	*		
35	74201612–74022000	*		
36	74031012–74031412*			
37	76031600–76032000*	*	*	
38	76110512–76111000	*	*	
39	76111812–76112300	*		
40	77011900–77012300*			
41	77020512–77021012*			
42	78010812–78011212		*	
43	78030100–78030500*			
44	79020300–79020712		*	
45	80011412–80011812		*	
46	80020612–80021012	*		
47	80021000–80021400*			
48	80111812–80112212*			
49	80112106–80112418	*	*	
50	81030500–81031000	*		
51	81031512–81032000	*	*	
52	81120412–81120812		*	
53	81121500–81121912	*	*	
54	81122912–82010300*			
55	82011300–82011900*	*		
56	82021200–82021600*	*		
57	83021000–83021500	*		
58	83021506–83021900*			
59	83102400–83102800	*	*	
60	83112400–83113012*	*		
61	83121900–83122400*			
62	84012912–84020312	*		
63	84032812–84040112	*	*	
64	85010400–85010900*	*	*	
65	85012512–85013012*			
66	85121512–85122112*			
67	86010212–86010612*			
68	88030700–88031012	*		

G.B. Mainly Grand Banks Storm
S.S. Mainly Scotian Shelf Storm
E.B. Mainly Georges Bank (Eastern Seaboard) Storm

Table 3.5 Grand Banks Verification Storms

STORM	Total Storm Duration	Analysis Duration
31	73102600–73102912	73102712–73102912
33	74010200–74010700	74010300–74010500
39	76111812–76112300	76111912–76112100
47	80021006–80021400	80021200–80021300
48	80111812–80112212	80112000–80112200
53	81121500–81121912	81121700–81121912
54	81122912–82010300	81123012–82010212
55	82011300–82011900	82011512–82011900
56	82021200–82021600	82021412–82021600
59	83102400–83102800	83102600–83102700
60	83112400–83113012	83112800–83113006
61	83121900–83122400	83122200–83122400
63	84032812–84040112	84032900–84033012
64	85010400–85010900	85010612–85010900
65	85012512–85013012	85012712–85013000
68	88030700–88031012	88030900–88031012

Table 3.6 Scotian Shelf Verification Storms

Storm	Total Storm Duration	Analysis Duration
27	72021812–72022200	72021912–72022100
34	74020400–74020800	74020500–74020700
36	74031012–74031412	74031100–74031312
41	77020512–77021012	77020606–77020712
42	78010812–78011212	78010912–78011200
48	80111812–80112212	80111900–80112100
49	80112106–80112418	80112118–80112412
50	81030500–81031000	81030612–81031000
51	81031512–81032000	81031712–81031912
52	81120412–81120812	81120600–81120812
53	81121500–81121912	81121600–81121812
55	82011300–82011900	82011500–82011900
56	82021200–82021600	82021400–82021512
57	83021000–83021500	83021212–83021412
59	83102400–83102800	83102500–83102700
60	83112400–83113012	83112600–83112900
61	83121900–83122400	83122012–83122300
62	84012912–84020312	84013112–84020212
63	84032812–84040112	84033000–84040100
64	85010400–85010900	85010512–85010812

Table 3.7 Grand Banks Buoy Codes and Positions

NUM	BUOY	NAME	TYPE	LAT	LONG	NEAREST GRID POINT	DEPTH
1	MEDS016	TORBAY	WR	47.6 N	52.4 W	3770	167 m
2	MEDS090	SEDCO J	WR	47.0 N	48.8 W	3744	91 m
3	MEDS091	SEDCO H	WR	45.3 N	54.4 W	3682	120 m
4	MEDS133	SEDCO 709	WR	46.7 N	48.8 W	3744	72 m
5	MEDS134	SEDCO 706	WR	46.9 N	48.7 W	3744	90 m
6	MEDS134	SEDCO 706	WR	47.2 N	47.6 W	3774	222 m
7	MEDS140	ZAPATA UGLAND	WR	47.1 N	48.0 W	3745	150 m
8	MEDS140	ZAPATA UGLAND	WR	47.1 N	48.7 W	3744	95 m
9	MEDS156	OCEAN RANGER	WR	46.7 N	48.8 W	3744	78 m
10	MEDS166	BOWDRILL I	WR	46.6 N	48.4 W	3744	98 m
11	MEDS167	VINLAND	WR	46.4 N	48.0 W	3716	90 m
12	MEDS168	JOHN SHAW	WR	46.9 N	48.0 W	3745	142 m
13	MEDS168	JOHN SHAW	WR	46.7 N	48.7 W	3744	88 m
14	MEDS169	WEST VENTURE	WR	46.7 N	48.8 W	3744	80 m
15	MEDS171	BOWDRILL II	WR	47.1 N	48.3 W	3744	133 m
16	MEDS172	BOWDRILL III	WR	46.7 N	48.5 W	3744	91 m
17	MEDS185	SEDCO 710	WR	46.5 N	48.5 W	3715	86 m
18	MEDS249	HIBERNIA (ESRF)	WC	46.7 N	48.8 W	3744	83 m

WR = Waverider Buoy
WC = WAVEC Buoy

Table 3.8 Scotian Shelf Buoy Codes and Positions

NUM	BUOY	NAME	TYPE	LAT	LONG	NEAREST GRID POINT	DEPTH
1	MEDS031	WESTERN HEAD	WR	44.0 N	64.6 W	3586	43 m
2	MEDS037	OSBORNE HEAD	WR	44.5 N	63.4 W	3616	57 m
3	MEDS091	SEDCO H	WR	43.8 N	61.8 W	3589	79 m
4	MEDS091	SEDCO H	WR	43.7 N	60.8 W	3589	53 m
5	MEDS091	SEDCO H	WR	43.1 N	62.3 W	3559	110 m
6	MEDS133	SEDCO 709	WR	43.6 N	60.1 W	3590	77 m
	MEDS133	SEDCO 709	WR	43.6 N	60.1 W	3589	85 m
7	MEDS133	SEDCO 709	WR	43.6 N	60.7 W	3589	68 m
8	MEDS142	ROWAN JUNEAU	WR	44.0 N	59.5 W	3590	24 m
	MEDS142	ROWAN JUNEAU	WR	43.9 N	59.5 W	3590	56 m
	MEDS142	ROWAN JUNEAU	WR	43.9 N	59.5 W	3590	50 m
	MEDS142	ROWAN JUNEAU	WR	44.0 N	59.6 W	3590	19 m
9	MEDS165	ZAPATA SCOTIAN	WR	44.1 N	59.5 W	3619	53 m
10	MEDS165	ZAPATA SCOTIAN	WR	44.0 N	59.6 W	3590	21 m
11	MEDS166	BOWDRILL I	WR	44.2 N	58.6 W	3620	85 m
12	MEDS167	VINLAND	WR	44.8 N	58.4 W	3649	100 m
13	MEDS167	VINLAND	WR	44.2 N	59.7 W	3619	160 m
14	MEDS170	SABLE ISLAND	WR	44.0 N	59.6 W	3590	22 m
15	MEDS171	BOWDRILL II	WR	43.2 N	62.2 W	3559	99 m
16	MEDS171	BOWDRILL II	WR	43.7 N	59.7 W	3590	101 m
17	MEDS185	SEDCO 710	WR	42.7 N	63.1 W	3530	1310 m
18	MEDS189	GLOMAR LABRADOR I	WR	44.4 N	58.4 W	3620	66 m
19	MEDS189	GLOMAR LABRADOR I	WR	44.2 N	58.9 W	3620	65 m
20	MEDS210	SOUTH GRIFFIN	WR	44.4 N	58.0 W	3621	55 m

WR = Waverider Buoy

Table 3.9 **Peak to Peak Comparison: GRAND BANKS**

Δ=Model–Buoy (Peak)

Storm	Date (Buoy)	Buoy	Depth (m)	Hs (m)	Tp (s)	Date (Model)	Grid	Hs (m)	Tp (s)	Δ
31	731028–12:00	2	91	10.06	11.40	73102814	3744	10.80	15.01	
33	740104–03:40	3	120	7.57	11.40	74010406	3682	7.42	11.82	
39	761120–03:30	1	167	9.40	13.70	76111922	3770	7.43	11.91	
47	800212–11:00	4	72	7.73	11.40	80021212	3744	8.38	11.78	
48	801121–00:00	7	150	8.17	15.20	80112100	3745	9.97	13.23	
53	811218–06:00	5	90	7.06	12.40	81121802	3744	9.35	15.65	
53	811218–13:48	8	95	7.26	11.40	81121802	3744	9.35	15.65	
53	811218–02:13	9	78	7.58	12.40	81121802	3744	9.35	15.65	
54	820101–18:00	1	166	8.00	17.10	82010104	3770	9.15	14.14	
54	820101–22:33	5	90	7.79	15.20	82010118	3744	10.20	14.72	
54	820101–05:00	8	95	8.41	13.70	82010118	3744	10.20	14.72	
54	820101–17:00	9	78	8.01	17.10	82010118	3744	10.20	14.72	
55	820116–13:08	5	90	10.29	13.70	82011616	3744	12.64	17.18	
55	820116–17:00	8	95	10.72	12.40	82011616	3744	12.64	17.18	
55	820116–18:27	9	78	10.54	13.70	82011616	3744	12.64	17.18	
56	820214–23:13	8	95	12.69	15.20	82021500	3744	13.45	16.80	
59	831026–17:06	1	166	7.21	11.40	83102610	3770	6.50	10.54	

Table 3.9 (con't) Peak to Peak Comparison: GRAND BANKS

Δ=Model–Buoy (Peak)

Storm	Date (Buoy)	Buoy	Depth (m)	Hs (m)	Tp (s)	Date (Model)	Grid	Hs (m)	Tp (s)	Δ
60	831129–10:00	6	222	8.68	15.20	83112908	3774	9.98	14.14	
60	831129–08:20	12	142	10.31	13.70	83112908	3745	10.28	14.19	
60	831129–03:51	14	80	9.58	12.40	83112908	3744	10.18	14.57	
60	831129–08:36	17	86	9.76	13.70	83112908	3715	10.15	14.39	
61	831222–16:05	1	166	10.10	17.10	83122218	3770	9.52	15.47	
61	831222–19:05	6	222	12.50	17.10	83122220	3774	13.86	16.43	
61	831222–22:59	12	142	13.26	17.10	83122220	3745	13.95	16.54	
63	840329–14:22	18	83	8.86	10.00	84032912	3744	6.85	11.04	
64	850106–17:09	10	98	8.43	11.40	85010704	3744	8.99	15.34	
64	850106–17:47	11	90	8.22	13.70	85010708	3716	9.01	15.84	
64	850108–01:03	13	88	7.07	13.70	85010704	3744	8.99	15.34	
64	850106–18:00	15	133	8.87	12.40	85010704	3744	8.99	15.34	
65	850128–21:21	10	98	10.75	13.70	85012900	3744	11.42	15.36	
65	850129–00:19	13	88	10.36	13.70	85012900	3744	11.42	15.36	
65	850129–03:34	15	133	11.03	13.70	85012900	3744	11.42	15.36	
65	850129–00:07	16	91	10.32	13.70	85012900	3744	11.42	15.36	
68	880309–15:50	1	166	6.69	13.30	88030912	3770	5.59	12.11	

Table 3.10 Peak to Peak Comparison: SCOTIAN SHELF

Δ= Model–Buoy (Peak)

Storm	Date (Buoy)	Buoy	Depth (m)	Hs (m)	Tp (s)	Date (Model)	Grid	Hs (m)	Tp (s)	Δ
27	720219–23:00	1	43	6.33	12.40	72022002	3586	8.44	12.18	
34	740205–09:00	3	79	6.85	9.80	74020600	3589	7.38	10.59	
36	740311–06:00	4	53	5.91	9.10	74031112	3589	7.31	10.66	
41	770206–09:00	5	110	5.57	9.10	77020614	3559	7.44	11.30	
42	780110–12:00	2	57	7.55	13.70	78011008	3616	9.76	14.68	
48	801119–17:00	8	24	7.07	9.80	80111920	3590	7.98	11.22	
49	801123–08:00	8	24	7.74	12.40	80112312	3590	6.76	11.00	
50	810307–12:00	8	56	6.82	11.40	81030714	3590	8.95	13.85	
51	810317–21:00	2	57	5.86	13.70	81031802	3616	7.07	12.80	
51	810318–03:50	8	56	7.79	13.70	81031802	3590	9.31	14.59	
52	811206–20:00	2	57	7.34	13.70	81120622	3616	6.71	11.89	
52	811206–21:00	8	50	5.87	15.20	81120708	3590	6.51	12.80	
53	811217–02:00	2	57	6.04	12.40	81121700	3616	7.78	14.23	
53	811217–12:00	8	50	8.44	12.40	81121708	3590	9.55	14.64	
55	820115–22:44	11	85	11.35	15.20	82011612	3620	9.17	12.88	
56	820214–12:50	11	85	9.76	11.40	82021416	3620	8.19	10.97	
57	830213–01:13	8	19	6.19	11.40	83021310	3590	6.35	10.07	
57	830213–10:03	9	53	6.99	10.50	83021308	3619	6.25	9.96	
57	830213–09:40	12	100	7.26	9.80	83021310	3649	6.27	9.84	
59	831025–11:54	6	77	7.01	9.10	83102516	3590	7.73	11.69	
59	831025–20:54	13	160	8.72	13.70	83102516	3619	7.74	11.70	
59	831025–22:58	15	99	7.42	13.70	83102514	3559	6.22	10.73	

Table 3.10 (con't) Peak to Peak Comparison: SCOTIAN SHELF

Δ= Model–Buoy (Peak)

Storm	Date (Buoy)	Buoy	Depth (m)	Hs (m)	Tp (s)	Date (Model)	Grid	Hs (m)	Tp (s)	Δ
60	831126–15:11	10	21	6.47	13.70	83112616	3590	9.66	14.64	
60	831126–13:45	13	160	5.33	12.40	83112616	3619	9.19	14.66	
60	831126–19:04	14	22	6.14	13.70	83112616	3590	9.66	14.64	
60	831126–09:40	15	99	8.64	11.40	83112616	3559	9.38	14.07	
60	831127–03:10	18	66	7.30	12.40	83112618	3620	8.99	15.03	
61	831221–18:13	13	160	6.65	9.80	83122118	3619	8.15	13.00	
61	831221–15:59	18	66	7.68	10.50	83122120	3620	8.69	13.30	
62	840201–06:00	2	57	5.32	12.40	84020106	3616	5.63	12.30	
62	840201–06:22	7	68	8.53	12.40	84020108	3589	8.34	13.39	
62	840201–09:14	10	21	6.37	11.40	84020110	3590	8.55	13.53	
62	840201–09:54	14	22	6.46	12.40	84020110	3590	8.55	13.53	
62	840201–09:54	16	101	7.78	12.40	84020110	3590	8.55	13.53	
62	840201–12:30	18	66	8.99	12.40	84020112	3620	8.31	13.80	
62	840201–11:49	20	55	7.79	12.40	84020114	3621	8.14	13.86	
63	840331–03:22	7	68	6.08	11.40	84033012	3589	8.01	11.91	
63	840330–13:46	10	21	6.82	11.40	84033014	3590	7.50	11.76	
63	840330–15:41	13	160	7.28	10.50	84033012	3619	7.66	11.38	
63	840330–13:06	14	22	5.43	11.40	84033014	3590	7.50	11.76	
63	840331–02:19	18	66	6.57	11.40	84033020	3620	7.27	11.74	
64	850106–18:17	6	85	7.81	10.50	85010620	3590	8.56	12.46	
64	850105–22:18	17	1310	6.67	11.40	85010618	3530	7.58	11.92	
64	850107–09:00	19	65	7.18	11.40	85010700	3620	8.96	13.00	

Table 3.11 H_S Statistics for Grand Banks Storms : Analysis Periods

STORM	BUOY	POINTS	AVE. OBS.	STD. DEV.	AVE. MODEL	STD. DEV.	BIAS (m)	RMSE (m)	SCATTER INDEX	CORR. COEFF.
31	2	24	6.18	1.94	7.54	2.21	1.35	1.51	24.39	0.95
33	3	16	5.00	1.10	6.44	1.01	1.44	1.62	32.51	0.74
39	1	11	6.29	1.70	6.41	0.83	0.12	1.12	17.77	0.78
47	4	10	6.74	0.72	7.63	0.48	0.89	0.93	13.85	0.95
48	7	20	6.49	0.99	8.12	1.53	1.63	1.88	28.97	0.79
53	5	31	5.17	1.27	6.36	1.53	1.19	1.53	29.69	0.77
53	8	22	5.41	1.08	6.60	1.39	1.19	1.65	30.47	0.58
53	9	29	5.36	1.33	6.50	1.49	1.14	1.50	28.09	0.75
54	1	34	5.68	1.46	6.74	1.63	1.06	1.63	28.68	0.67
54	5	28	5.57	1.27	7.70	2.04	2.14	2.47	44.34	0.81
54	8	37	5.99	1.49	7.88	1.88	1.88	2.17	36.22	0.81
54	9	17	6.87	0.65	8.86	1.23	2.00	2.18	31.76	0.70
55	5	42	6.55	1.92	7.84	2.53	1.29	1.64	25.08	0.93
55	8	43	6.86	1.99	7.90	2.53	1.04	1.47	21.38	0.92
55	9	42	6.60	1.84	7.91	2.56	1.31	1.75	26.57	0.91
56	8	18	8.40	2.48	9.57	2.51	1.17	1.48	17.64	0.93
59	1	13	5.28	1.16	5.62	0.87	0.34	0.74	13.97	0.81
60	6	25	5.83	1.50	6.62	1.98	0.79	1.10	18.79	0.94
60	12	29	5.72	1.87	6.53	2.00	0.81	0.99	17.37	0.96
60	14	29	5.80	1.88	6.58	1.99	0.78	0.94	16.12	0.96
60	17	24	6.06	1.89	6.96	2.11	0.91	1.14	18.77	0.94
61	1	23	6.61	2.11	6.90	1.96	0.30	1.22	18.45	0.83
61	6	25	7.37	2.58	9.16	3.02	1.79	2.13	28.88	0.92
61	12	24	7.95	2.47	9.47	2.98	1.53	1.87	23.60	0.93
63	18	18	5.11	0.76	5.69	0.81	0.58	1.00	19.52	0.43
64	10	24	6.23	0.80	8.28	0.80	2.05	2.18	34.96	0.54
64	11	30	5.73	0.98	7.66	1.45	1.93	2.11	36.73	0.82
64	13	21	6.07	0.45	8.35	0.82	2.28	2.37	39.08	0.59
64	15	19	6.24	1.22	8.19	0.86	1.96	2.28	36.58	0.36
65	10	31	7.18	1.80	8.65	2.39	1.47	1.68	23.37	0.96
65	13	31	6.98	1.73	8.65	2.39	1.67	1.94	27.78	0.93
65	15	29	6.95	1.91	8.54	2.43	1.59	1.83	26.36	0.94
65	16	30	6.84	1.81	8.57	2.38	1.73	1.94	28.30	0.95
68	1	19	4.35	1.32	4.78	0.69	0.44	0.98	22.64	0.77

Table 3.11 (con't) T_p Statistics for Grand Banks Storms : Analysis Periods

STORM	BUOY	POINTS	AVE. OBS.	STD. DEV.	AVE. MODEL	STD. DEV.	BIAS (s)	RMSE (s)	SCATTER INDEX	CORR. COEFF.
31	2	24	11.23	1.86	12.29	2.30	1.06	1.89	16.87	0.72
33	3	16	10.26	0.93	11.16	0.61	0.91	1.12	10.89	0.69
39	1	11	11.15	2.03	11.41	0.87	0.26	1.37	12.25	0.82
47	4	10	11.72	0.79	12.66	1.24	0.94	1.38	11.80	0.52
48	7	20	12.97	1.82	13.82	0.93	0.85	2.25	17.33	–0.12
53	5	31	10.79	1.57	12.60	1.69	1.81	2.44	22.64	0.48
53	8	22	11.25	1.17	12.86	1.61	1.60	2.46	21.87	0.08
53	9	29	11.11	1.84	12.73	1.67	1.62	2.24	20.20	0.60
54	1	34	13.02	2.76	12.94	1.84	–0.08	1.42	10.92	0.88
54	5	28	12.50	2.79	12.93	2.50	0.43	2.09	16.72	0.70
54	8	37	13.43	2.20	13.04	2.19	–0.40	1.62	12.09	0.74
54	9	17	15.23	1.40	14.35	0.64	–0.88	1.33	8.73	0.73
55	5	42	11.98	1.77	13.42	2.11	1.45	2.16	18.07	0.66
55	8	43	12.02	2.06	13.48	2.12	1.46	2.21	18.37	0.68
55	9	42	11.97	2.03	13.48	2.14	1.51	2.15	17.93	0.73
56	8	18	12.51	2.43	13.44	2.20	0.93	1.84	14.68	0.76
59	1	13	10.05	0.84	10.32	1.63	0.27	1.38	13.71	0.50
60	6	25	13.04	1.41	13.00	0.83	–0.04	1.31	10.02	0.38
60	12	29	13.11	0.95	12.99	0.80	–0.11	1.07	8.15	0.24
60	14	29	12.70	1.24	13.06	0.92	0.36	1.37	10.80	0.25
60	17	24	12.71	1.31	13.30	0.91	0.59	1.62	12.72	0.07
61	1	23	15.00	1.78	14.20	1.18	–0.80	1.63	10.86	0.59
61	6	25	14.51	2.35	14.25	1.71	–0.26	1.45	10.00	0.79
61	12	24	14.14	2.21	14.50	1.59	0.35	1.62	11.44	0.68
63	18	18	10.39	0.79	11.26	0.34	0.86	1.20	11.57	–0.02
64	10	24	12.19	1.66	14.76	0.59	2.57	3.03	24.82	0.21
64	11	30	11.81	1.92	14.38	1.10	2.57	3.13	26.48	0.38
64	13	21	12.06	1.31	14.88	0.52	2.82	3.13	26.00	0.03
64	15	19	11.97	2.22	14.65	0.65	2.67	3.30	27.55	0.49
65	10	31	11.99	1.78	13.20	2.36	1.21	1.77	14.80	0.83
65	13	31	11.75	1.62	13.20	2.36	1.44	2.21	18.81	0.69
65	15	29	12.40	2.26	13.09	2.40	0.69	1.27	10.22	0.89
65	16	30	12.03	1.65	13.13	2.37	1.10	1.87	15.55	0.76
68	1	19	10.74	1.82	10.79	0.67	0.06	1.49	13.89	0.58

Table 3.12 H_s Statistics for the Scotian Shelf Storms : Analysis Periods

STORM	BUOY	POINTS	AVE. OBS.	STD. DEV.	AVE. MODEL	STD. DEV.	BIAS (m)	RMSE (m)	SCATTER INDEX	CORR. COEFF.
27	1	19	4.84	0.88	6.55	1.31	1.72	2.05	42.29	0.51
34	3	25	4.67	1.29	5.85	1.21	1.18	1.86	39.76	0.32
36	4	28	4.32	0.73	5.54	1.11	1.22	1.39	32.12	0.82
41	5	15	4.32	0.75	5.83	1.27	1.51	1.78	41.31	0.64
42	2	24	4.91	1.38	7.42	2.10	2.51	2.67	54.35	0.94
48	8	25	4.22	1.63	6.12	1.41	1.91	2.14	50.77	0.79
49	8	22	5.50	1.42	5.90	0.64	0.40	1.18	21.41	0.62
50	8	29	3.89	1.50	6.82	1.71	2.94	3.07	78.89	0.85
51	2	22	3.92	1.02	4.43	1.38	0.51	1.04	26.59	0.74
51	8	23	5.64	1.05	6.86	1.57	1.22	1.47	26.06	0.87
52	2	31	3.29	1.29	4.66	1.59	1.37	1.64	49.74	0.82
52	8	26	3.94	1.10	4.99	1.27	1.05	1.33	33.73	0.77
53	2	31	3.66	1.16	4.88	1.99	1.23	1.58	43.13	0.93
53	8	31	4.74	1.79	6.62	2.00	1.88	2.00	42.24	0.94
55	11	46	6.30	2.32	6.19	2.17	–0.11	0.96	15.21	0.91
56	11	19	5.86	1.87	6.16	1.52	0.30	1.17	19.87	0.79
57	8	18	3.47	1.31	5.06	1.11	1.58	1.90	54.58	0.62
57	9	19	4.80	1.65	4.79	1.16	–0.01	0.68	14.09	0.94
57	12	25	4.75	1.68	4.77	1.29	0.02	0.59	12.37	0.95
59	6	24	3.84	1.57	4.81	1.81	0.97	1.18	30.61	0.93
59	13	25	4.34	2.02	4.98	1.72	0.64	0.76	17.46	0.99
59	15	20	4.42	1.88	3.92	1.42	–0.50	0.91	20.60	0.93
60	10	65	3.96	0.96	6.90	1.60	2.94	3.05	76.94	0.92
60	13	36	3.75	0.79	6.50	1.48	2.75	2.91	77.53	0.82
60	14	66	3.82	1.17	6.93	1.61	3.11	3.20	83.73	0.90
60	15	36	5.37	2.03	6.30	2.07	0.93	1.19	22.11	0.93
60	18	34	5.20	1.03	6.74	1.37	1.55	1.64	31.64	0.93
61	13	29	4.26	1.51	5.36	1.96	1.10	1.65	38.83	0.77
61	18	28	5.06	1.68	6.08	2.06	1.02	1.54	30.38	0.82
62	2	25	2.83	1.15	3.37	1.84	0.54	1.07	37.66	0.91
62	7	24	4.13	1.85	4.70	2.17	0.58	0.97	23.53	0.93
62	10	25	3.56	1.40	4.71	2.20	1.15	1.45	40.81	0.97
62	14	21	3.40	1.31	4.65	2.17	1.26	1.58	46.55	0.96
62	16	23	3.98	1.83	4.69	2.29	0.71	0.98	24.67	0.97
62	18	25	4.13	1.62	4.69	2.25	0.56	1.03	24.85	0.95
62	20	25	3.94	1.46	4.88	2.22	0.94	1.33	33.84	0.95
63	7	25	4.84	0.70	6.81	1.00	1.97	2.03	41.99	0.89
63	10	24	5.18	0.97	6.65	0.82	1.47	1.53	29.56	0.90
63	13	25	5.06	0.92	6.61	1.05	1.55	1.66	32.86	0.82

63	14	24	3.89	0.77	6.65	0.82	2.76	2.78	71.55	0.92
63	18	25	4.97	1.12	6.36	0.96	1.39	1.49	30.04	0.87
64	6	37	4.71	1.81	6.07	2.24	1.36	1.57	33.40	0.94
64	17	37	3.95	1.74	4.94	2.15	0.99	1.18	29.79	0.97
64	19	35	5.00	1.84	6.65	2.32	1.65	1.86	37.24	0.94

Table 3.13 T_p Statistics for the Scotian Shelf Storms : Analysis Periods

STORM	BUOY	POINTS	AVE. OBS.	STD. DEV.	AVE. MODEL	STD. DEV.	BIAS (s)	RMSE (s)	SCATTER INDEX	CORR. COEFF.
27	1	19	11.94	1.45	11.75	1.56	–0.18	0.69	5.74	0.90
34	3	25	9.30	1.57	9.75	1.00	0.44	1.34	14.42	0.57
36	4	28	8.62	0.62	9.54	0.77	0.92	1.17	13.62	0.45
41	5	15	9.32	1.81	10.29	0.78	0.97	2.27	24.40	–0.23
42	2	24	11.95	2.18	13.62	2.45	1.67	2.19	18.33	0.81
48	8	25	10.24	1.68	11.03	1.10	0.79	1.53	14.92	0.61
49	8	22	12.09	1.89	11.14	1.11	–0.95	1.59	13.16	0.74
50	8	29	10.16	2.80	13.53	1.86	3.37	3.82	37.58	0.77
51	2	22	12.47	1.66	12.21	1.59	–0.25	1.08	8.63	0.78
51	8	23	12.95	1.90	12.90	1.32	–0.05	1.25	9.68	0.74
52	2	31	10.35	2.25	10.76	1.96	0.40	1.97	18.99	0.57
52	8	26	12.33	1.69	10.98	2.30	–1.35	3.12	25.29	–0.01
53	2	31	11.09	1.78	11.83	2.20	0.73	1.22	11.00	0.90
53	8	31	11.30	2.60	12.00	2.01	0.70	1.38	12.18	0.89
55	11	46	12.08	2.11	11.49	1.51	–0.59	1.26	10.47	0.86
56	11	19	9.72	1.87	10.53	1.52	0.81	1.32	13.61	0.82
57	8	18	10.86	1.10	10.02	1.39	–0.84	1.74	15.99	0.23
57	9	19	9.37	1.82	9.20	1.07	–0.17	1.07	11.43	0.84
57	12	25	9.82	1.36	8.95	1.47	–0.87	2.12	21.64	0.02
59	6	24	9.63	2.38	9.92	1.88	0.29	1.72	17.87	0.69
59	13	25	10.60	2.93	10.04	1.81	–0.56	1.97	18.61	0.77
59	15	20	10.29	2.51	9.32	2.37	–0.97	2.63	25.54	0.47
60	10	65	11.39	2.32	12.52	1.72	1.13	1.75	15.36	0.82
60	13	36	9.48	2.22	12.30	1.95	2.82	3.20	33.79	0.74
60	14	66	12.07	2.43	12.54	1.71	0.47	1.29	10.72	0.88
60	15	36	10.37	2.28	11.47	2.06	1.09	1.56	15.07	0.87
60	18	34	10.30	1.72	12.55	1.94	2.25	2.54	24.64	0.79
61	13	29	8.56	1.05	10.99	1.76	2.43	2.78	32.53	0.62
61	18	28	9.50	1.07	11.49	1.70	1.98	2.33	24.54	0.68
62	2	25	10.08	1.83	10.89	1.57	0.81	1.58	15.68	0.68
62	7	24	10.59	1.73	10.77	2.04	0.18	1.43	13.49	0.72
62	10	25	10.22	2.39	10.85	2.09	0.64	1.82	17.77	0.71
62	14	21	10.47	2.57	10.89	2.17	0.42	1.44	13.76	0.84
62	16	23	9.94	2.09	10.76	2.16	0.81	1.35	13.58	0.87
62	18	25	10.18	1.64	10.77	2.67	0.60	2.15	21.13	0.61
62	20	25	10.18	2.16	11.16	1.85	0.98	1.79	17.59	0.72
63	7	25	10.08	1.81	11.96	1.29	1.88	2.65	26.31	0.28
63	10	24	10.23	2.20	11.68	1.52	1.46	2.22	21.74	0.63
63	13	25	9.56	1.46	11.70	1.57	2.14	2.36	24.72	0.78
63	14	24	10.77	2.18	11.68	1.52	0.91	1.72	15.93	0.73
63	18	25	9.34	1.69	11.47	1.65	2.13	2.51	26.90	0.67

64	6	37	9.96	2.00	10.85	1.96	0.88	1.58	15.88	0.77
64	17	37	8.61	1.74	9.96	1.64	1.36	1.72	19.95	0.80
64	19	35	9.79	1.67	11.22	2.23	1.44	1.72	17.55	0.92

Table 3.14 Peak to Peak Statistics for East Coast Storms

VAR	AREA	POINTS	AVE. OBS.	STD. DEV.	AVE. MODEL	STD. DEV.	BIAS	RMSE	SCATTER INDEX	CORR. COEFF.
Hs (m)	GB	34	9.21	1.70	10.05	2.03	0.84	1.42	15.39	0.82
	SS	44	7.12	1.21	7.99	1.07	0.88	1.58	22.23	0.32
Tp (s)	GB	34	13.66	1.91	14.71	1.76	1.05	2.30	16.87	0.36
	SS	44	11.88	1.54	12.58	1.47	0.70	1.68	14.15	0.47

Table 3.15 Analysis Period Statistics for East Coast Storms

VAR	AREA	POINTS	AVE. OBS.	STD. DEV.	AVE. MODEL	STD. DEV.	BIAS	RMSE	SCATTER INDEX	CORR. COEFF.
Hs (m)	GB	868	6.25	1.81	7.58	2.23	1.33	1.71	27.41	0.88
	SS	1241	4.42	1.61	5.81	1.95	1.40	1.87	42.27	0.77
Tp (s)	GB	868	12.29	2.14	13.21	1.93	0.92	2.00	16.29	0.62
	SS	1241	10.48	2.25	11.30	2.06	0.82	1.96	18.70	0.66

3.3 HALLOWEEN STORM VALIDATION

3.3.1 Introduction

The so–called Halloween storm occurred on October 30–31, 1991. This storm is of particular interest to this study since it provided the highest ever measured waves not only in this region, but also anywhere else, with peak significant wave height of about 17 meters. This value exceeded the estimated 100–year wave height for this location by more than 4–5 meters. Another unique feature of this particular event is that an excellent network of buoys were operational along the storm track. It provided excellent records of the storm evolution and gave a very good coverage both spatially and temporally. This operational array of deep ocean moored buoys is shown in Figure 3.12. The measured H_S exceeded 14 meters at two of these buoys (44137, 44141), which exceeds the largest previously measured H_S in Canadian east coast waters. At buoy 44137 the peak H_S of 16.86 m, as averaged over three consecutive hourly estimates, is among the highest measured sea states ever reported in any basin. This storm was hindcast in a separate study as reported by Cardone and Callahan (1992). That hindcast used the ODGP model adapted in a deep water mode. The grid system differed from that used for the previous PERD study (described in previous sections of this report), but the resolution of 0.5 degree latitude by longitude adopted is comparable to that of the fine mesh of the nested grid system used for the 3–year hindcast and the PERD storm hindcasts. In a more recent study (Cardone et al., 1995), hindcasts made by four different wave models, including the ODGP, and driven by a common wind field are validated against wind and wave measurements made by all US and Canadian buoys moored in deep water. In this section we present the validation of only the ODGP hindcast. The meteorological evolution of this storm, described below, was not typical of storms in the population hindcast for the previous wave climate study, but this case provides a unique opportunity to validate the hindcast methodology against truly deep water measurements representing a very wide dynamic range of sea states.

The evolution of the main meteorological systems comprising the Halloween storm have been described in detail by Cameron and Parkes (1992) using mainly operational analyses produced at AES, and NOAA, using the NOAA NMC products. Figure 3.13 shows the tracks of what were initially two separate storm systems which comprise this event. The southern subtropical system formed late on the 25th about 300 nm south of Bermuda, intensified to tropical storm strength early on the 26th and hurricane strength (Grace) late on the 26th. Grace moved slowly northwestward on the 27th. The surface wind field about Grace during this period was characterized by winds of gale to storm force over a large area, up to 300 nm from the centre. Grace slowed and turned northward on the 28th while weakening, then turned toward the east and moved for a time eastward toward Bermuda early on the 29th. While the storm was losing its tropical characteristics and its inner core of near hurricane force winds (not well resolved on the 0.5 degree grid) it still at this time possessed a large circulation with winds in excess of 40 knots covering a large area. Late on the 29th, the remnants of Grace turned northeastward, sparing Bermuda significant impact, and on the 30th became absorbed into the northern cyclonic system.

The northern system formed out of a weak wave which had been moving eastward out of New England along a strong basically east–west oriented cold front laid out along the St. Lawrence Valley early on the 27th. As the wave reached the eastern tip of Nova Scotia at about 12 UT on the 28th, it evidently turned abruptly southward and began to intensify rapidly; 24 hours later, the center was near 41^{o}N, 55^{o}W, its central pressure having fallen about 24 mb. The cyclone then turned toward the west–southwest and continued to intensify over the next 24–hours during the 30th, before slowing and filling on the 31st. The center executed a counterclockwise loop on the 31st October and 1 November while filling. Beyond 1 November, the cyclone turned northward and for a time intensified and acquired tropical characteristics before weakening and entering Nova Scotia just west of Halifax on the 2nd.

3.3.2 Validation

Time histories of hindcast and measured H_s and T_p at nine offshore buoys moored in deep water are compared in Figures 3.13 through 3.21. At NOAA buoys 41001 and 41002, the sea state peaks on the 31st consist mainly of propagated swell. At NOAA buoy 44008 the water depth of 60 meters is marginally shallow for these wave periods, and the model positive bias may be attributed to the shallow water processes. At NOAA buoy 44011, with water depth 88 m, the hindcast is in excellent agreement with the measurements. In the Canadian array, the hindcast is in excellent agreement with the measurements at some buoys (e.g. 44138, 44139, 44140) and is biased low at others (44137, 44141). Note that at these strictly deep sites, the ODGP model does not exhibit the consistently positive bias seen when hindcasts are compared to the MEDS data from buoys moored in marginally deep water or shallow water. The hindcast and measured H_s and T_p storm peaks are compared in Table 3.16 for the 7 buoys within the main part of the storm circulation. The mean difference in H_s is –0.85 m, which is caused mainly by the large negative bias at 44137 and 44141. Cardone et al. (1995) found that this negative mean difference in the H_s peaks at these buoys is reduced but not eliminated even in hindcasts made by a third–generation model. The extreme peak storm seas observed at 44137 in this storm were evidently generated by efficient coupling of the wave generation along a dynamic fetch associated with a propagating feature in the surface wind field termed a low level ”jet streak” by Cardone et al., (1995). At 44141, the hindcast H_s is lower than measured not only near the peak of the storm but also over a considerable part of the storm duration. This was found also for all other wave models. Cardone et al., (1995) attribute the difficulty at this buoy to either a remaining systematic error in the wind field near and upwind of this buoy or perhaps to an interaction of the wave generation and ocean currents.

The validation of the time histories of H_s and T_p at all 9 buoys is given in Table 3.17. The scatter index in H_s varies from as low as 8.45% at 41001 to 25.63% at 44008. Within the Canadian array, the scatter index varies between 10.9% and 22.71% with correlation coefficient between 0.93 and 0.98. These indicate significantly greater skill than achieved in the PERD storms (see Table 3.15). This is attributed to the greater accuracy in the wind fields for this storm, made possible by the surface wind measurements made available by the dense array of NOAA and AES buoys.

HALLOWEEN STORM

Buoy Locations and Nearest ODGP Gridpoints
For Period: Oct. 28 – Nov. 3, 1991

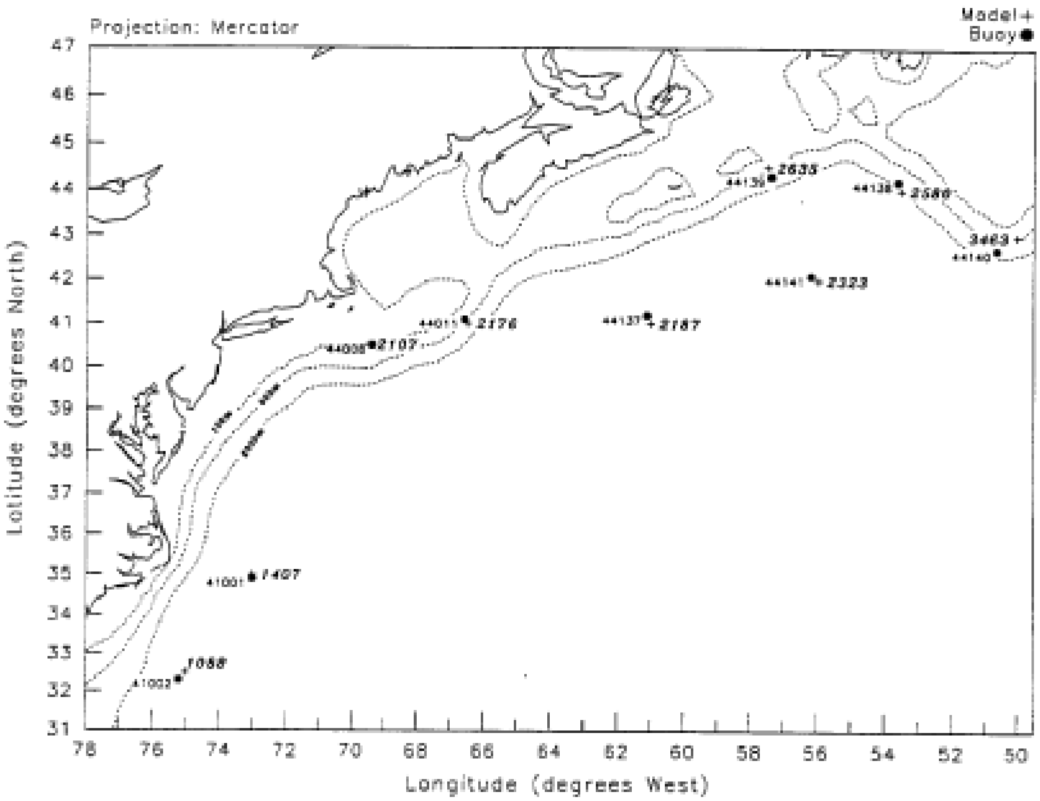

Figure 3.12 Halloween Storm Map

Figure 3.12 Halloween Storm Map

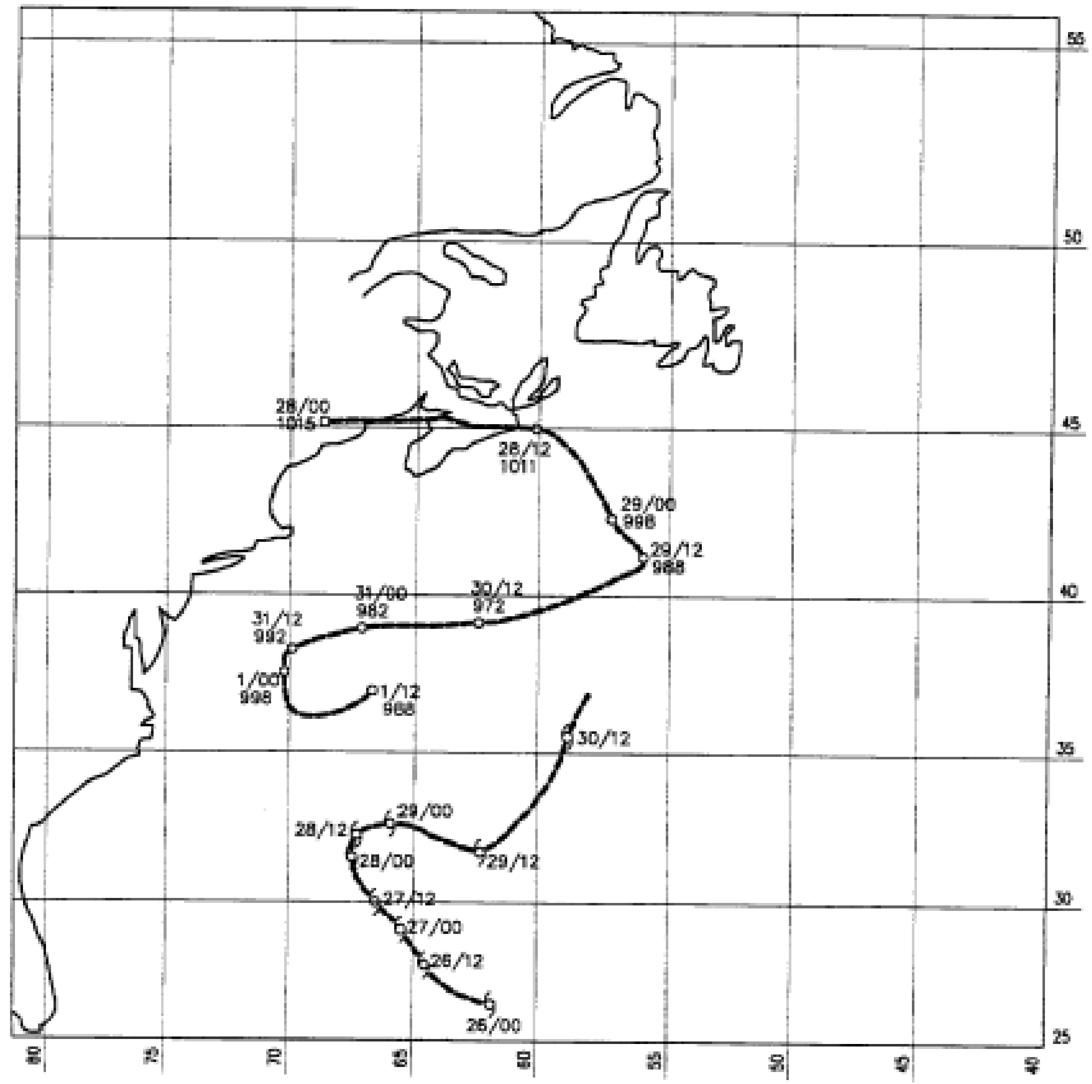

Figure 3.13 Halloween Storm Track with Central Pressure Indicated (Oct. 26-Nov. 1, 1991)

Figure 3.13 Halloween Storm Track with Central Pressure Indicated (Oct. 26–Nov. 1, 1991)

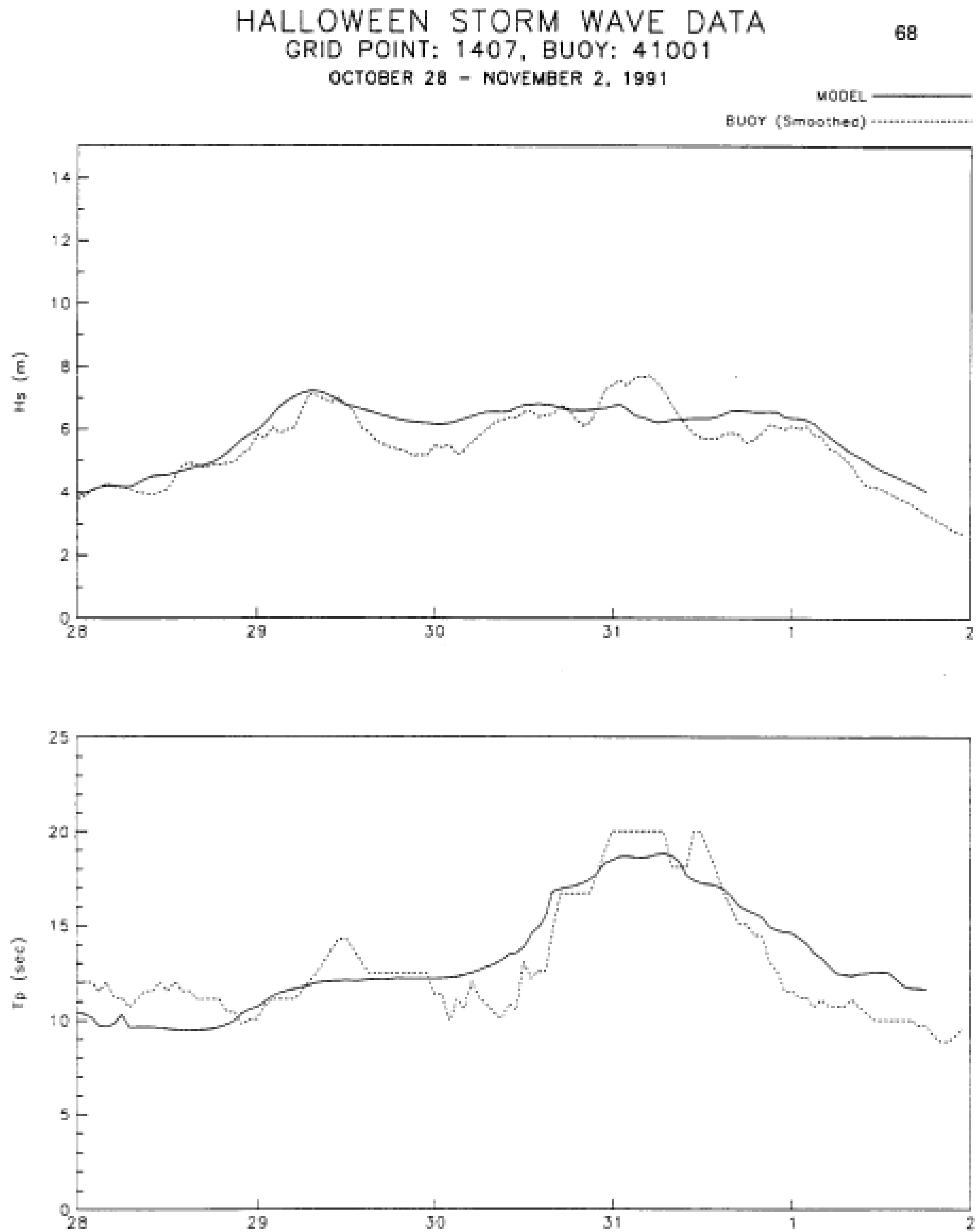

Figure 3.14 Halloween Storm Verification

Figure 3.14 Halloween Storm Verification

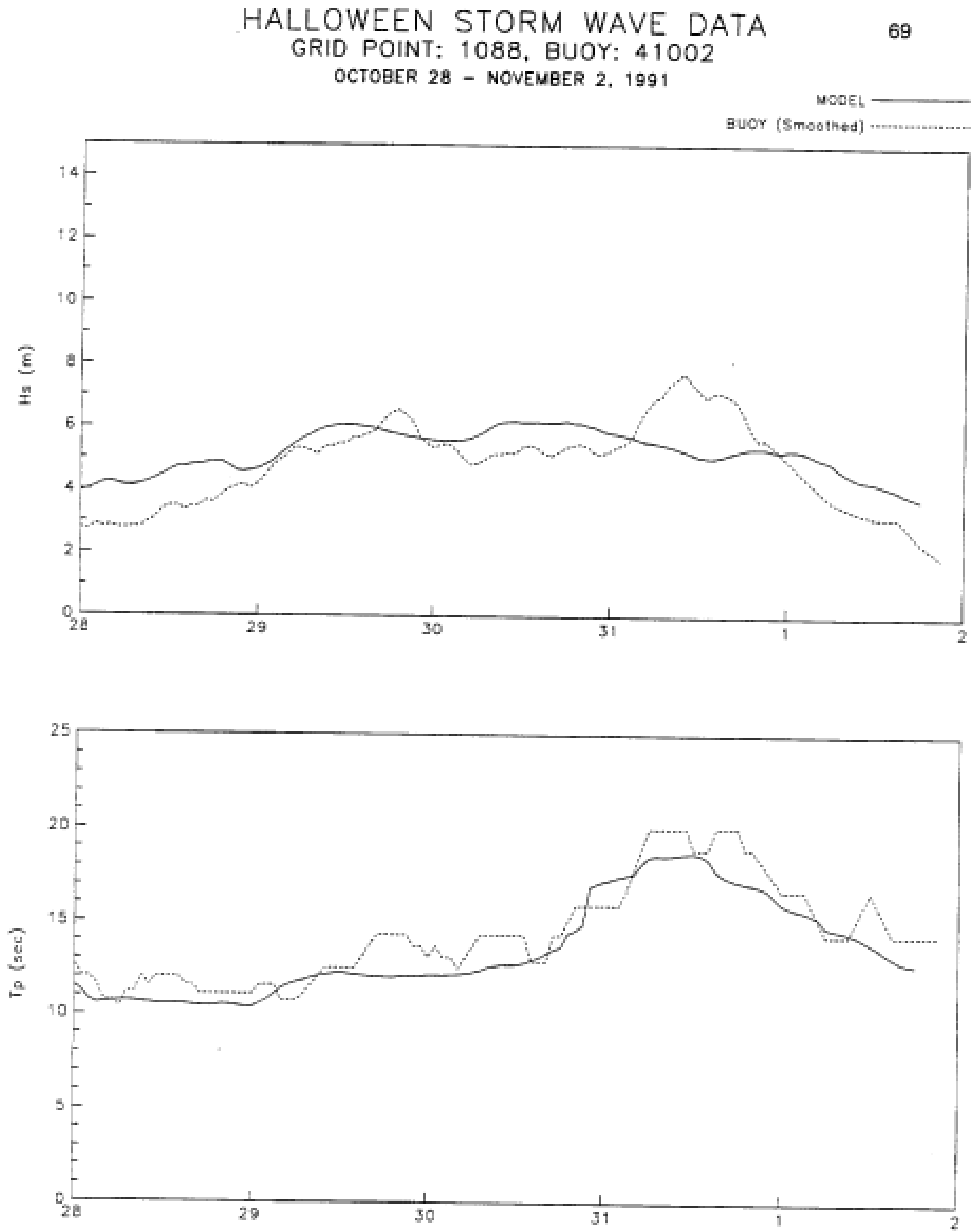

Figure 3.15 Halloween Storm Verification

Figure 3.15 Halloween Storm Verification

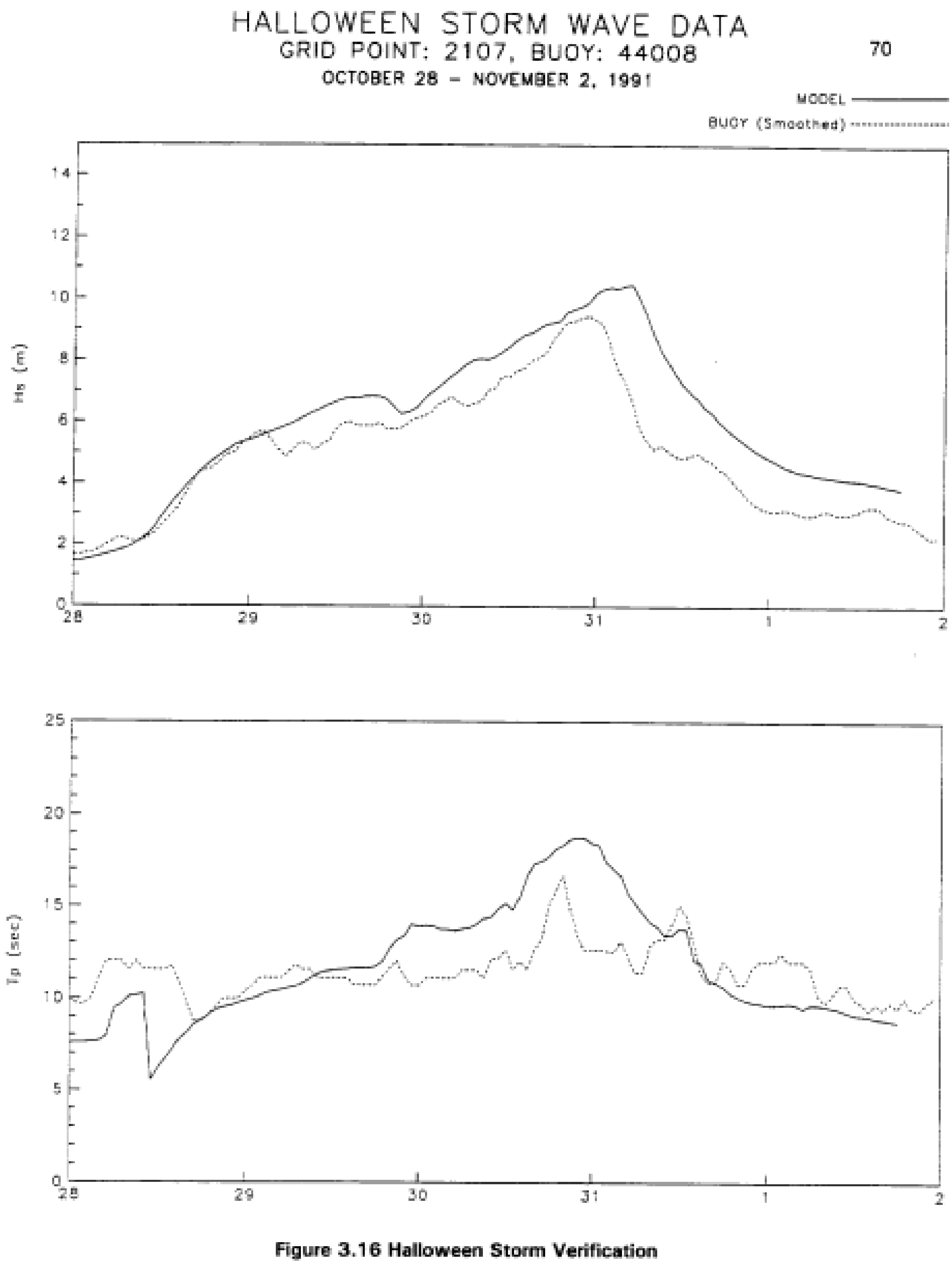

Figure 3.16 Halloween Storm Verification

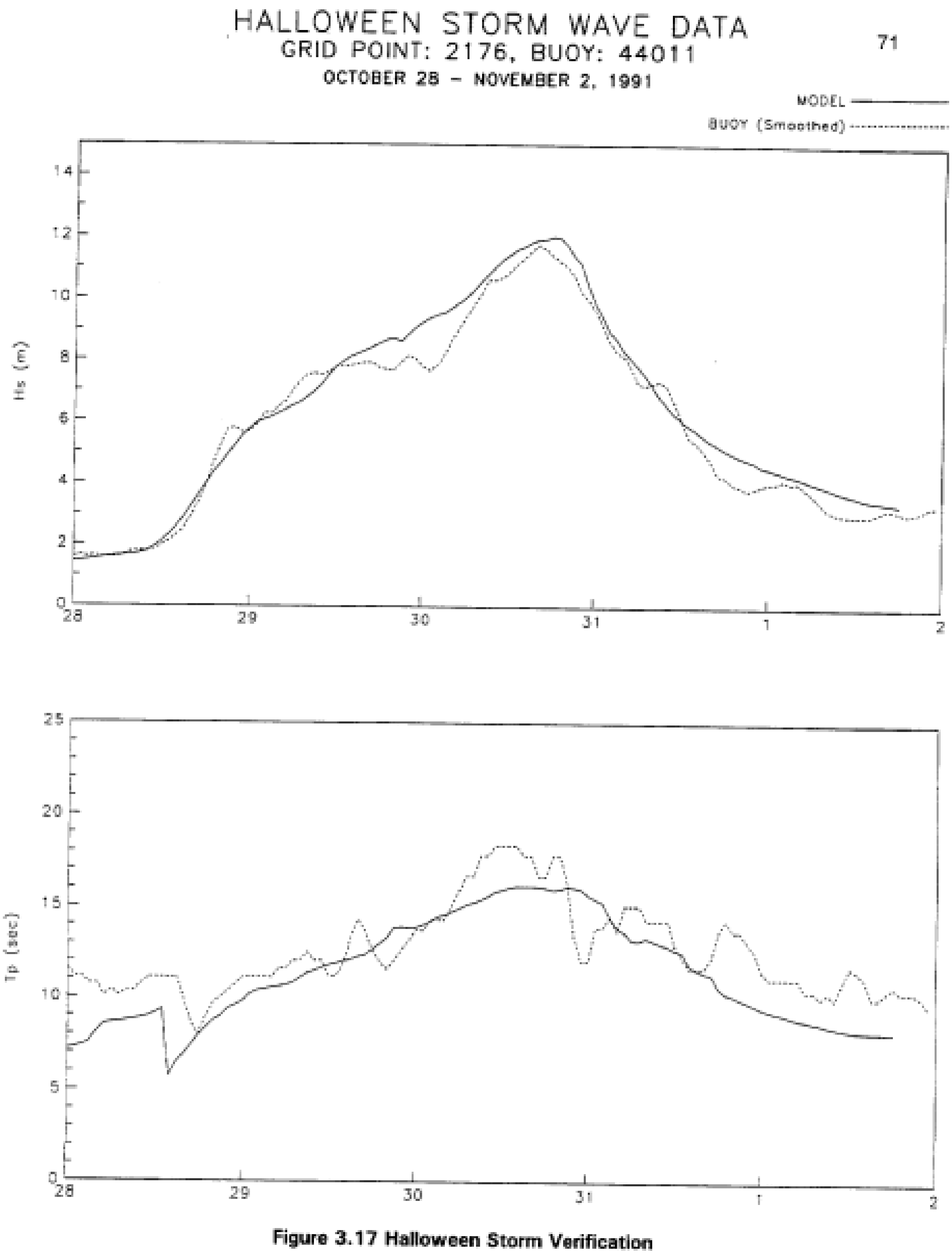

Figure 3.17 Halloween Storm Verification

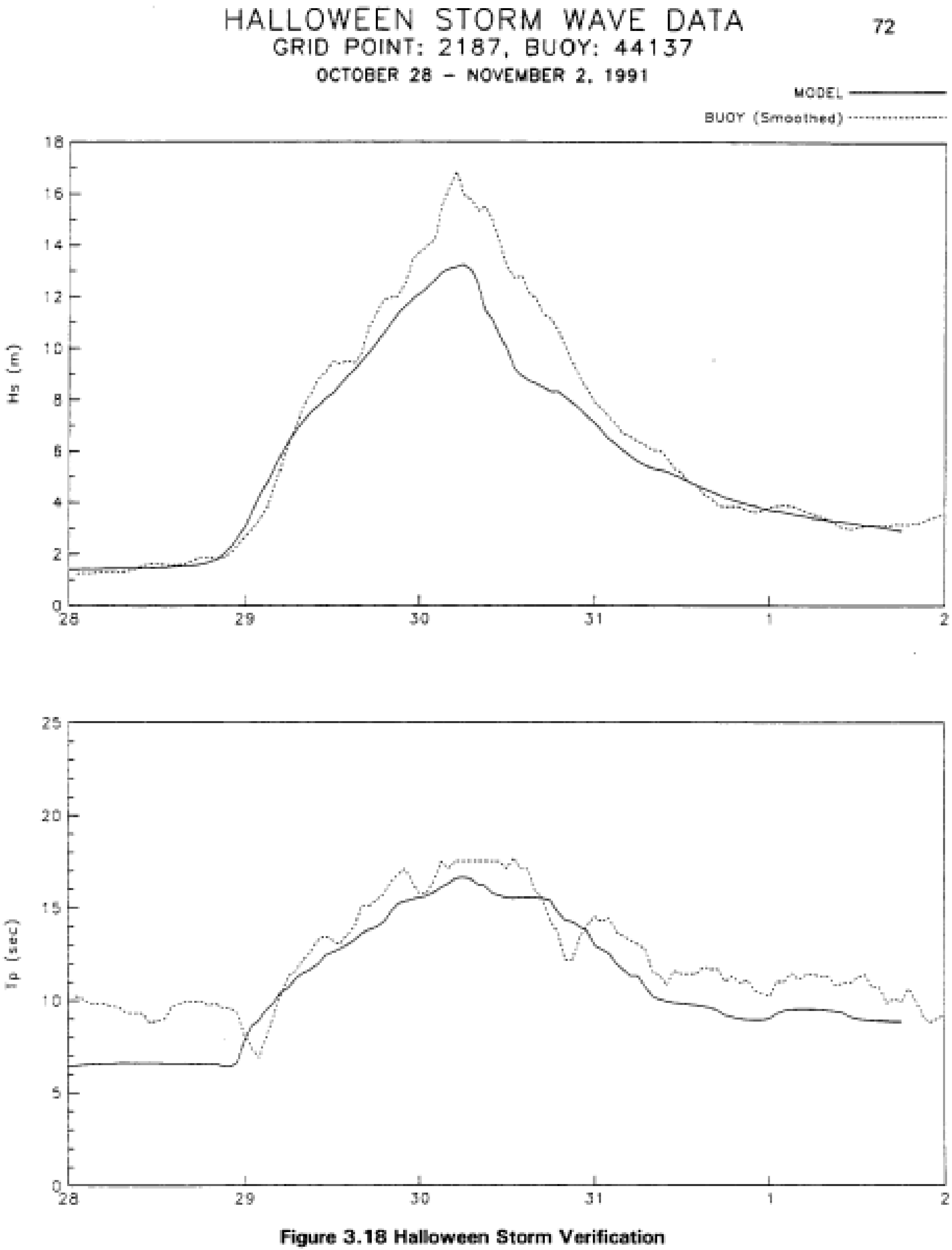

Figure 3.18 Halloween Storm Verification

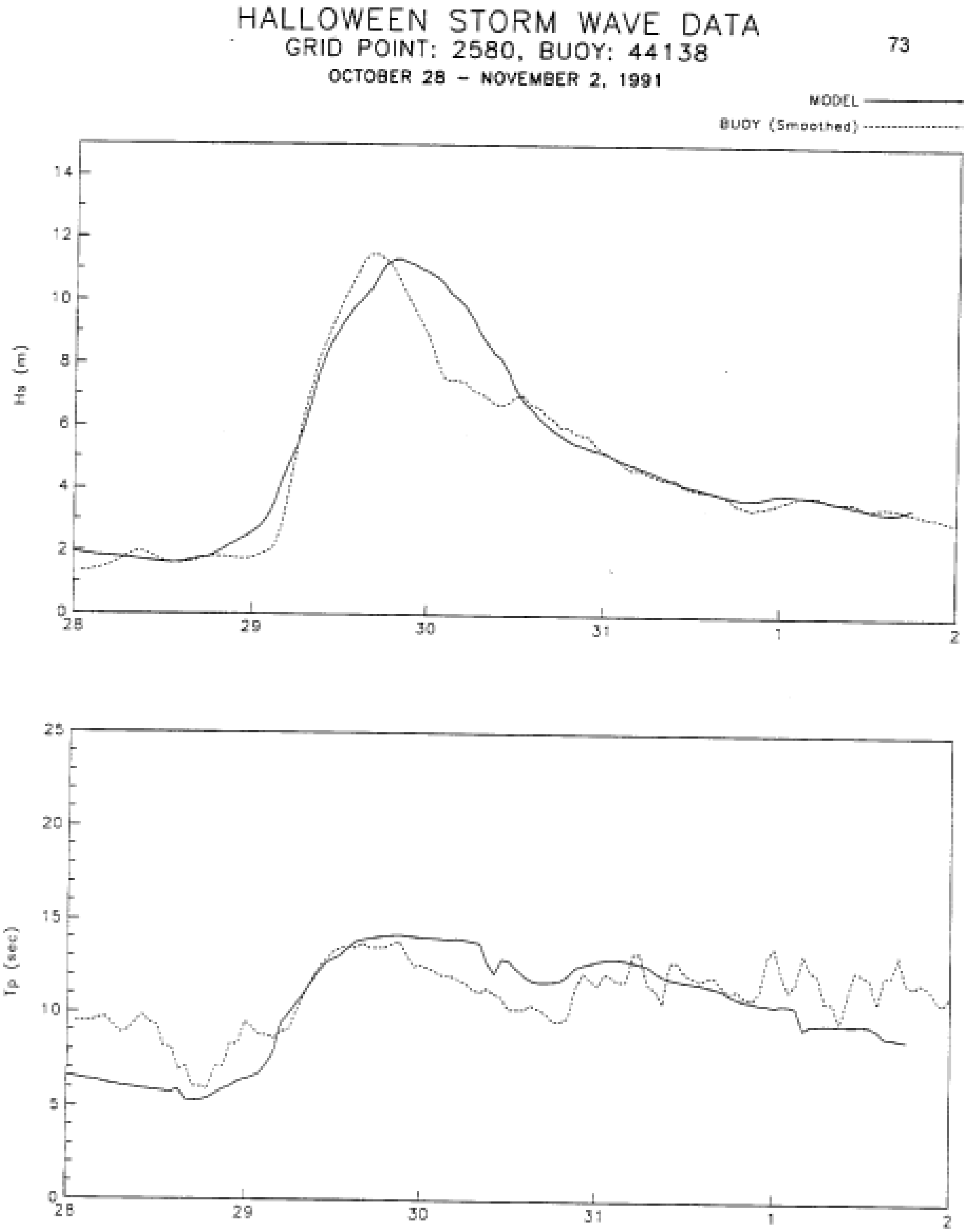

Figure 3.19 Halloween Storm Verification

Figure 3.19 Halloween Storm Verification

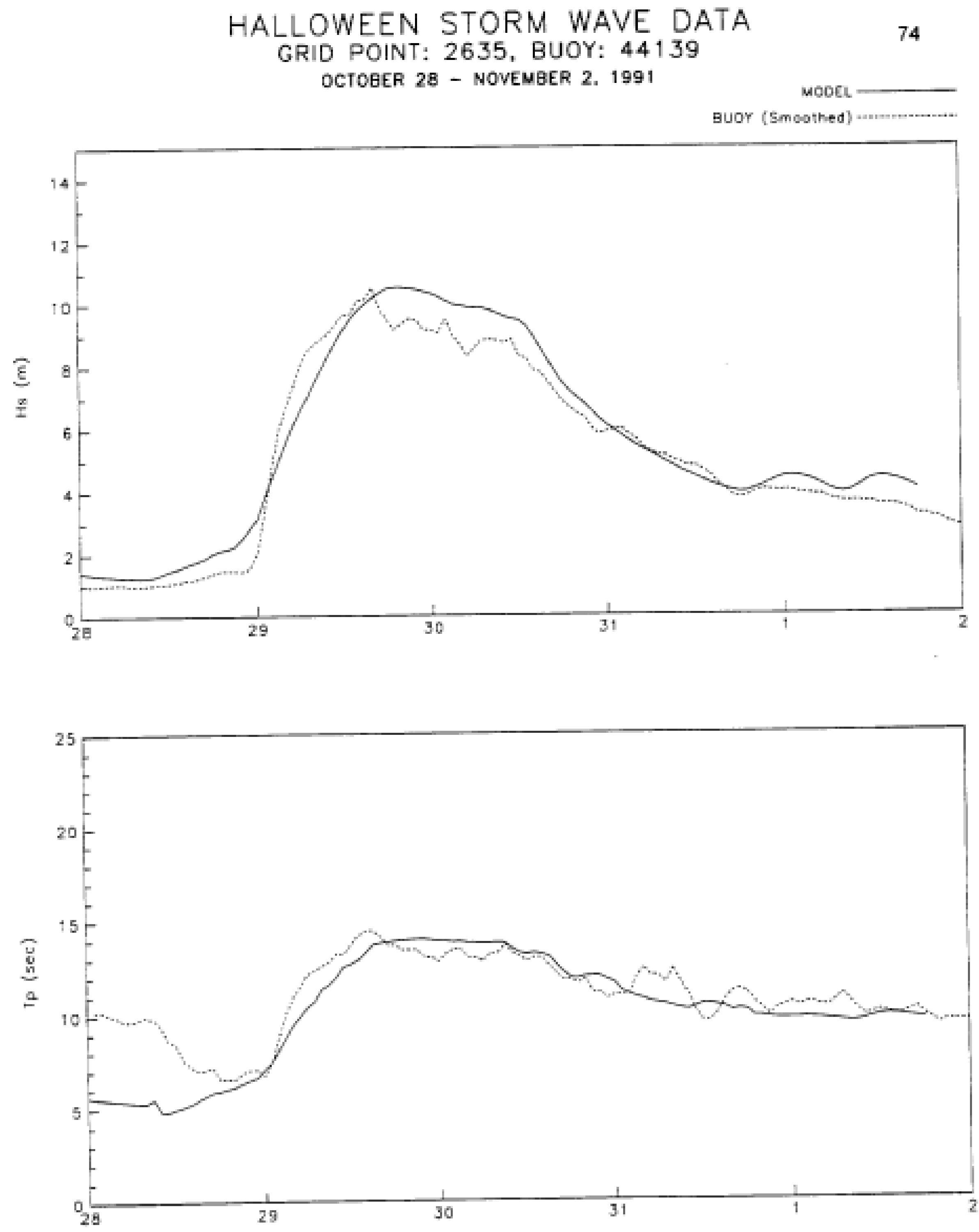

Figure 3.20 Halloween Storm Verification

Figure 3.20 Halloween Storm Verification

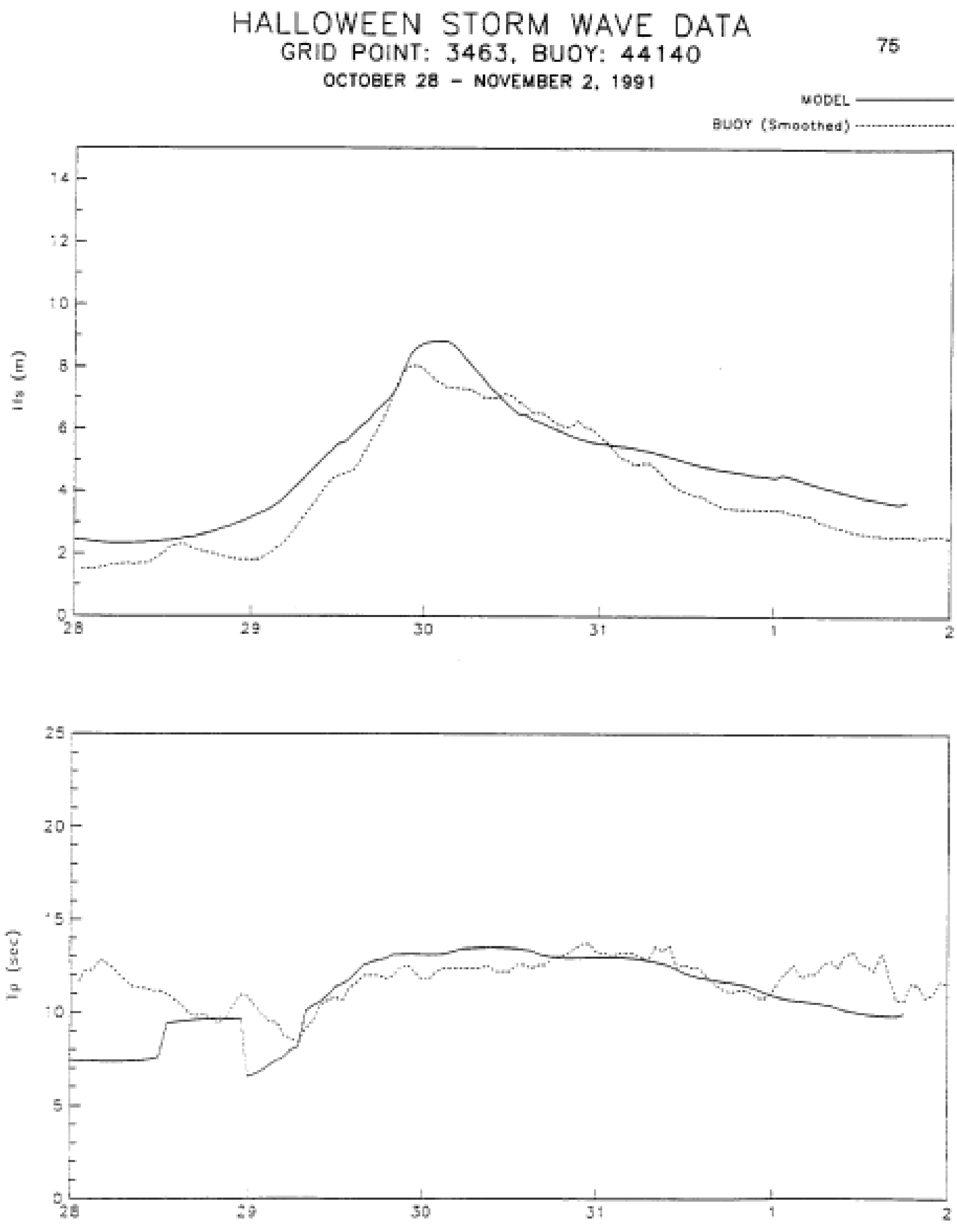

Figure 3.21 Halloween Storm Verification

Figure 3.21 Halloween Storm Verification

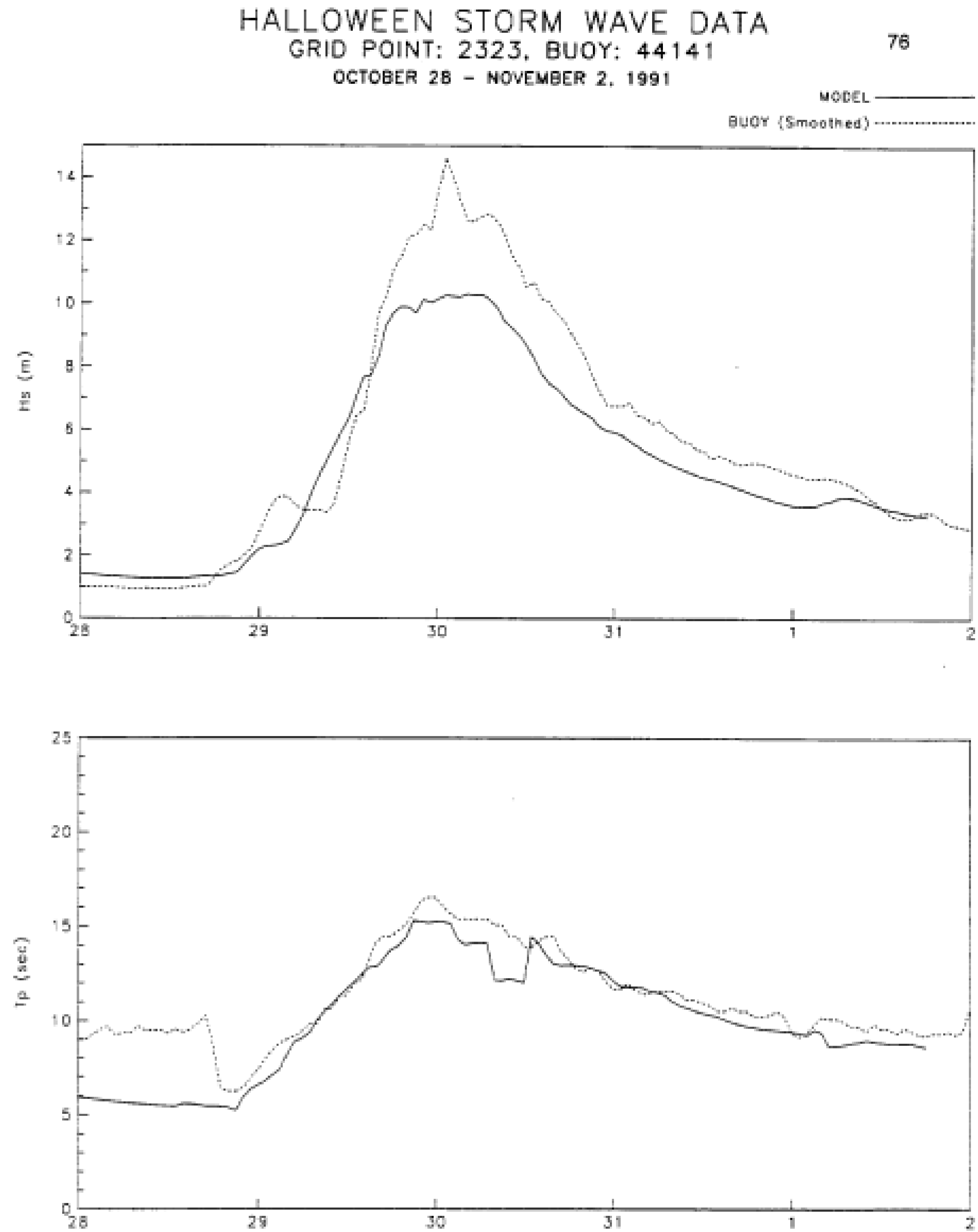

Figure 3.22 Halloween Storm Verification

Figure 3.22 Halloween Storm Verification

Table 3.16 Halloween Storm: Peak To Peak Comparison

Buoy Measurements					Model Hindcast					
Date (Buoy)	**Buoy**	**Depth (m)**	**Hs (m)**	**Tp (s)**	**Date (Model)**	**Grid**	**Hs (m)**	**Tp (s)**	**ΔDate (hr)**	**ΔHs (m)**
911030–23	44008	60	9.47	12.63	911031–05	2107	10.48	15.74	6.0	1.01
911030–16	44011	90	11.77	17.80	911030–18	2176	12.03	16.06	2.0	0.26
911030–05	44137	4500	16.86	17.53	911030–06	2187	13.26	16.64	1.0	–3.60
911029–16	44138	1500	11.47	13.73	911029–20	2580	11.33	14.16	4.0	–0.14
911029–16	44139	1100	10.52	14.20	911029–19	2635	10.54	14.00	3.0	0.02
911029–23	44140	1500	8.05	12.20	911030–02	3463	8.82	13.15	3.0	0.77
911030–01	44141	4500	14.61	16.00	911030–04	2323	10.31	14.06	3.0	–4.30

Δ = Model – Buoy (Peak)

Table 3.17 Halloween Storm Data: Analysis Period: Oct. 29 – Nov. 1, 1991

VAR	GRID	BUOY	POINTS	AVE. OBS.	STD. DEV.	AVE. MODEL	STD. DEV.	BIAS (m)	RMSE	SCATTER INDEX	CORR. COEFF.
Hs (m)	1407	41001	72	6.24	0.69	6.56	0.27	0.32	0.69	11.00	0.46
	1088	41002	71	5.76	0.80	5.69	0.39	–0.07	0.99	17.17	–0.32
	2107	44008	72	6.22	1.54	7.50	1.58	1.27	1.60	25.63	0.81
	2176	44011	71	7.88	2.14	8.28	2.20	0.40	0.67	8.45	0.97
	2187	44137	72	8.96	4.04	7.83	2.95	–1.13	1.74	19.43	0.98
	2580	44138	72	6.26	2.61	6.66	2.72	0.40	1.04	16.67	0.93
	2635	44139	72	7.00	2.18	7.24	2.44	0.24	0.76	10.90	0.96
	3463	44140	72	5.20	1.75	5.85	1.48	0.65	0.89	17.07	0.94
	2323	44141	72	7.75	3.39	6.46	2.54	–1.29	1.76	22.71	0.96
Tp (s)	1407	41001	72	14.33	3.28	14.58	2.66	0.24	1.44	10.04	0.90
	1088	41002	71	15.07	2.92	14.24	2.74	–0.83	1.35	8.95	0.93
	2107	44008	72	11.99	1.31	13.51	2.69	1.52	2.60	21.70	0.63
	2176	44011	71	13.87	2.18	13.19	2.07	–0.68	1.68	12.09	0.74
	2187	44137	72	13.64	2.78	12.69	2.66	–0.95	1.43	10.46	0.92
	2580	44138	72	11.56	1.39	12.11	1.83	0.55	1.37	11.84	0.73
	2635	44139	72	11.98	1.58	11.79	1.81	–0.20	0.89	7.42	0.88
	3463	44140	72	11.90	1.28	11.99	1.86	0.09	1.10	9.21	0.82
	2323	44141	72	12.40	2.31	11.76	2.16	–0.64	0.98	7.88	0.95

3.4 SHALLOW WATER EFFECTS

Further investigation of possible shallow water effects was carried out only to try to explain the over–prediction by the deep water model when compared with actual measurements taken in relatively shallow waters. As clearly shown in section 3.2.3 , the large over–prediction of wave height by the model is mainly due to shallow water effect. As shown in Table 3.1.4, the average peak period varied from about 12 s on the Scotian Shelf to 14 s on the Grand Banks; this corresponds to a wave length of 225 m to 300 m. As also shown, most of these measurements were taken in water depths of less than 100 m (i.e. the water depth ranges of most interest to offshore industry, e.g. 80 m at Hibernia and about 45 m at Cohasset/Panuke oil fields). This means that the ratio of wave length to water depth (L/d) is greater than 2, where shallow water effects become significant.

The comparison of time series histories of wave height and period and the verification statistics (Tables 3.9 – 3.15) suggests that in most severe storms on the Grand Banks and Scotian Shelf, shallow water effects must be considered to accurately hindcast sea states, and accurate deep water hindcasts will provide conservative results in such water depths which are of most interest to offshore industry (i.e. less than 100 m).

This study strongly recommends that further study of shallow water effects should be carried out. These would include not only incorporation of shallow water source term and inclusion of refraction and shoaling in wave model, but also investigation of the effects of shallow water on the estimation of maximum individual wave height and crest height.

4.0 THE WEST COAST

This chapter contains results from studies that modelled the wave climate of the North Pacific Ocean in order to provide wave climate of the west coast of Canada. Datasets that were compiled in this study are:

a) Three year spectral wave model hindcast database (Jan. 1, 1987–Dec. 31, 1989) which was carried out by MPL and OWI as part of this study.

b) Extreme wave hindcast study carried out by MPL and OWI, in which 51 storms on the west coast were hindcast (Canadian Climate Centre, 1992).

c) Four recent severe storm events that were hindcast after the above study was completed. These were also carried out as part of this study.

In each of these studies the wave model used was the Ocean Data Gathering Program (ODGP) model. Similar to the East Coast Version (NATWAV), The Pacific Version (PACWAV) is a deep water, fully directional, spectral wave model; 24 directions by 15 frequencies. For a description of the model physics and hindcast techniques, see Eid et al. (1989), MacLaren Plansearch (1985); and Cardone et al. (1976). To date, it has been used in many studies of wave spectra as discussed in previous sections, and its output has been determined to be of a high degree of accuracy. For instance, when the wind input error is of the order of ± 2 m/s in speed and $\pm 20^o$ in direction, the scatter index for the significant wave height and peak frequency is about 15%. Being a deep water model, there will tend to be a consistent over prediction of the wave regime in shallow water conditions. Fortunately, shallow water areas are found only in inland waters along the B.C. coast, though numerous islands that exist off this coast do pose a challenge to the model. Overall, the model performs well in the offshore areas of this region.

The Pacific Ocean model produces wave spectral information on two grids: a coarse and fine grid. The coarse grid contains 755 gridpoints, with spacing of 1.25 degrees latitude by 2.5 degrees longitude, and extends across much of the northern Pacific Ocean, from 30^{o}N to 60^{o}N. See Figure 4.1. The fine grid is used specifically for the B.C. coast of Canada. It contains 173 gridpoints, with a spacing of 0.625 degrees latitude by 1.25 degrees longitude, and covers a rectangular area from 45^{o}N to 60^{o}N. See Figure 4.2

4.1 WEST COAST THREE–YEAR HINDCAST

The main objective of this study was to produce a 3 year continuous hindcast database of the wave climate of the Northeast Pacific Ocean. In addition, it was necessary to verify the output of the ODGP spectral wave model used against buoy data from the area. The hindcast spanned the years of 1987–1989 inclusive. The area of interest is the offshore and inshore areas of the Pacific Ocean, near the west coast of Canada. Specifically, the area extended from the shoreline to approximately 144^{o}W longitude, and from 45^{o}N to 60^{o}N latitude.

The hindcast method used is as follows:

(a) 12–hourly gridded fields of ECMWF surface pressure, air temperature, and sea temperature were collected for the years 1986–1988.

(b) This data was converted to a beta–spline field on an 800 km grid for the entire Pacific Ocean.

(c) The Interactive Graphics Editor, INGRED, was utilized to edit each 12 hourly surface pressure chart in accordance with the 6 hourly surface analyses from the U.S. National Meteorological Centre (NMC). The microfilmed NMC charts proved to be a more accurate depiction of the pressure fields over the Pacific, for certain time periods than the ECMWF data.

(d) The edited 12 hourly surface charts were then passed through an interpolation routine to linearly interpolate the charts to 2 hour intervals for the complete 3 year period; since the wave model utilized a 2 hour time step.

(e) Using the Marine Planetary Boundary Layer Model (MPBL), wind fields were calculated, at 2 hourly time–steps for each of the model's gridpoints. Winds were calculated at a 20 m height.

(f) The gridded wind fields were then input into the wave model to produce spectral wave data for 58 specified gridpoints.

Two basic data sources were utilized to provide the starting fields of 12 hourly pressure, air–temperature and sea surface temperature. The first source is the so–called WMO archive of ECMWF global analyses, which provides gridded fields of geopotential height, winds, air temperature and humidity on a 2.5^{o} latitude–longitude grid for the decade of the 1980's. These analyses are derived from the higher resolution operational analyses produced by ECMWF in real time. We converted the fields of 1000 geopotential height to surface pressure using the hypsometric relationship expressed in terms of the 1000 mb air temperature. The 1000 mb air–temperature was also taken as an approximation to the surface air temperature for the stability parameter (air–sea temperature difference) required by the planetary boundary layer used to derive surface winds. The sea surface temperature (SST) grids were interpreted from a long term climatology of mean–monthly sea–surface temperature. The source was the mean–monthly SST resolved on a global 1–degree grid contained in the CD–ROM data base "U.S. Navy Climatic Atlas of the Oceans". Each of the above fields was interpolated bi–linearly to the 800–km grid which forms the nodal points of the beta–spline grid used by INGRED. A 400–km resolution was also considered, but a separate experiment (personal communication, B. Thomas) in which INGRED derived analyses for the two resolutions were compared found little difference in the resulting wind and wave analyses. This is not to be considered a general conclusion but rather merely reflects that smaller scales of motion are not resolved in the particular source grids used.

The interpolation routine in INGRED (described below) produced 2 hourly fields of surface pressure, air and sea surface temperature, for the three year hindcast period of 1986–1988. These fields were then converted to gridded wind fields, by a routine based on the Marine Planetary

Boundary Layer (MPBL) model, (see Cardone, 1969, and Cardone, 1978). The model calculates ”effective neutral” winds at 20 m in height, by taking atmospheric stability into account. Effective neutral winds are winds in a thermally neutral atmosphere that would result in the same stress on the ocean surface as would be present in a thermally stratified atmosphere.

By the process described above, the gridded wind fields, were calculated from the beta–spline field, then input into the ODGP spectral wave model. Model hindcast parameters, such as significant wave height (H_s), peak period (T_p), wind speed (W_s), wind direction (W_d), wave direction ($Wave_d$), and friction velocity u_* were generated by the model for 58 specified gridpoint locations.

The output from the wave model was then verified against buoy data in the area (See Figure 4.2.) Time series plots and standard statistics were prepared and are included in this report. It was found that the model's output was in good agreement with actual data from the region, and that the statistics were consistent with other studies that used this model.

4.1.1 INGRED – Interactive Graphical Editor

On–Screen Editing

Manipulating the 12–hourly charts was made easier by the use of the Interactive Graphics Editor, INGRED, that was developed by Environment Canada to be used as a forecast assistant for meteorologists. INGRED also allowed for on–screen editing of the 12 hourly charts, as was done frequently in this study. This undertaking proved very valuable, as the output of atmospheric numerical weather models inevitably falters over large expanses of water, such as the Pacific Ocean, due mainly to sparsity of real–time data (buoys, ships, planes, etc) that is a necessary input to these weather models. To correct errors that do arise, it is necessary for a meteorologist to edit the 12 hourly weather model charts, by a comparing the model output with a more reliable form of the data. In this study, the ECMWF output was corrected according to a comparison that was made between the ECMWF model and the 6–hourly manual surface analyses provided by the U.S. National Meteorological Centre (NMC). This process was performed on the surface pressure charts only. The low and high pressure centres were deepened or strengthened accordingly, and pressure gradients were manipulated in strength and orientation to agree more closely with the surface analysis charts.

Linking

Another feature of INGRED that proved valuable to this type of work, allows the user to ”link” weather patterns, such as pressure centres, ridges, and troughs, between consecutive 12 hourly weather charts. Linking is the term that refers to the process that informs the interpolation routine that particular atmospheric features are continuous between weather charts. In cases such as quickly propagating systems, this could improve the interpolation process, thus improving the calculation of gridded wind fields. On the west coast, a sensitivity analysis was performed to quantify the difference in the results that occurred when pressure centres were linked, as compared to when the systems were not linked. In both cases, the wind fields were calculated, the wave model was run, and the significant wave height results were compared to buoy data. This test was conducted for the first three months of 1987, which was a relatively severe winter in terms of wave conditions off the west coast. The comparison between the linked and unlinked model runs shows very little difference between the two methods; the results show an average change of less than 2%. Since the linking process increased processing time by upwards of 40%, it was decided that the linking of the pressure features was not warranted for this study. To add justification for this decision, it is worth pointing out that the pressure systems off the B.C. coast were relatively slow moving. Because the displacements of the pressure systems changed by relatively small amounts between the 12 hourly charts, errors introduced by the interpolation scheme are reduced.

4.1.2 Verification

To verify the accuracy of this 3 year hindcast, the wave model output was compared to buoy data that was available for the west coast area. Buoys that collected data consistently during the model period were used for model validation. The model gridpoints that were nearest to these buoys were extracted from the hindcast database for comparison. Here, data from NOAA buoys 46004, 46036, 46184, and MEDS buoy 503 were compared to data from gridpoints 768, 682, 852, and 1283 respectively (see Figure 4.3).

Originally, time series plots and scattergrams were produced, accompanied by standard statistics calculated for each wave parameter. It was found that the model generally performed well in all areas of the model domain, although it was evident that the model was consistently underpredicting wave heights at most locations, and that this underprediction varied with season. For example, winter months showed a larger bias than the summer months, where the climate was less severe.

Wind data existed only for NOAA buoys 46004, 46036, and 46184; therefore, wind statistics were calculated for the buoys. Wind speeds were adjusted according to the stability of the atmospheric boundary layer determined from air–sea temperature differences. Since model wind data are given at 20 m height above sea level, the buoy data was adjusted to that height. Statistics compiled for this adjusted data set showed that correlation coefficients were in the range of 0.61 to 0.74, and biases that ranged from –0.05 m/s to –0.85 m/s. Average scatter indices for wind speed were near 40%, which is slightly higher than those found for H_s and T_p. Average wind directions for these model grid locations 682, 768, 852 were SSW with a standard deviation of near 80°. The average buoy wind direction veered by 12° from the model data (i.e. bias = –12° {model–buoy}). Scatter indices were similar to those calculated for wind speeds and they ranged from 33% to 38%. Correlation coefficients for wind direction ranged from 0.50 to 0.67 for these three verification sites (see Tables 4.1 and 4.2).

It is important to note that the model generally under predicted the wave heights for offshore buoys while it over predicting some inshore sites, eg. gridpoint 1218. Since the model is a deep water wave model, this over prediction can be expected at shallow water sites.

To counteract the consistent under prediction of wave heights in offshore areas, a linear regression analysis was performed on the significant wave height data. Correction factors based on this analysis were applied to the data. Since these affects have a seasonal dependency, the regression analysis was undertaken for each of the four seasons (i.e. Dec.–Feb. = Winter; Mar.–May. = Spring; etc.) for gridpoints 682, 768, 852, 1283. Significant wave height calculated by the model was adjusted by these correction factors α and ß through the simple relation $y=\alpha x+ß$. This procedure was carried out for the verification gridpoints 682, 768, 852, 1218, 1283, and 1365. Gridpoints 682, 768, 852, and 1283 were adjusted with the correction factors calculated at those points, while the inshore sites of 1218, and 1365 were adjusted by the factors calculated for site 1283. This was justified since all three are considered inshore sites. Statistics show that bias essentially is reduced to 0.0 m; with negligible changes to the scatter index, and correlation coefficient between the adjusted and unadjusted data. These statistically–adjusted values provided climate summaries (normals) which are in good agreement with the corresponding measured buoy data over the entire 3 year period.

From Table 4.3, it is shown that over the three year period, correlation coefficients for H_s were on average near 0.82, and the scatter index ranged from 30% to 50%. For T_p, the correlation was lower at 0.34, while the scatter indices were similar to those found for H_s (See Table 4.4). The lower correlations for T_p is typical due to the inherent variability in the measurement of this parameter.

During the hindcast period, there existed only one WAVEC buoy from which wave directional data could be obtained and compared to the model output. Results from this buoy (MEDS buoy 211) agreed well with the model output as can be seen in Table 4.5.

4.2 STORM HINDCASTS

4.2.1 West Coast Study Storm Population

A west coast storm hindcast study was carried out by MPL and OWI (CCC, 1992) in order to describe the extreme wave climate on the West Coast of Canada. In that study, 51 storms were hindcast with the deep water version of the ODGP model. The grid system is shown in Figures 4.1 and 4.2. The storm selection process was essentially the same as that used to identify high–ranked historical storms in the East Coast study. Wind fields were also prepared for each storm selected using the same methodology. The study included a model validation phase. In this section we carry out a more expansive validation consisting of comparisons in all available storms where buoy data exist.

Since the completion of the west coast study, several storms have occurred in which extreme sea states (H_S greater than 12 meters) have been recorded by buoys in the Canadian west coast buoy array. The four most severe of these storms were hindcast in this study using exactly the same methodology as used to hindcast the full population of 51 storms. The additional storms hindcast are:

1. *November 10–16, 1990*. In this storm H_S greater than 14 m was measured at three buoys: 46004, 46205 and 46208. The peak measured H_S of 15.7 meters with associated T_P of 17.10 seconds was measured at 46208.

2. *December 18–24, 1991*. This storm was notable because it generated a peak H_S of 14.32 meters with associated T_P for 15.10 seconds, inside Hecate Strait as measured at buoy 46185.

3. *December 11–17, 1992*. This storm was associated with an eastward propagating band of very strong westerly winds, which approached the Dixon Entrance. Three buoys measured peak H_S exceeding 12 meters in this event, including 14.10 meters at 46184 located about 200 nm west of Dixon Entrance, and 13.76 meters at 46205 located a few miles outside Dixon Entrance.

4. *January 16–20, 1993*. Measurements are available in no less than 11 buoys in this event, which like storm 2 was notable because it generated extreme sea states inside Hecate Strait. Buoy 46185 measured a peak H_S of 13.10 meters, while no buoy offshore recorded a peak H_S greater than 9.23 meters.

4.2.2 Measured Buoy Data

As shown in Figure 4.4, an excellent array of buoy networks of NOAA and AES buoys is well established offshore the west coast of Canada and U.S.A. (along the edge of the ODGP model fine grid domain). In addition, AES has maintained an excellent buoy network along the west coasts of Queen Charlotte Island, Vancouver Island and in Queen Charlotte Sound, Hecate Strait and Dixon Strait. In addition, MEDS, through their west coast wave climate program have provided an excellent coverage of wave measurements using both non–directional (wave only) and directional waverider buoys within the inshore. These buoys (both MET/OCEAN and MEDS buoys) provided an excellent coverage both spatially and temporally with over 5 years of measured data at most locations. The NOAA and AES MET/OCEAN buoys are similar to those described in section 3.2.2

4.2.3 Comparison of Storm Hindcast and Measured Data

Of the total of 55 storms hindcast, measurements were available at least at one buoy in 42 storms. The comparison of peak hindcast and measured H_S and associated T_P, and vector mean wave direction, wind speed and wind direction is given in Table 4.6 for all available data. In the first half of these storms, measurements are available only at either M103, a MEDS waverider buoy moored in shallow water off Tofino, or at the US NOAA offshore buoys 46004, 46005. In storms which occurred after 1987, measurements are typically available in a given storm at ten or more sites.

The west coast array of buoys presents a wide range of exposures. For example, the bathymetry of the west coast is such that is possible to have a buoy in very deep water yet sheltered by nearby land or offshore islands. Therefore the comparison statistics are stratified by grouping the buoys into the following categories:

Offshore Deep	NOAA,AES 46004
	NOAA,AES 46005
	NOAA,AES 46036
	NOMAD 46184
Inshore Deep	AES 46041
	AES 46205
	AES 46206
	AES 46207
	AES 46208
	MEDS 503
Deep, Inshore, Sheltered	AES 46145
	AES 46183
	AES 46185
	AES 46204
	MEDS 211
	MEDS 213
	MEDS 226
	MEDS 257
	MEDS 502
Shallow	MEDS 103

The peak–peak statistics are summarized in Table 4.7 for H_s and T_p for the above categories and overall (all buoys). These differ little from those presented in the west coast hindcast study of extremes. For example, the deep–offshore category in the previous study the mean difference in peak H_S was found to be +0.51 meters. For the expanded validation of this study, Table 4.7 indicates that the mean difference is +0.38 meters. The scatter index for this category is 16.24% with correlation coefficient of 0.83. The mean error in T_P is exceptionally low at .05 second with scatter index of only 11.8%. These indicate that in this study, skill typical of that achieved in other studies of this type carried out in mid–latitude NH basins, was also achieved here. Errors are generally higher for the other categories. However, for the shallow water category, the statistics differ little from those of the deep water category, except that the positive bias is increased to +0.53 m, which is lower than the positive bias of about 0.85 m seen in the East Coast comparisons. The worst statistics are for the sheltered category, with mean difference of –0.8 meters and scatter index of 24.70% for H_S, and mean difference of 0.50 seconds and scatter index of 22.03% for associated T_P. This mainly reflects the significant under hindcast of peak H_s at the buoy inside Hecate Strait in southwesterly storms. This deficiency has been attributed to either a shallow water effect or to wave–current interaction, as discussed in the West Coast study.

4.3 LARGE STORM EVENTS

Further analysis of storm events on the West Coast of Canada shows that some events were under–predicted by the model. Situations such as this tend to occur in very large storm events where wave heights exceed 10 m. In this section, we identify which storm events were under–predicted by the wave modelling on each coast and draw conclusions on the reason for the discrepancies. The time period for this analysis is from 1962 to 1993 on the West Coast.

The largest storms that occurred were assessed in order to determine if hindcast results adequately detailed the event. Of primary interest was significant wave height. Wave model results were obtained from previous studies completed by MPL/OWI (CCC, 1992). Buoy data for the selected storms was obtained from MEDS (which also includes NOAA and AES buoys).

Results

The selection process resulted in 11 storm events (with a total of 19 verification entries) being chosen on the West Coast (see Table 4.8) where the model significantly under–predicted the wave height. Statistical analysis were compiled for each event (Tables 4.9–4.10). It should be noted that statistics were not compiled for the complete storm period, but rather for a shorter ”analysis” period which spanned only the time period of the storms where the largest wave heights occurred (see Table 4.9).

Results from the peak to peak analysis are found in Table 4.9. ΔHs between the model and the buoy ranged from –1.24 m to –5.40 m, with a mean value of –2.47 m. Statistical results (Table 4.10) for the storm analysis periods show that the storm events were described well by the wave model despite the under–prediction of the peak value. The correlation coefficients for H_s ranged from 0.81 to 0.98; and scatter indices ranged from 6.4% to 28.6%. For T_p RMSE varied from 0.8 to 2.55 and S.I. from 5.6% to 18.3%.

Discussion of Results

In order to explain the discrepancies found, time series plots were analyzed to quantify the history of each storm event. Wind error, wind funnelling, shallow water effect, wave sheltering and/or wave–current interaction were noted and are summarized in Table 4.11. It was found that on the West coast wind error was not a factor in causing the wave heights to be under–predicted by the model; as in all cases the modelled wind speed was greater than the measured wind speed. Wave–current interaction was determined to be a possible factor for error along the B.C. coast. The prevailing surf or current direction was S or SW, which was directionally aligned with the wave direction in most storm events. The surface current speed averaged 2 kts or more which could lead to higher wave heights being recorded by the buoys that were produced by the model. Wind funnelling, which increases wind speed; such as the interior waters along the B.C. coast (inlets/bays); was a factor in 6 of the 18 storm events. Shallow water effects were not a factor for error on the West coast except at the Tofino location.

Although the islands off the B.C. coast were accounted for in the model, discrepancies in the accuracy of island representation may be a source of error. Here, modelled waves could be artificially sheltered, thus leading to lower wave heights or vice versa. Six storms were selected on the West coast that potentially could include errors due to this effect.

It should also be noted here that the ”measured” buoy winds were used in the hindcast wind fields, and therefore error statistics would be influenced as shown in the good correlation results between measured and hindcast values. However, the buoy wind, especially in these very large sea states is believed to largely under–predict the true speed. This requires extensive research work which is beyond the scope of this study.

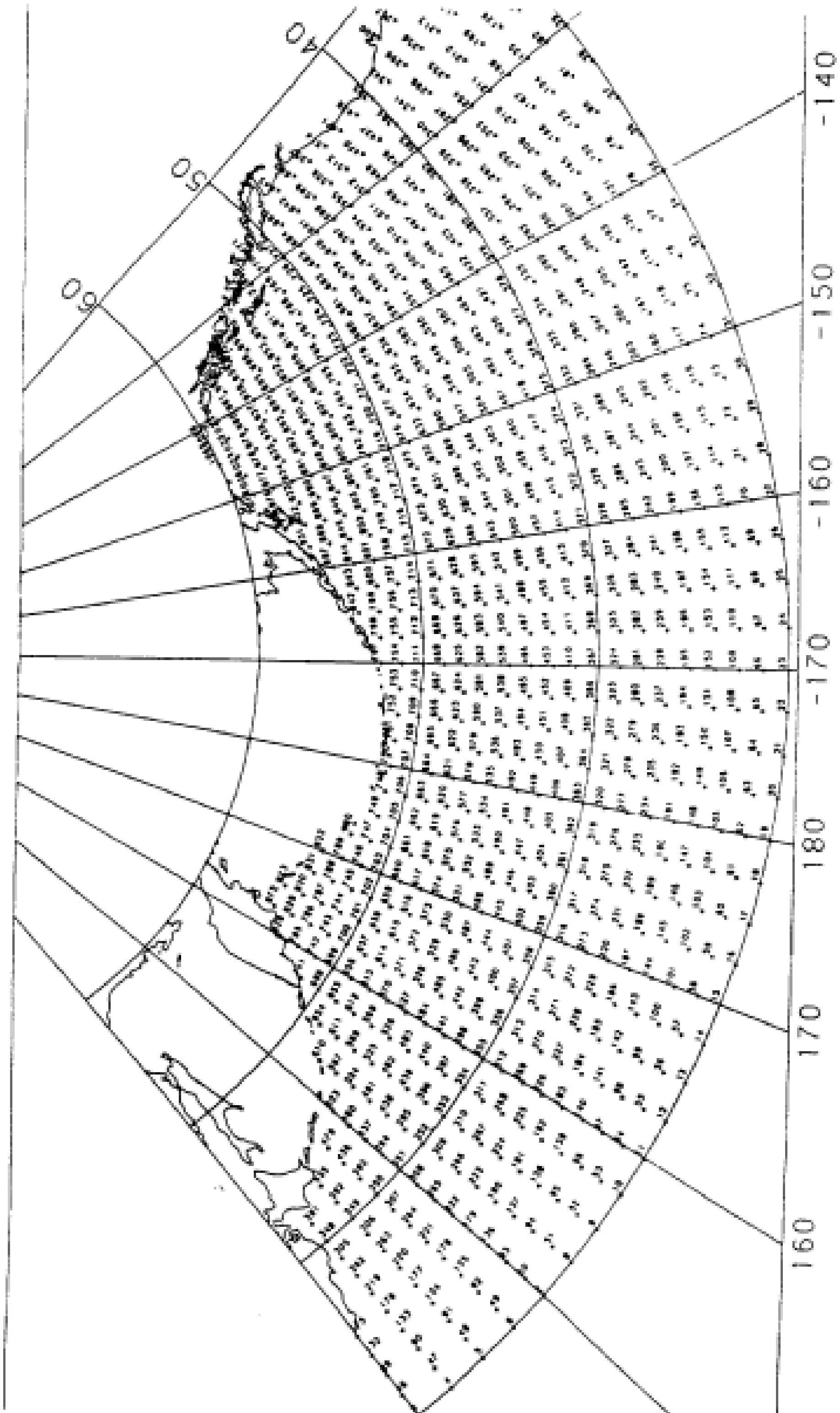

Figure 4.1 ODGP North Pacific Model Grid (PACWAV)

Figure 4.1 ODGP North Pacific Model Grid (PACWAV)

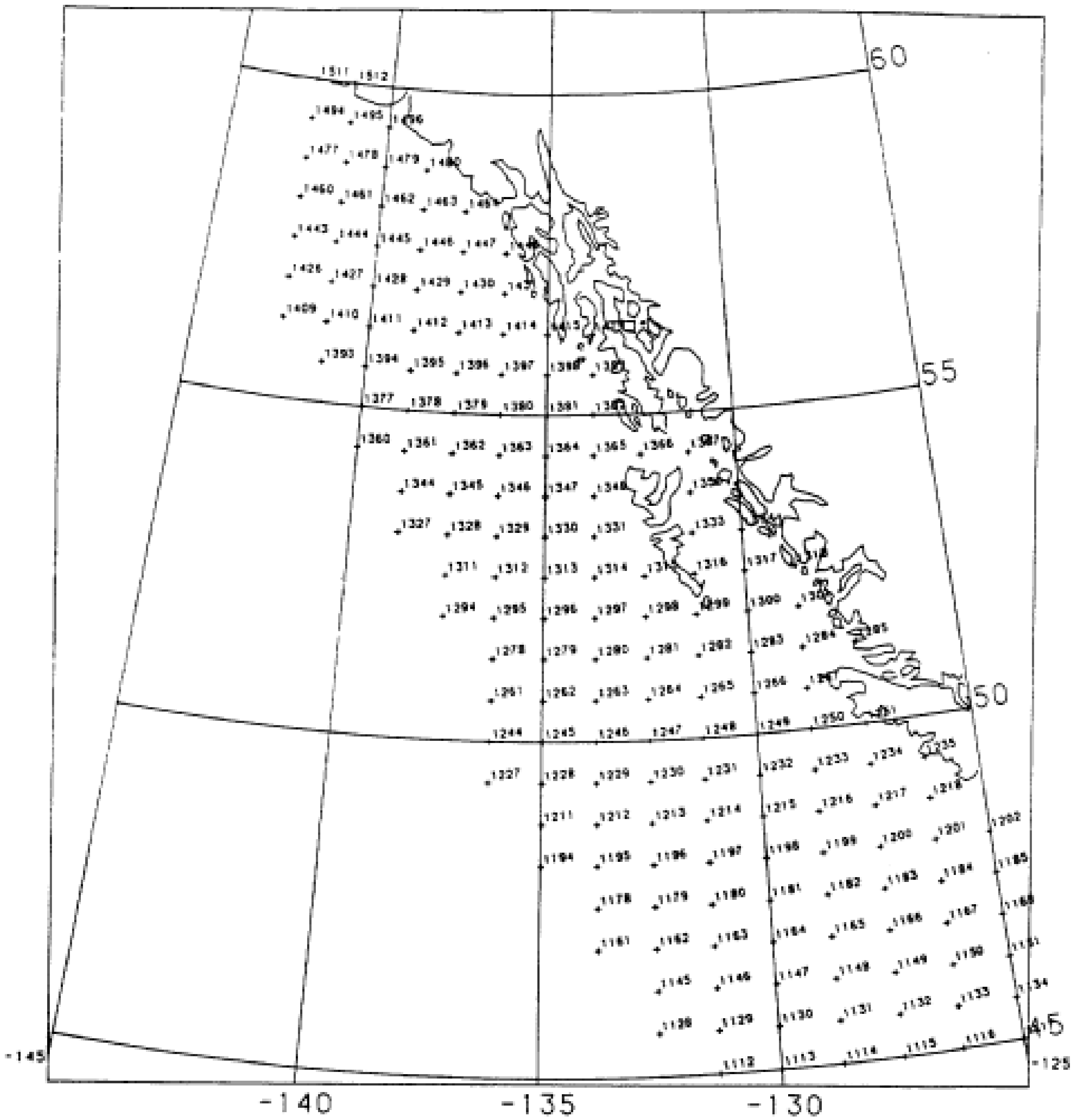

Figure 4.2 ODGP Nested West Coast Fine Grid

Figure 4.2 ODGP Nested West Coast Fine Grid

VERIFICATION OF 3–YEAR HINDCAST

MODEL GRIDPOINTS AND NEAREST BUOYS

Date Range: 1987–01–01 through 1989–12–31

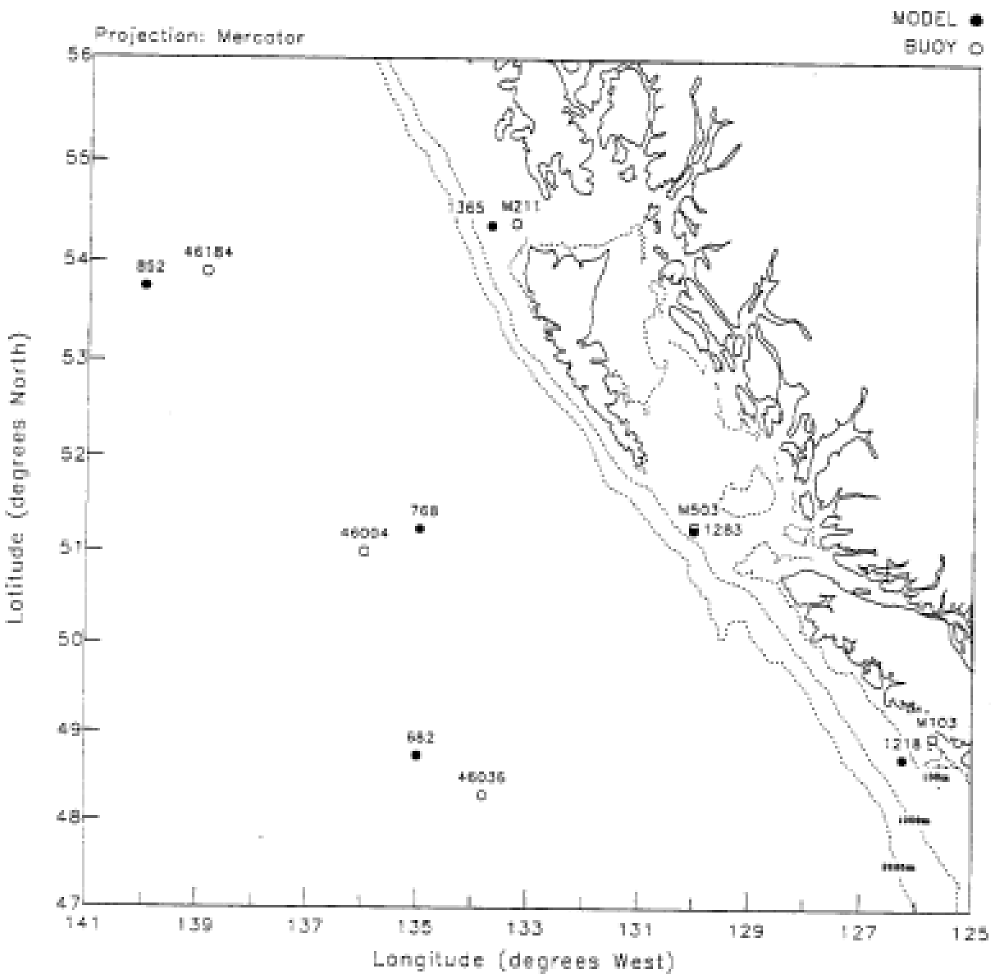

Figure 4.3 Hindcast Verification Map Locations (Buoy & Model Grid)

Figure 4.3 Hindcast Verification Map Locations (Buoy & Model Grid)

Table 4.1 Verification Statistics For H_s: Period 1987–1989

Buoy	Max (m)	Min (m)	Mean (m)	σ (m)	Grid	Max (m)	Min (m)	Mean (m)	σ (m)	Bias (m)	RMSE (m)	Scatter Index
46036	12.30	0.50	2.99	1.48	**682**	10.89	0.00	3.00	1.78	0.01	0.96	32.08
46004	14.80	0.60	3.13	1.51	**768**	11.93	0.00	3.14	1.79	0.01	0.94	30.08
46184	11.00	0.60	2.98	1.50	**852**	11.82	0.33	2.98	1.76	0.00	0.92	30.85
M103	8.68	0.37	2.17	1.15	**1218**	11.79	0.00	2.62	1.79	0.45	1.20	55.29
M503	11.27	0.48	2.65	1.44	**1283**	11.88	0.00	2.66	1.76	0.00	0.99	37.21
M211	10.52	0.56	2.70	1.44	**1365**	9.17	0.11	2.66	1.73	–0.03	1.12	41.63

Table 4.2 Verification Statistics For T_p: Period 1987–1989

Buoy	Max (s)	Min (s)	Mean (s)	σ (s)	Grid	Max (s)	Min (s)	Mean (s)	σ (s)	Bias (s)	RMSE (s)	Scatter Index
46036	23.30	4.20	11.28	2.84	**682**	19.47	3.41	9.53	2.65	–1.76	3.56	31.57
46004	25.00	3.70	11.03	2.86	**768**	19.76	3.87	9.56	2.59	–1.46	3.31	30.05
46184	21.30	4.30	10.96	2.69	**852**	18.02	3.26	8.99	2.37	–1.97	3.58	32.72
M103	22.22	3.45	11.73	3.22	**1218**	20.32	2.76	9.77	2.89	–1.96	4.20	35.80
M503	21.33	4.49	11.40	2.90	**1283**	19.16	1.79	9.27	2.69	–2.12	3.89	34.16
M211	22.20	3.70	11.33	3.17	**1365**	19.96	3.36	9.66	2.90	–1.67	3.76	33.21

Table 4.3 Verification Statistics For Ws: Period 1987–1989

Buoy	Max (m/s)	Min (m/s)	Mean (m/s)	σ (m/s)	Grid	Max (m/s)	Min (m/s)	Mean (m/s)	σ (m/s)	Bias (m/s)	RMSE (m/s)	Scatter Index
46036	25.70	0.00	7.52	3.32	**682**	23.33	0.00	7.01	3.75	–0.52	2.85	37.90
46004	24.30	0.00	7.74	3.72	**768**	26.32	0.10	7.70	4.10	–0.05	3.47	44.78
46184	24.50	0.00	8.24	3.70	**852**	27.03	0.00	7.39	4.22	–0.85	3.04	36.93
M103	*	*	*	*	**1218**	23.01	0.00	6.70	3.60	*	*	*
M503	*	*	*	*	**1283**	23.60	0.00	6.53	3.80	*	*	*
M211	*	*	*	*	**1365**	21.74	0.18	7.58	4.39	*	*	*

Table 4.4 Verification Statistics For Wd: Period 1987–1989

Buoy	Max (°T)	Min (°T)	Mean (°T)	σ (°T)	Grid	Max (°T)	Min (°T)	Mean (°T)	σ (°T)	Bias (°T)	RMSE (°T)	Scatter Index
46036	360.00	0.00	107.44	82.29	**682**	359.00	0.00	128.96	75.18	–1.52	42.60	39.65
46004	360.00	0.00	119.87	78.93	**768**	359.00	0.00	160.26	70.95	–12.69	53.09	44.29
46184	360.00	0.00	119.53	90.62	**852**	359.00	0.00	147.38	80.57	–4.99	40.75	34.09
M103	*	*	*	*	**1218**	359.00	0.00	203.10	96.16	*	*	*
M503	*	*	*	*	**1283**	359.00	0.00	215.33	88.31	*	*	*
M211	*	*	*	*	**1365**	358.00	0.00	201.79	74.93	*	*	*

Table 4.5 Verification Statistics For Wave Direction: Period 1987–1989

Buoy	Max (°T)	Min (°T)	Mean (°T)	σ (°T)	Grid	Max (°T)	Min (°T)	Mean (°T)	σ (°T)	Bias (°T)	RMSE (°T)	Scatter Index
M211	357.00	67.00	115.21	36.80	**1365**	354.00	1.00	138.72	47.55	–20.45	45.61	39.58

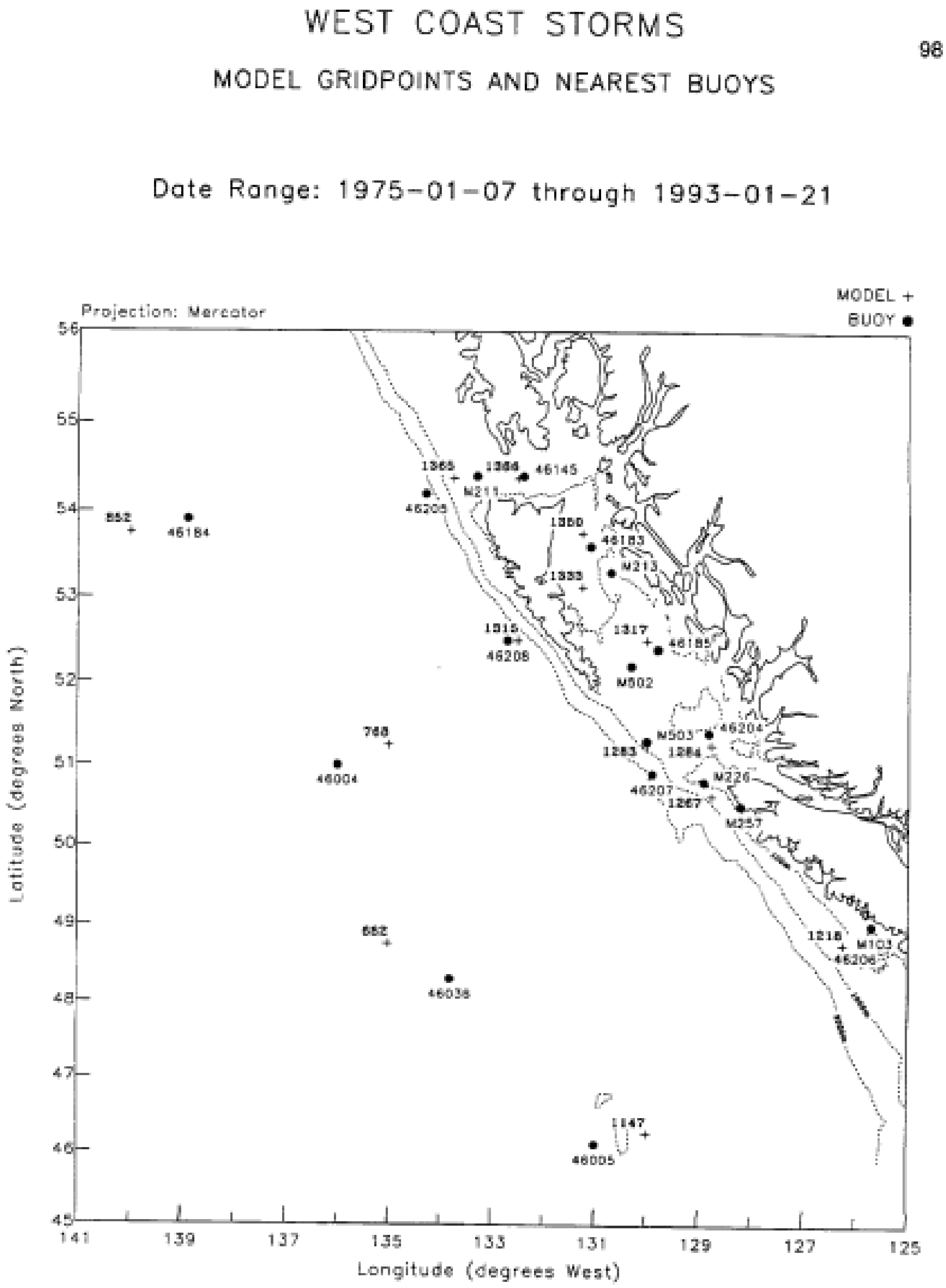

Figure 4.4 West Coast Storms Verification Locations

Table 4.6 Peak to Peak Comparison Using All Available Data

Peak to Peak Comparison (no Smoothing applied)

Date YYMMDD	Stn	BUOY Hs	Tp	Ws	Wdir	ODGP GP	Hs (ODGP)	Tp	VMD from	Ws	Wdir
750107	M103	6.93	15.20			1235	6.3	12.7	257	17.1	273
751113	M103	7.75	12.40			1235	8.6	16.0	206	20.9	187
751221	M103	4.41	10.50			1235	6.5	12.5	178	18.2	155
760127	M103	4.82	12.40			1235	6.8	14.2	229	9.5	192
760222	M103	4.19	9.80			1235	4.7	11.9	220	10.1	156
761026	46004	4.80	10.00	17.4	203	768	5.9	11.9	216	15.0	214
761025	46005	5.50	14.29	15.4	287	1147	6.0	11.8	280	16.3	279
761025	M103	5.49	13.70			1235	5.2	12.2	226	15.9	210
761030	46004	8.00	16.67	17.3	223	768	9.8	15.1	225	22.6	220
761031	46005	5.80	16.67	6.7	201	1147	6.5	14.2	256	13.1	222
761031	M103	6.39	17.10			1235	5.7	15.0	245	14.4	200
770115	46004	6.40	16.67	10.1	187	768	7.8	16.8	221	9.7	179
770117	M103	4.70	17.10			1235	5.7	16.7	240	11.8	181
770213	46004	8.10	14.29	10.9	208	768	8.9	15.1	228	20.6	220
770221	46004	8.50	16.67	20.5	187	768	11.1	15.9	192	22.0	183
771024	46005	7.80	14.29	15.9	238	1147	9.8	15.5	233	18.0	210
771025	M103	8.98	17.10			1235	8.2	17.2	234	15.4	200
780108	M103	4.22	10.50			1235	4.4	12.9	181	14.4	140
780109	46005	5.00	14.29	15.5	134	1347	5.6	11.7	196	11.4	156
781031	46004	7.70	14.29	17.2	220	768	8.3	13.8	225	21.5	206
781031	46005	4.50	14.29	9.9	213	1147	5.8	13.0	255	4.1	284
781102	M103	3.59	13.70			1235	4.9	12.9	252	4.6	295
781214	46004	8.10	16.67	22.6	282	768	9.5	15.4	280	21.6	290
781215	46005	6.10	16.67	12.8	327	1147	7.5	14.9	297	12.5	286
781215	M103	5.33	15.20			1235	6.4	13.2	279	18.2	290
790216	46004	4.40	12.50	5.3	155	768	5.4	10.8	234	16.3	225
790218	46005	4.70	14.29	12.2	220	1147	5.3	11.2	245	12.8	247
790218	M103	5.44	12.40			1235	4.6	11.5	231	8.4	217
790305	46004	6.10	12.50	15.0	223	768	8.2	14.0	233	19.6	233
790307	46005	4.20	12.50	9.1	219	1147	6.9	13.5	227	11.8	201
791121	46004	8.60	14.29	21.0	191	768	11.4	16.5	194	23.1	200
791121	46005	7.30	12.50	12.4	201	1147	10.5	15.6	218	14.5	210
791122	M103	* 6.81	17.10			1235	8.1	16.1	219	13.4	180
791217	M103	* 5.19	9.80			1235	6.2	14.1	212	8.4	171
791218	46005	4.40	16.67	8.2	164	1147	7.5	13.2	206	12.4	191
791222	46004	6.30	14.29	14.6	262	768	6.8	13.1	205	11.1	194
811201	46004	8.80	16.67	15.5	206	768	8.2	14.9	251	17.8	240
811201	46005	7.00	12.50	16.7	267	1147	7.1	14.4	260	12.6	227
811201	M103	5.37	13.70			1235	6.2	14.6	250	13.1	216
840409	M103	7.41	10.50			1235	7.7	14.2	240	10.5	218
840410	46004	8.70	16.67	7.4	196	768	8.8	15.5	236	13.1	216
840411	46005	9.70	16.67			1147	9.1	16.5	266	13.3	245

Table 4.6 (con't) Peak to Peak Comparison Using All Available Data

Peak to Peak Comparison (no Smoothing applied)

Date	Stn	BUOY				ODGP					
YYMMDD		Hs	Tp	Ws	Wdir	GP	Hs	Tp	VMD from	Ws	Wdir
841012	46005	10.70	16.67	20.4	266	1147	10.3	15.3	244	21.0	236
841013	46004	7.50	11.11	12.7	261	768	8.9	12.1	268	23.4	287
841013	M103	8.38	17.10			1235	9.9	16.4	230	22.1	230
841102	46005	10.40	14.29	23.7	270	1147	12.5	16.3	253	24.9	260
841103	M103	7.55	12.40			1235	8.5	15.5	217	14.4	230
850211	M213	8.91	12.40			1333	7.0	13.4	191	23.9	217
850212	M103	6.99	13.70			1235	6.9	14.0	249	11.3	265
850215	46004	11.40	14.29	15.5	251	768	10.9	14.9	237	24.2	240
860107	46004	10.00	14.29	13.8	214	768	9.2	14.1	200	21.1	200
860107	M226	8.27	9.80			1267	6.8	13.9	178	18.0	143
860108	M103	6.68	10.50			1235	5.8	14.5	187	17.0	150
860112	M211	8.19	18.20		225	1365	8.7	14.5	182	20.5	173
860227	46004	9.80	14.29			768	10.5	14.2	184	24.8	179
860227	46005	7.80	16.67	9.9	191	1147	6.4	14.0	228	9.7	205
860228	M103	4.56	15.20			1235	5.2	14.1	233	2.9	207
860228	M211	10.66	18.20		211	1365	9.0	14.8	191	21.3	190
860228	M226	7.14	12.40			1267	6.5	14.6	225	5.8	215
860424	M211	5.45	9.10		119	1365	4.3	8.5	145	17.0	111
860424	M213	7.99	12.40			1333	4.2	10.2	144	15.4	120
860424	M226	7.21	9.10			1267	8.3	14.1	243	14.8	226
860425	46004	8.70	14.29			768	8.4	13.2	299	23.1	320
860425	46005	8.20	14.29	12.7	289	1147	7.6	13.4	271	17.7	266
860425	M103	5.48	13.70			1235	7.5	14.8	254	14.9	240
861118	46004	7.80	11.11	16.3	321	768	7.8	11.3	322	24.1	334
861118	M211	4.73	9.10		83	1365	5.0	9.3	113	21.1	90
861118	M213	5.53	13.70			1333	4.8	9.3	137	20.3	120
861118	M502W	8.83	11.60			1317	5.8	12.2	178	12.7	164
861118	M503W	9.56	16.00			1283	8.1	13.4	217	14.9	190
861119	M103	8.13	17.10			1235	9.2	16.4	248	18.3	236
861123	46004	14.10	16.67	16.2	245	768	11.3	17.2	234	22.1	235
861123	M213	7.37	10.50			1333	4.9	11.9	197	18.4	213
861123	M503W	10.76	16.00			1283	9.9	17.2	243	17.5	250
861124	M103	7.12	15.20			1235	7.5	17.4	256	10.2	292
861124	M211	9.24	18.20		227	1365	9.3	14.8	241	21.1	250
861224	M503W	8.87	14.20			1283	9.0	14.2	244	19.3	241
861225	M213	9.81	12.40			1333	5.6	12.3	187	19.7	193
861226	46004	10.20	16.67	13.3	222	768	10.9	15.6	224	23.1	220
861226	46005	8.10	20.00	8.1	204	1147	7.2	15.1	245	10.1	205
861226	M103	6.69	17.10			1235	6.2	15.3	239	8.8	209
861226	M211	8.22	18.20		248	1365	9.0	15.0	208	19.5	200
870109	46004	7.00	11.11	15.5	187	768	6.8	11.8	197	18.2	181
870109	M211	9.05	11.80		213	1365	6.9	12.6	192	19.1	186
870109	M213	9.16	12.40			1333	5.3	11.2	180	19.9	187
870110	M257	5.73	12.40			1267	5.7	11.8	201	14.0	197
870110	M503W	6.76	10.70			1283	6.3	12.1	203	17.5	185
870111	M103	5.12	9.10			1235	5.5	12.5	207	14.9	204
870112	46005 *	7.10	14.29	13.0	200	1147	6.5	13.0	223	16.5	199

Table 4.6 (con't) Peak to Peak Comparison Using All Available Data

Peak to Peak Comparison (no Smoothing applied)

Date	Stn	BUOY				ODGP					
YYMMDD		Hs	Tp	Ws	Wdir	GP	Hs	Tp	VMD from	Ws	Wdir
870416	46004	10.60	14.29	16.0	247	768	9.7	14.5	241	22.3	233
870416	46005	6.60	16.67	3.5	253	1147	5.8	14.0	273	4.8	279
870416	46036	7.54	14.30			682	7.6	14.7	254	16.2	234
870416	M103	6.49	15.40			1235	5.1	14.7	265	10.7	277
870416	M211	10.52	12.50		245	1365	9.4	14.0	233	23.1	240
870416	M213	5.61	9.80			1333	4.8	9.6	204	20.1	216
870416	M257	5.47	15.20			1267	6.7	14.8	258	11.8	257
870416	M502W	5.01	10.20			1317	6.5	12.5	223	17.9	223
870416	M503W	7.80	14.20			1283	7.3	15.1	251	14.1	241
871208	M103	7.62	13.30			1235	8.3	14.8	185	21.5	161
871208	M503W	11.27	13.50			1283	9.3	13.9	165	22.6	154
871210	46004	9.10	12.50	13.4	272	768	9.1	15.9	253	17.8	263
871210	46005	10.40	14.29	16.5	258	1147	9.3	15.4	256	13.7	251
871210	46036	11.10	14.20	10.1	57	682	10.9	16.2	259	22.5	255
871210	46041	* 7.13	16.70	10.0	260	1185	8.9	15.4	251	16.6	265
880112	M503W	8.82	11.60			1283	9.4	14.8	227	16.6	230
880113	46004	8.90	16.67	11.7	133	768	9.4	14.5	243	21.3	240
880115	46005	11.00	14.29	16.4	251	1147	10.3	15.8	241	20.5	240
880115	46036	7.20	13.50	12.1	281	682	9.0	14.9	240	19.3	247
880115	M103	7.32	13.30			1235	8.4	15.7	228	19.0	240
880116	46041	7.30	14.30	13.0	240	1185	9.6	15.9	234	15.4	234
880304	46184	7.70	12.80	10.4	155	853	8.5	13.8	222	20.4	222
880304	M502W	7.71	12.20			1317	8.5	14.9	217	20.6	217
880305	46004	8.90	12.50	14.2	242	768	10.1	14.5	230	24.2	230
880305	46005	11.00	16.67			1147	10.9	15.8	246	22.1	240
880305	46036	12.00	14.20	4.7	100	682	10.4	14.2	257	25.3	276
880306	46041	7.22	16.70	12.0	240	1185	9.8	15.9	252	15.9	266
880306	M103	8.49	18.20			1235	9.8	16.2	239	20.6	240
881121	M502W	* 5.91	10.70			1317	9.1	15.5	235	23.1	240
881122	46004	9.90	12.20	20.0	305	768	11.7	16.1	281	25.0	284
881122	46036	11.20	14.20	15.9	294	682	11.7	16.0	279	23.9	284
881123	46041	9.20	16.70	10.0	270	1185	9.1	16.1	262	15.7	269
881123	46184	7.80	14.20	8.5	244	853	9.8	15.1	284	23.4	297
881123	46205	8.90	12.20	14.9	302	1365	6.7	13.9	264	16.6	283
881123	46206	9.20	15.10	12.6	288	1218	9.6	16.1	256	18.0	250
881123	M103	8.06	16.70			1235	8.7	15.9	253	18.5	250
881127	46004	14.80	17.10	19.1	250	768	12.9	16.6	238	27.2	228
881127	46036	10.10	18.30	14.6	248	682	10.2	16.2	251	21.6	236
881127	46184	10.50	12.20	17.6	296	853	10.8	14.1	261	26.2	290
881127	46205	12.80	17.10	13.3	187	1365	11.4	15.7	229	25.7	240
881127	M502W	6.89	11.60			1317	8.1	17.3	226	17.0	220
881128	46041	6.32	16.70	5.0	260	1185	6.9	15.8	270	13.2	295
881128	46206	7.70	18.30	9.7	276	1218	7.5	16.2	261	12.6	283
881128	M103	7.64	18.20			1235	6.8	16.1	258	11.8	274
881129	46184	7.90	12.80	15.8	179	853	9.6	14.0	195	22.1	180
881130	46004	10.10	12.80	18.2	205	768	9.1	14.4	205	23.7	190
881130	46036	7.00	12.80	10.4	227	682	7.2	14.6	216	20.0	186
881130	46205	12.20	14.20	17.1	219	1365	9.4	14.7	211	23.7	230
881130	46206	4.10	13.50	8.2	138	1218					
881130	M502W	6.94	11.10			1317	6.7	14.6	203	21.1	180

Table 4.6 (con't) Peak to Peak Comparison Using All Available Data

Peak to Peak Comparison (no Smoothing applied)

Date	Stn	BUOY				ODGP					
YYMMDD		Hs	Tp	Ws	Wdir	GP	Hs	Tp	VMD from	Ws	Wdir
881201	M103	4.12	13.30			1235					
881202	46206	4.40	12.20	8.8	310	1218	4.7	12.3	224	12.4	182
881203	46004	* 7.40	15.10	9.4	224	768	8.5	13.6	187	20.5	176
881203	46036	* 6.40	16.00	11.0	173	682	8.0	13.4	195	20.4	183
881203	46184	* 7.10	12.80	13.5	188	853	8.2	14.1	179	18.6	168
881203	46205	9.60	15.10	15.9	153	1365	7.1	13.7	181	18.0	169
881203	M211	7.91	15.40		222	1365	7.1	13.7	181	18.0	169
881204	M103	3.40	13.30			1235	4.3	12.5	222	12.7	180
890120	46004	*11.20	16.00	16.8	232	768	11.1	17.4	230	24.2	220
890120	46005	6.30	16.67	8.5	231	1147	6.9	16.1	268	10.1	262
890120	46036	* 6.40	16.00	13.8	199	682	9.9	16.2	253	21.6	240
890120	46184	* 7.60	15.10	7.8	243	853	10.3	17.0	211	19.8	213
890120	46205	* 7.90	13.50	14.8	175	1365	9.8	15.2	211	20.9	200
890120	M503W	* 5.00	12.80			1283	9.0	17.3	242	18.7	237
901027	46036	8.80	15.10	12.60	233	682	9.60	16.20	223	22.12	200
901027	46004	12.60	15.00	21.16	199	768	11.10	16.00	222	22.64	210
901027	46184	9.70	13.50	16.10	115	852	9.80	15.00	220	22.12	220
901027	46206	5.20	14.20	11.00	381	1218	6.20	15.40	240	10.29	200
901027	M103	5.83	14.29	-99.00	-099	1218	6.20	15.40	240	10.29	200
901027	46207	7.80	16.00	9.00	185	1283	8.20	16.20	216	16.46	190
901027	46204	5.90	18.30	7.80	174	1284	7.50	16.40	226	13.89	190
901027	46208	10.40	17.10	12.30	183	1315	9.60	16.10	216	19.55	210
901027	46205	15.00	17.00	18.16	167	1365	9.60	15.40	193	22.12	170
901112	46036	8.90	15.10	12.10	238	682	11.03	15.26	225	26.75	230
901112	46004	14.00	16.00	23.90	220	768	12.43	15.94	215	30.91	222
901112	46184	9.30	12.20	19.30	038	852	7.53	11.11	359	25.24	337
901112	46208	15.70	17.10	16.80	189	1315	11.95	16.36	211	25.21	200
901112	46205	14.70	17.10	17.10	163	1365	10.68	15.73	189	23.91	170
901113	46206	6.00	15.10	7.40	256	1218	7.40	14.17	240	7.06	271
901113	M103	6.36	15.38	-99.00	-099	1218	7.40	14.17	240	7.06	271
901113	46207	9.50	16.00	8.80	199	1283	10.22	16.36	213	23.15	190
911219	46145	6.13	15.10	12.70	280	1366	6.27	12.71	276	19.55	290
911220	46036	8.53	12.20	17.10	161	682	7.68	12.82	193	18.05	193
911220	46005	8.30	12.50	-99.00	-099	1147	9.26	13.82	202	22.06	193
911220	46207	10.92	10.20	21.90	158	1283	9.37	12.87	174	23.43	163
911220	46204	9.67	12.20	17.80	138	1284	8.53	14.77	199	17.17	192
911220	46208	9.44	12.80	13.60	179	1315	8.55	13.26	166	21.63	156
911220	46185	14.32	15.10	22.20	129	1317	9.91	13.09	159	28.82	142
911220	46183	9.80	12.80	20.00	138	1350	7.77	13.02	151	24.16	140
911221	46004	9.50	14.20	8.20	251	768	8.34	13.75	218	18.81	230
911221	46184	9.51	15.10	11.50	243	852	7.25	12.06	294	21.86	300
911221	46206	6.60	12.80	6.80	193	1218	7.51	15.21	205	15.06	176
911221	M103	7.20	13.33	-99.00	-099	1218	7.51	15.21	205	15.04	176
911221	46205	7.99	13.50	11.80	254	1365	7.01	13.09	162	18.01	150
921212	46185	8.35	9.85	16.10	130	1317	7.24	17.85	240	18.52	240
921213	46184	14.10	17.07	19.20	130	852	12.96	18.48	233	25.72	250
921213	46183	6.71	11.13	16.30	137	1350	4.92	8.74	232	21.09	240
921214	46036	9.68	18.29	10.10	284	682	10.24	18.08	258	17.15	242
921214	46004	13.84	17.07	16.40	260	768	12.08	19.02	248	21.13	237
921214	46005	7.08	16.67	-99.00	-099	1147	7.69	17.26	275	12.92	298
921214	46206	7.18	17.07	9.00	279	1218	7.75	18.58	268	11.90	284
921214	46207	9.36	17.07	11.50	260	1283	9.64	18.25	254	15.61	243
921214	46204	8.95	17.07	8.20	280	1284	9.16	18.14	255	14.92	250
921214	46205	13.76	19.69	22.90	274	1365	12.18	16.46	243	24.57	240
921214	46145	11.25	17.07	14.60	231	1366	10.01	16.61	249	21.79	233

Table 4.6 (con't) Peak to Peak Comparison Using All Available Data

Peak to Peak Comparison (no Smoothing applied)

Date	Stn	BUOY				ODGP					
YYMMDD		Hs	Tp	Ws	Wdir	GP	Hs	Tp	VMD from	Ws	Wdir
930117	46184	4.97	8.98	7.60	170	852	4.86	11.99	244	11.83	250
930118	46004	6.89	10.24	14.50	162	768	6.42	10.80	188	21.09	160
930118	46205	8.26	10.24	4.30	183	1365	6.57	11.32	162	16.64	140
930118	46145	4.34	7.42	17.80	143	1366	5.79	10.40	148	23.66	140
930119	46005	7.69	12.50	-99.00	-099	1147	7.16	12.72	218	19.20	210
930119	46206	5.75	9.85	0.00	180	1218	6.70	14.40	197	18.70	156
930119	M103	5.46	10.53	-99.00	-099	1218	6.70	14.40	197	18.70	156
930119	46207	9.23	12.19	14.50	147	1283	8.86	12.84	188	22.12	190
930119	46204	7.38	9.85	20.10	123	1284	8.70	12.36	171	26.24	140
930119	46185	13.10	12.80	18.80	136	1317	9.04	13.23	175	22.64	169
930119	46183	8.75	11.64	19.50	144	1350	7.30	12.25	158	23.15	150

Notes : For M211, values are Hs, Tp and peak direction
* indicates value may not be at a peak

Table 4.7 West Coast Storm Peak to Peak Comparison Statistics (Using All Available Measured Data)

Var	Model	Num of Points	Ave. Obs.	Std. Dev.	Ave. Model	Std. Dev.	MeanError	RMSE	Scatter Index	Corr. Coeff.
Hs (m)	Offshore Deep	86	8.52	2.37	8.90	1.95	0.38	1.38	16.24	0.83
	Inshore Deep	39	9.01	2.74	8.64	1.65	–0.38	1.89	20.96	0.74
	Sheltered	40	7.95	2.19	7.15	1.69	–0.80	1.96	24.70	0.59
	Shallow	38	6.25	1.46	6.78	1.52	0.53	1.01	16.23	0.83
	All Buoys	203	8.08	2.44	8.11	1.98	0.03	1.57	19.38	0.77
Tp (s)	Offshore Deep	86	14.54	2.05	14.60	1.78	0.05	1.72	11.80	0.60
	Inshore Deep	39	14.69	2.43	15.05	1.65	0.36	1.76	12.00	0.70
	Sheltered	40	12.77	2.96	13.27	2.42	0.50	2.81	22.03	0.47
	Shallow	38	13.98	2.61	14.58	1.55	0.60	2.12	15.18	0.61
	All Buoys	203	14.12	2.52	14.42	1.94	0.30	2.06	14.60	0.61

Table 4.8 West Coast Storms

STORM	STORM PERIOD	ANALYSIS PERIOD	BUOY	GRID
1	86112100–86112518	86112300–86112500	46004	768
2A	87120400–87121018	87120512–87120612	M503	1283
2B	87120400–87121018	87120800–87120900	M503	1283
3	88030200–88030712	88030512–88030612	46036	682
4A	88112500–88112818	88112706–88112812	46205	1365
4B	88112700–88120112	88112700–88112812	46004	768
5	88112700–88120112	88113000–88120106	46205	1365
6	88120100–88120500	88120312–88120400	46205	1365
7A	90102600–90102812	90102612–90102800	46004	768
7B	90102600–90102812	90102612–90102800	46205	1365
8A	90111000–90111600	90111212–90111312	46208	1315
8B	90111000–90111600	90111212–90111312	46205	1365
8C	90111000–90111600	90111200–90111400	46004	768
9A	91121700–91122400	91122000–91122112	46207	1283
9B	91121700–91122400	91122000–91122112	46185	1317
10A	92121100–92121600	92121312–92121512	46205	1365
10B	92121100–92121600	92121400–92121500	46145	1366
10C	92121100–92121600	92121312–92121500	46004	768
11	93011600–93012100	93011818–93012000	46185	1317

Table 4.9 West Coast Storms: Peak to Peak Analysis

Storm	Date (Buoy)	Buoy	Hs (m)	Tp (s)	Wd (fr)	Ws (m/s)	Date (Model)	Grid Point	Hs (m)	Tp (s)	VMD (fr)	Ws (m/s)	Wd (fr)
1	861123–15:00	46004	14.10	16.67	245	16.17	861123–14	768	11.31	17.17	234	22.13	235
2A	871205–19:57	M503W	10.42	11.60	–99	–99.0	871205–20	1283	8.95	12.33	177	23.97	154
2B	871208–07:57	M503W	11.27	13.50	–99	–99.0	871208–08	1283	9.31	13.90	165	22.58	154
3	880305–21:13	46036	12.00	14.20	319	1.20	880305–20	682	10.50	14.20	257	25.21	280
4A	881127–17:27	46205	12.70	16.00	206	12.70	881127–18	1365	11.42	15.73	229	25.72	240
4B	881127–12:49	46004	14.80	17.10	250	19.10	881127–14	768	12.85	16.55	238	27.19	228
5	881130–19:27	46205	12.20	14.20	219	17.10	881130–18	1365	9.39	14.66	211	23.66	230
6	881203–19:27	46205	9.60	15.10	153	15.90	881203–20	1365	7.13	13.74	181	18.02	169
7A	901027–00:39	46004	12.60	15.00	199	21.16	901027–08	768	11.10	16.00	222	22.64	210
7B	901027–06:41	46205	15.00	17.00	167	18.16	901027–10	1365	9.60	15.40	193	22.12	170
8A	901112–22:52	46208	15.70	17.10	189	16.80	901113–00	1315	11.95	16.36	211	25.21	200
8B	901112–22:52	46205	14.70	17.10	163	17.10	901113–02	1365	10.68	15.73	189	23.91	170
8C	901112–18:47	46004	14.00	16.00	220	23.90	901112–20	768	12.43	15.94	215	30.91	222
9A	911220–17:52	46207	10.92	10.20	158	21.90	911220–22	1283	9.37	12.87	174	23.43	163
9B	911220–16:52	46185	14.32	15.10	129	22.20	911220–20	1317	9.91	13.09	159	28.82	142
10A	921214–05:52	46205	13.76	19.69	274	2.90	921214–08	1365	12.18	16.46	243	24.57	240
10B	921214–06:34	46145	11.25	17.07	231	14.60	921214–08	1366	10.01	16.61	249	21.79	233
10C	921214–03:47	46004	13.84	17.07	260	16.40	921214–02	768	12.08	19.02	248	21.13	237
11	930119–08:52	46185	13.10	12.80	136	18.80	930119–14	1317	9.04	13.23	175	22.64	169

Δ = Model–Buoy

Table 4.10 Statistics for Selected Large Storms on the West Coast: Analysis Periods

VAR	STORM	POINTS	AVE. OBS.	STD. DEV.	AVE. MODEL	STD. DEV.	BIAS (m)	RMSE (m)	SCATTER INDEX	CORR. COEFF.
HS (m)	1	25	7.62	2.63	8.14	1.96	0.52	1.07	14.05	0.96
	2A	8	7.17	1.72	7.85	0.78	0.67	1.30	18.08	0.81
	2B	5	7.99	2.46	7.87	1.60	–0.11	1.00	12.50	0.94
	3	12	8.93	1.67	9.04	1.16	0.12	0.57	6.35	0.98
	4A	15	9.26	2.12	8.89	1.86	–0.37	0.84	9.06	0.93
	4B	18	9.13	2.39	9.39	2.09	0.26	0.91	9.92	0.93
	5	15	8.93	1.68	7.82	1.42	–1.11	1.22	13.64	0.96
	6	4	8.10	0.78	6.95	0.17	–1.15	1.28	15.83	0.83
	7A	18	6.92	2.51	7.94	2.35	1.02	1.53	22.13	0.88
	7B	18	7.14	3.71	6.56	1.99	–0.59	2.04	28.61	0.92
	8A	12	9.23	3.69	9.40	1.88	0.18	1.95	21.18	0.94
	8B	13	8.41	3.18	7.64	2.30	–0.77	1.74	20.74	0.87
	8C	25	6.12	3.02	7.30	2.89	1.19	1.75	28.54	0.90
	9A	19	7.94	2.08	7.32	1.85	–0.62	1.17	14.78	0.87
	9B	18	8.36	3.40	7.28	1.98	–1.08	2.24	26.77	0.85
	10A	25	8.62	2.95	7.71	2.40	–0.91	1.39	16.08	0.94
	10B	13	7.84	1.78	7.86	1.53	0.01	0.83	10.59	0.87
	10C	18	9.83	2.53	9.93	1.75	0.10	1.46	14.83	0.82
	11	16	8.28	2.80	6.84	1.52	–1.44	2.07	25.04	0.92

Table 4.10 (con't) Statistics for Selected Large Storms on the West Coast: Analysis Periods

VAR	STORM	POINTS	AVE. OBS.	STD. DEV.	AVE. MODEL	STD. DEV.	BIAS	RMSE	SCATTER INDEX	CORR. COEFF.
T_P (s)	1	25	13.83	2.88	14.28	1.98	0.45	1.55	11.20	0.87
	2A	8	12.31	1.63	12.30	0.98	–0.02	0.69	5.64	0.96
	2B	5	12.72	0.83	13.50	0.63	0.78	1.02	8.01	0.53
	3	12	12.83	1.37	13.60	0.77	0.77	1.05	8.16	0.91
	4A	15	14.32	2.41	14.23	1.43	–0.09	1.34	9.34	0.86
	4B	18	14.11	2.60	14.41	1.62	0.30	1.41	9.99	0.88
	5	15	13.10	1.10	13.87	0.56	0.77	1.41	10.78	0.01
	6	4	15.10	0.73	13.78	0.26	–1.32	1.53	10.16	–0.57
	7A	18	12.22	2.32	13.12	2.27	0.90	2.11	17.27	0.63
	7B	18	12.44	2.31	12.48	2.19	0.03	1.34	10.80	0.81
	8A	12	13.46	2.39	14.73	1.56	1.27	1.91	14.22	0.80
	8B	13	12.78	3.44	12.60	2.77	–0.17	1.13	8.87	0.95
	8C	25	11.00	2.11	12.55	2.46	1.54	2.01	18.30	0.84
	9A	19	11.97	1.84	11.59	2.24	–0.38	1.95	16.33	0.55
	9B	18	12.37	2.41	11.65	2.34	–0.71	1.63	13.22	0.80
	10A	25	15.27	2.47	14.42	1.69	–0.85	1.32	8.66	0.94
	10B	13	16.72	1.69	15.64	0.67	–1.08	1.86	11.14	0.35
	10C	18	15.42	1.57	17.02	1.64	1.60	2.46	15.93	0.29
	11	16	11.08	1.78	11.42	1.77	0.34	0.80	7.20	0.91

Table 4.11 Possible Sources of Error for Large Storms on the West Coast

STORM	BUOY	GRID POINT	ΔHs (m)	CORR COEF	BIAS (m)	WIND FUNNEL	SHALLOW WATER	WAVE SHELTER	CURRENT –WAVE
1	46004	768	–2.79	0.96	0.52	NO	NO	NO	NO
2A	M503W	1283	–1.47	0.81	0.67	NO	NO	NO	NO
2B	M503W	1283	–1.96	0.94	–0.11	NO	NO	NO	NO
3	46036	682	–1.50	0.98	0.12	NO	NO	NO	NO
4A	46205	1365	–1.28	0.93	–0.37	NO	NO	NO	NO
4B	46004	768	–1.95	0.93	0.26	NO	NO	NO	NO
5	46205	1365	–2.81	0.96	–1.11	NO	NO	NO	NO
6	46205	1365	–2.47	0.83	–1.15	NO	NO	NO	NO
7A	46004	768	–1.50	0.88	1.02	NO	NO	NO	NO
7B	46205	1365	–5.40	0.92	–0.59	YES	NO	NO	NO
8A	46208	1315	–3.75	0.94	0.18	NO	NO	YES	NO
8B	46205	1365	–4.02	0.87	–0.77	YES	NO	YES	NO
8C	46004	768	–1.57	0.90	1.19	NO	NO	NO	NO
9A	46207	1283	–1.55	0.87	–0.62	YES	NO	NO	NO
9B	46185	1317	–4.41	0.85	–1.08	YES	?	YES	NO
10A	46205	1365	–1.58	0.94	–0.91	NO	NO	NO	NO
10B	46145	1366	–1.24	0.87	0.01	YES	?	YES	NO
10C	46004	768	–1.76	0.82	0.10	NO	NO	NO	NO
11	46185	1317	–4.06	0.92	–1.44	YES	?	YES	NO

5.0 SUMMARY AND CONCLUSIONS

5.1 SUMMARY

This study has attempted to accomplish two objectives:

(1) Verify wave hindcasts in Canadian waters, including Great Lakes, East Coast and West Coast of Canada all made with contemporary wave models.

(2) Summarize and assess the error characteristics of the hindcast series and the reliability of the wave climate descriptions derived from the hindcasts.

Various models were used to provide wave climate in the Great Lakes. The models accuracy varied from one lake to another. The WIS hindcast, which covered all lakes appeared to provide a consistent and reasonably acceptable hindcast results.

All hindcast studies made for the East Coast and West Coast offshore areas were made with the same model: namely, the ODGP deep water fully discretized spectral wave model, thus simplifying somewhat the study because even though the model's physics and numerics might contribute to some error in the hindcast these factors should not contribute to differential behaviour in hindcasts seen in different studies. The following assessments are therefore restricted exclusively to the studies carried out using the ODGP model. This model has also been used in a large number of hindcast studies in other basins and has been compared recently in controlled hindcasts with the performance of other well tuned spectral models, including the third generation (3G) WAM model.

Table 5.1 gives a concise summary of the errors in the continuous and storm hindcast studies made with the ODGP model off the East and West Coasts.

The results for the West Coast were derived from the continuous three–year hindcasts carried out as part of this study as described in section 4.1 . The results from the East Coast study are from a previous study in which wind fields were generated by quite a different procedure. The statistics from the West Coast study are from comparisons of hindcasts and measurements at NOAA and AES offshore buoys moored in deep water. There were no buoys with comparably deep water exposure available for evaluation of the East Coast three year hindcast study, though most are in deep enough water for waves of low to moderate intensities (not storm sea states) to be considered deep water. The east coast comparisons are mainly against waverider buoys maintained by MEDS as part of the exploratory drilling programs. Despite these differences of approach and verification the errors in H_S and T_P are not substantially different between the different basins. Scatter index in H_S is exactly 31% in both studies. The hindcast spectral peak period is biased low in both basins, by 0.4 seconds on the East Coast and 1.7 seconds on the West Coast. This bias is probably attributable to the difficulty of resolving background swells, an effect which is likely to be greater in comparisons on the eastern margin of a major ocean than on the western margin. The scatter in T_P hindcasts in the continuous studies is also larger off the West Coast than off the East Coast. This scatter is contributed to also by the more common occurrences of double peaks in measured spectra than in hindcast spectra.

The hindcasts for East Coast and West Coast storms are both made from wind fields of potentially greater accuracy than the winds derived for the three–year hindcasts. The energy level of storm generated sea states is also, of course, greater on average than those of continuous hindcasts. For these reasons, the verification of storm hindcasts exhibit greater relative skill than the continuous hindcasts, with scatter index of H_S and T_P of 10%–20%, which is comparable to reported skill in storm hindcasts made with the ODGP and other well tuned models in other world basins and for a wide range of storm types. The positive bias in H_S seen in the East Coast storm verification appears to arise mainly in the unavoidable use of verification sites of water depths in the range of 50–100 m, a depth range which may be considered deep water for moderate immature sea states, but shallow water for high–amplitude, long period storm generated seas and swells. Interestingly, while the absolute error of H_S (e.g. RMSE) for storms is greater than for the continuous hindcasts, the absolute error for peak storm T_P is lower for storms. We attribute this to the tendency for spectra of peak sea states in storms to be single– peaked with little swell content.

While the bias in H_S in the storm verification is positive (hindcast greater than measured) in both basins, this masks a definite characteristic for the hindcast to under specify the peak sea states in the largest storm peaks, when peak H_S exceeds about 12 m. This effect was especially shown in the West Coast verification because more such peaks were measured at the offshore deep–water buoys. Water depth limitations at the verification sites used for the East Coast storms may have limited the occurrence of these very extreme sea states in the East Coast storm verification comparison data base. However, within the past few winters a number of very extreme storms have occurred off the East Coast following the deployment of AES buoys in deep water south off Nova Scotia and the Grand Banks. The verification of the Halloween storm hindcast peaks, summarized in this report as well, show the model hindcasts to exhibit a negative bias which derives mainly from the storm peaks above 12 meters. A similar result is found in the hindcast of the so–called ”Storm of the Century” of March 1993 (Cardne et al., 1995).

Wind fields derived from these recent storms are probably more accurate than wind fields derived for the earlier historical storms hindcast in the West Coast and East Coast studies. This is because of the enhancement of the MET/OCEAN buoy network in both areas. The recent wind fields appear to resolve surface wind ”jet streaks” much better than earlier storms. These are features which maintain spatial and temporal coherency of at least 24 hours and propagate at speeds of 10–20 m/sec. Maximum wind speeds (1–hour average at 20 m height) in these jet streaks may range as high as 35 m/sec. Buoys which measure peak H_S in excess of about 12 m seem to lie directly in the path of these jet streaks. Outside of these features ODGP model hindcasts of storm peaks H_S and T_P are nearly unbiased with scatter index of 10–15%.

5.2 SOURCES OF ERROR

In this section we discuss the sources of errors in the hindcasts found in this study. We draw these tentative conclusions from results of this study and also from results of several related studies recently completed, namely the SWADE hindcast study (Cardone et al., 1994) in which alternative hindcasts of a moderate storm of the US East Coast was carried out with the WAM model using 6 different wind fields, and the study of the ”Halloween Storm” and ”Storm of the Century” (Cardone et al., 1995) carried out with one wind field and four different models, including the ODGP model.

5.2.1 Wind Errors

There seems to be little doubt that errors in surface wind fields are the largest single source of error in ODGP model hindcasts of deep water offshore sea states for both ”continuous” and ”storm” regime hindcasts. The only exception to this conclusion, at least for the stated model and regimes, may be in the specification of extreme storm waves (H_S greater than about 12 m) generated along rapidly propagating ”jet streaks”, where some other effect seems to be contributing to a tendency for the model hindcasts to systematically under specify peak sea states by up to 20%. Outside of these regimes, it appears that if wind fields could be significantly more accurately specified than possible for the historical series hindcast for these studies (such as they were in SWADE), ODGP model hindcast technology leads to errors in storm peak sea states of negligible bias and scatter index as low as 10% in H_S and T_P.

Within the core of energetic ”jet streaks” a wave model deficiency (either physics or numerics) may be responsible for the negative bias. However, it should be noted that even in recent studies the standard used for assessment for accuracy of wind fields has been measurements of wind from moored buoys, mainly vector averaged wind speeds from anemometers mounted at 4–5 m height on NOMAD hull buoys. It is quite possible that even after ”adjusting” the raw buoy wind speed measurements for averaging interval, anemometer height and thermal stability to produce an effective neutral 1–hour average at 20–m, that the adjusted winds are still biased low in extreme sea states.

Recommendation

With the increasing proliferation of small hulled moored buoys with low–mounted anemometers, better understanding of the accuracy of measured buoy surface winds is needed. One approach is to calibrate the measurements over a wide–range of sea states against data acquired from a fixed platform with a well exposed high–mounted anemometer. A large number of suitable platforms exist in the North Sea where the harsh wave climate provides an opportunity to sample a wide range of conditions in one winter season. Also the LASMO rig off the east coast at Cohasset/Panuke oil field could provide such an opportunity. An alternative approach is to equip a standard AES NOMAD buoy so as to record the measured winds at high–frequency, preferably at two heights, correlate wind measurements with buoy motion, and compare scalar and vector averaged wind speeds.

5.2.2 Model Physics

This study has identified errors associated with two clear limitations of the ODGP model applied here, namely: lack of shallow water physics and wave–current interaction mechanisms. Shallow water effects appear to be primarily responsible for the correlation of storm hindcast peak–peak errors with water depth in the East Coast storm hindcast data set. The absence of wave–current interaction mechanisms in the ODGP model appear to be responsible for the large negative bias in storm sea states seen in the approaches to Hecate Strait and Dixon Entrance. These effects may also introduce some variability in the verification in other regions, for example, in the Halloween Storm verification, there appears to be a noticeable systematic underestimation of hindcast H_S time series induced by currents at the AES deep water offshore buoy located in the Gulf Stream meander during this event. In addition, on the continental shelf, shallow water limitations may manifest themselves at a given site only in high–energy long period sea states.

Recommendation

Many high–quality verification sites are located in areas where waves may be expected to be affected at least at times by shallow water effects and ocean current interactions. These data sources provide an opportunity to evaluate and possibly refine additional source terms of wave models designed to account for these effects. Additional hindcast and verification studies are needed to properly isolate the separate contributions of wind errors, shallow water refraction and attenuation, current refraction, and deep–water source terms (atmospheric input, wave breaking, wave–wave interaction) to the total error. In strictly deep–water verification, differences between the ODGP model and well tuned 2G and 3G formulations are slight except perhaps in the core of ”jet streaks”. To gain a better understanding of the differential model behaviour in this type of wave regime, further hindcast verification studies should be carried out in which each model is driven by high–quality wind fields of weather systems exhibiting ”dynamic fetch” wave generation modes, including hindcasts of well–documented tropical cyclones, the quintessential ”dynamic fetch” system.

5.2.3 Model Numerics

Even in strictly deep water areas, the time step and grid spacing used for the hindcasts verified in this study may not be optimum for all wave regimes encountered and for all verification sites. One obvious manifestation of this effect is along the West coast where the H_S RMSE and scatter index for ”inshore deep” areas are degraded by about 25% from the ”offshore deep” areas. Statistics for the ”sheltered” sites are even further degraded. Wave model temporal and spatial resolution should also be compatible with the time and space scales of the wind fields associated with the meteorological systems being modeled. This compatibility criteria is usually satisfied for typical scales of motion of open ocean extratropical cyclones. However, even higher spatial resolution and smaller time steps may be required to fully model the small scale rapidly propagating ”jet streak” features resolved in some extreme events as discussed above.

Recommendation

A straightforward hindcast sensitivity study of selected storm cases using models of increasingly finer grids would help define the optimum grid for near shore wave field resolution and for assessment of the sensitivity of the wave solution to grid resolution for storm systems in which wave generation along dynamic fetch excites extreme waves.

5.3 IMPLICATIONS OF RELIABILITY OF SIMULATED WAVE CLIMATES

5.3.1 Normals

The long term wave climate descriptions generated in the three–year East Coast and West Coast studies are accurate enough for most operational purposes with the following exceptions:

1. Grid limitations prevent accurate resolution of near shore gradients even in deep water regions, with near shore defined as any area within two grid distances of the open coast, or an offshore island.

2. Physics limitations may lead to unrepresentative climates in shallow water areas and in areas susceptible to strong currents.

3. A three–year sample is probably not long enough to represent the true long–term climate.

Recommendation

The interactive graphics (INGRED/FPA) method used to specify winds for the West Coast 3–year hindcast offers a promising approach to the specification of the long continuous time series of winds. This approach should be further refined and considered for the specification of continuous winds of a 10–year period for both East Coast and West Coast basins. These winds should be used to drive a wave model with obvious deficiencies removed, including the addition of shallow water terms, possible addition of wave–current interactions, and an extended domain for better resolution of distant swell sources.

5.3.2 Extremes

The wave height peaks hindcast in East Coast storms are weakly positively biased in the Grand Banks and Scotian Shelf, but this positive bias appears to be caused by the neglect of shallow water processes in the wave model used. Hindcast extremes, therefore, may actually be negatively biased in deep water portions of the domain, where, unfortunately, there were no verification sites available. On the other hand, the model hindcasts appear to be biased negatively in deep water in very severe storms where measurement sites lie in the path of the core of rapidly propagating and energetic jet streaks. Since little is known about the climatology of jet streaks the effect of this deficiency on design wave extremes is not estimable at this time.

Recommendation

Further detailed hindcast studies of recent storms which have been well sampled in the dense buoy network off the East and West Coasts (as carried out already for the Halloween and Storm of the Century) should be carried out with the 1–G ODGP as well as 3G type models to further characterize the dynamic fetch generation associated low level jet streaks, and to allow the estimation of the effect of these systems on the extreme wave climates in different areas.

TABLE 5.1 SUMMARY OF VERIFICATION

		CONTINUOUS 3–YEAR HINDCAST		STORMS = Pk–Ph	
		East Coast[2]	West Coast[3]	East Coast[2]	West Coast[3]
H_S	**No. of Obs.**	5427	28726	78	86
	Ave. Obs.(m)	2.56	3.04	8.03	8.52
	Bias[1]((m)	0.25	0.01	0.86	0.38
	RMSE (m)	0.79	0.94	1.51	1.38
	S.I.	0.31	0.31	0.19	0.16
T_P	**No. of Obs.**	5315	28726	78	86
	Ave. Obs.(s)	9.21	11.11	12.65	14.54
	Bias[1](s)	~0.41	–1.69	0.85	0.05
	RMSE (s)	2.24	3.47	1.97	1.72
	S.I.	0.24	0.31	0.16	0.12

[1] Hindcast–measurement

[2] All Scotian Shelf and Grand Banks buoy

[3] ”Offshore deep” buoys only

[4] ”Peak to peak statistics

6.0 REFERENCES

Baird, W.F. and J.S. Readshaw, 1981. A comparison of hindcast and recorded wave data. Marine Environmental Data Services, DFO, Contractor Report No. 1, Ottawa, Ont.

Beal, R.C. (editor), 1991. Directional ocean wave spectra: measuring, modelling, predicting and applying. John Hopkins sites in Each and Space Science Report series, the John Hopkins University Press.

Businger, J.A., J.C. Wynagaard, U. Izumi, and E.F. Bradley, 1971. Flux–Profile Relationships in the Atmospheric Surface Layer, J. of the Atmospheric Sciences, Vol. 28, pp. 181–189.

Cameron, D. and G. Parkes, 1992. A Meterological Overview of the Halloween Storm of 1991. Supplement, 3rd International Workshop on Wave Hindcasting and Forecasting, Montreal, Quebec, May 1992, pp. 1–44

Canadian Climate Centre 1991. Wind/wave hindcast extremes for the east coast of Canada, Volume I. Prepared under contract No: KM169–7–6678 by MacLaren Plansearch Limited and Oceanweather Inc., 109p. Plus appendices. Downsview, Ont.

Canadian Climate Centre, 1992. Wind/wave hindcast extremes for the west coast of Canada, Volume I. Prepared under contract No: KM169–8–7418 by MacLaren Plansearch Limited and Oceanweather Inc., 143p. Plus appendices. Downsview, Ont.

Cardone, V., 1969. Specification of the Wind Field Distribution in the Marine Layer for Wave Forecasting. Report TR–69–1, Geophys. Sci. Lab., New York University. Available from NTIS AD#702–490.

Cardone, V.J., W.J. Pierson, and E.G. Ward, 1976. Hindcasting the Directional Spectrum of Hurricane Generated Waves. J. of Petrol. Tech.,28,385–394.

Cardone, V.J. , 1978. Specification and Prediction of the Vector Wind on the United States Continental Shelf for Application to an Oil Slick Trajectory Forecast Program. Final Report, Contract T–35430 NOAA, U.S. Dept. of Commerce, Silver Spring, Maryland.

Cardone, V.J., A.J. Broccoli, C.V. Greenwood, and J.A. Greenwood, 1980. Error Characteristics of Extratropical Storm Wind Fields Specified from Historical Data J. of Petrol. Tech., 32, 873–850.

Cardone, V.J., D. Szabo and F. Della Stritto, 1989. Development of wind and wave criteria for Hibernia. Proceedings 2nd International Workshop on Wave Hindcasting and Forecasting. April 1989, Vancouver, B.C. pp. 75–88.

Cardone, V.J. and B.T. Callahan, 1992. Kinematic Analysis of the Surface Wind Field in the Halloween Storm and a preliminary Spectral Model Hindcast. Supplement, 2nd International Workshop on Wave Hindcasting and Forecasting. Montreal, Quebec, May 1992. pp. 101–118.

Cardone, V.J., H.C. Graber, R.E. Jensen, S. Hasselmann and M. J. Caruso, 1994: In search of the true surface wind field in SWADE IOP–1: Ocean Wave modelling perspective. Submitted to The Atmosphere–Ocean System.

Cardone, V.J., R.E. Jensen, D.T. Resio, V.R. Swail and A.T. Cox, 1995: Evaluation of Contemporary Ocean Wave Models in Rare Extreme Events: ”Halloween Storm” of October, 1991 ”Storm of the Century” of March, 1993. Accepted by J. Atmosphere Ocean Tech.

Clodman, S., 1983. Testing and future application of the Numerical Lake Wave Model; Internal Report No. MSRB–83–4, Atmospheric Environment Service, Downsview, Ontario.

Clodman S. and B. Eid., 1988. Adapting a Lake Wind Wave Model to a Small Enclosed Sea. Fourth Conference on Meteorology and Oceanography of Coastal Zone. January 31–February 5, 1988, Araheim, California, pp.62–65.

Coastal Engineering Research Centre, 1984. Shore Protection Manual, Volume 1. Department of the Army, U.S. Army Corps of Engineers, Washington, D.C. 20314.

Donelan, M.A., 1978. A simple numerical model fro wave and wind stress prediction. Report, National Water Research Institute, CCIW, Burlington, Ontario.

Driver, D.B., et al. 1991. ”Hindcast Wave Information for the Great Lakes: Lake Erie,” WIS Report 22, US Army Engineer Waterways Experimental Station, Vicksburg, MS, USA.

Driver, D.B., et al. 1992. ”Hindcast Wave Information for the Great Lakes: Lake Superior,” WIS Report 23, US Army Engineer Waterways Experiment Station, Vicksburg, MS, USA.

Eid, B.M., C. Morton and E. Dunlap, 1992. Development of wind and wave climate atlas for the east coast of Canada and the Great Lakes. Proceedings 3rd International Workshop on Wave Hindcasting and Forecasting; May 1992, Montreal, Québec, pp. 339–350.

Eid, B.M., C.M. Morton, V.J. Cardone and J.A. Greenwood, 1989. Development and evaluation of a wave climate database. Proceedings of The 2nd International Workshop on Wave Hindcasting and Forecasting, Vancouver, B.C., April 25–28, 1989, p.140–150.

Environment Canada, 1992. Supplement to The 3rd International Workshop on Wave Hindcasting and Forecasting, Montreal, Quebec, May 19–22, 1992.

Gilhousen, D.B., 1987. ”Field Evaluation of NDBC Moored Buoy Winds”. J. Atmos Ocean Tech., 4, 94–104.

Hubertz, J.M., 1989. A Wind–Wave Hindcast of the Great Lakes 1956–1987. Proceedings of The 2nd International Workshop on Wave Hindcasting and Forecasting. Vancouver, pp. 171–181.

Hubertz, J.M., 1991. ”Hindcast Wave Information for the Great Lakes: Lake Michigan,” WIS Report 24, US Army Engineer Waterways Experiment Station, Vicksburg, MS, USA.

Juszko, B. and R. Graham, 1992. ”Frequency and Directional Evaluation of the Ocean Data Gathering Program (ODGP) Wave Spectra at Hibernia. Atmosphere – Ocean Volume 30(3), pp. 441–456.

MacLaren Plansearch Limited, 1985. Evaluation of the Spectral Ocean Wave Model (SOWM) for supporting real–time wave forecasting in the Canadian east coast offshore. Prepared under contract for Atmospheric Environment Service, Downsview, ONT.

MacLaren Plansearch Limited, 1988. Wave Hindcast Database for Lake Ontario and Lake Superior. Report submitted to Ontario Ministry of Natural Resources, Toronto, March 1988 pp.

MacLaren Plansearch Limited, 1989. Preparation of a Wind and Wave Climate Atlas, Phase I Interim, Report – Initialization, Planning, Data Compilation, and Methodology, Report submitted to Transportation Development Centre, Transport Canada, Montréal, Québec, March 1989, Transport Canada Publication No.10867E.

MacLaren Plansearch Limited, 1991. ”Wind and Wave Climate Atlas Volume I, The East Coast of Canada.” Transport Canada Publication No. TP10820E.

MacLaren Plansearch Limited, 1992. Wind and Wave Climate Atlas, Volume III, The Great Lakes. Transport Canada Publication No. TP10820E.

MacLaren Plansearch Limited, 1993. ’Wind and Wave Climate Atlas, Volume IV, West Coast of Canada.” Transport Canada Publication NO. TP10820E.

Phillips and Irbe, 1978. ”Lake to Land Comparison of Wind, Temperature and Humidity on Lake Ontario during the International Field Year for the Great Lakes (IFYGL).” Canadian Climate Centre, Report #CLI–2–77, AES, Downsview, Ontario.

Philpott Associates Coastal Engineers Limited, 1988. Wave Hindcast Database for Ontario’s Great Lakes Lake Huron/Georgian Bay. Report submitted to Ontario Ministry of Natural Resources, Toronto, March 1988.

Pierson, W.J., L.J. Tick and L. Baer, 1966. Computer Based Procedures for Preparing Global Wave Forecasting and Wind Field Analyses Capable of Using Wave Data Obtained by a Spacecraft. In Sixth Naval Hydrodynamics Symposium, ACR–136, Office of Naval Research, Dept. of the Navy, Washington, D.C., 499–532.

Reinhard, R.D., et al. 1991a. ”Hindcast Wave Information for the Great Lakes: Lake Huron,” WIS Report 26, US Army Engineer Waterways Experiment Station, Vicksburg, MS, USA.

Reinhard, R.D., et al. 1991b. ”Hindcast Wave Information for the Great Lakes: Lake Ontario”, WIS Report 25, U.S. Army Engineer Waterways Experiment Station, Vicksburg, MS, USA.

Reece, A.M. and V.J. Cardone, 1982. Test of wave hindcast model results against measurements during four different meterological systems. Offshore Technology Conference Paper 4323.

Resio, D.T., 1989: A revised deep water wave model. Coastal Engineering Research Centre, U.S. Army Engineers Waterways Experiment Station, Vicksburg, MS .

Resio, D.T. and C.L. Vincent, 1976. Design of wave information for the Great Lakes. Report 1 – Lake Erie; Report 2 – Lake Ontario; Report 3 – Lake Michigan; Report 4 – Lake Huron. U.S. Army Waterways Experiment Station (WES), Report No. TR–H–76–1.

Resio, D.T. and C.L. Vincent, 1977. Estimation of Winds Over the Great Lakes. American Society of Civil Engineering, Waterway Port. and Coast. Ocean Div. J. 102, 265–283.

Sandwell Swan Wooster Inc., 1988. Wave Hindcast Database for Lakes Erie and St. Clair. Report submitted to Ontario Ministry of Natural Resources, Toronto, March 1988.

Schwab, D.J., J.R. Bennett, P.C. Liu, M.A. Donelan, 1984. Application of a simple numerical wave prediction model to Lake Erie, Journal of Geophysical Research, Vol. No. 89, No. C3, pp. 3586–3592.

Schwab, D.J., J.R. Bennett, and E.W. Lynn,1986. A Two Dimensional Wave Prediction System. Environmental Software, Vol. 1, No. 1, pp. 4–9.

Steele, K.E. and T. Mettlach, 1993. "NDBC wave data – current and planned." Proc. WAVES '93.ASCE, New Orleans, LA,.

Swail, V.R., V.J. Cardone and B.M. Eid, 1989. Wind/Wave Hindcast Extremes for the East Coast of Canada. Proceedings of the 2nd International Workshop on Wave Hindcasting and Forecasting, Vancouver, B.C., April 25–28,1989.

Swail, V.R., V.J. Cardone and B.M. Eid, 1992. An extreme wind and wave hindcast off the west coast of Canada. Proceedings 3rd International Workshop on Wave Hindcasting and Forecasting; Montreal, Québec, May 19–22, 1992, pp. 339–350.

Vincent, C.L., R.E. Jensen, P.A. Wittman and H.C. Graber., 1992. A wind wave hindcast for the Halloween northeaster in 1991 in the Atlantic Ocean Coastal Waters. Supplement to The 3rd International Workshop on Wave Hindcasting and Forecasting, Montreal, Quebec, May 19–22, 1992.